NASA TECHNICAL TRANSLATION NASA TT F-16,097

NEW METHODS OF STUDYING TELESCOPIC LENSES WITH REMARKS ON ASSESSING QUALITY

Y. Vaisala

(NASA -TT-F- 16097) NEW METHODS OF STUDY TELESCOPIC LENSES WITH REMARKS ON ASSESSING QUALITY KANNER (Leo) Associates) 98p HC $4.75 N75-13616

CSCL 20F Unclas G3/74 04984

Translation of "Neue Methoden zur Untersuchung der Objektive nebst Bemerkungen über die Beurteilung ihrer Güte," Annales Universitatis Fennicae Aboensis, Series A, Vol. 1, No. 2, Turku, Finland, 1922, pp. 3-129

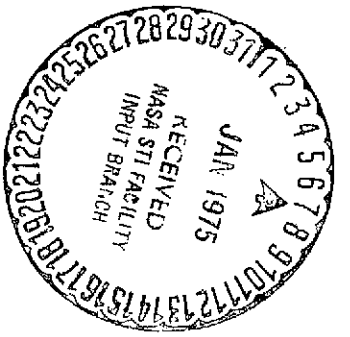

NATIONAL AERONAUTICS AND SPACE ADMINISTRATION
WASHINGTON, D.C. 20546 DECEMBER 1974

STANDARD TITLE PAGE

1. Report No. NASA TT F-16,097	2. Government Accession No.	3. Recipient's Catalog No.
4. Title and Subtitle NEW METHODS OF STUDYING TELESCOPIC LENSES WITH REMARKS ON ASSESSING QUALITY		5. Report Date December 1974 6. Performing Organization Code
7. Author(s) Y. Vaisala		8. Performing Organization Report No. 10. Work Unit No.
9. Performing Organization Name and Address Leo Kanner Associates, P.O. Box 5187, Redwood City, California 94063		11. Contract or Grant No. NASw-2481 13. Type of Report and Period Covered Translation
12. Sponsoring Agency Name and Address NATIONAL AERONAUTICS AND SPACE ADMINISTRATION, WASHINGTON, D.C. 20546		14. Sponsoring Agency Code

15. Supplementary Notes

Translation of "Neue Methoden zur Untersuchung der Objektive nebst Bemerkungen über die Beurteilung ihrer Güte," Annales Universitatis Fennicae Aboensis, Series A, Vol. 1, No. 2, Turku, Finland, 1922, pp. 3-129.

16. Abstract

Quantitative methods are developed for determining the aberrations of objectives, utilizing interference effects. Zonal aberrations are found by several methods to ascertain the curvature of the light front and its deviation from a perfect sphere. Astigmatism and coma are also ascertained by these techniques. The methods are applied to two transits, a refracting telescope, and a parabolic mirror. Parameters reflecting the quality of a lens are discussed and compared. Finally, the methods and results are applied to objectives in various observatories on the basis of literature data.

17. Key Words (Selected by Author(s))	18. Distribution Statement
	Unclassified - Unlimited

19. Security Classif. (of this report)	20. Security Classif. (of this page)	21. No. of Pages	22. Price
Unclassified	Unclassified	96	

NEW METHODS OF STUDYING TELESCOPIC LENSES WITH REMARKS ON ASSESSING QUALITY

Y. Vaisala

I. Introduction /3*

1. The most natural method for testing telescopic objectives in the observatory is to view a celestial body directly through the telescope. In general, close double stars have been considered suitable objects for this purpose. Nevertheless, a much more reliable and detailed picture of the quality of an objective is obtained by viewing extrafocal images of the stars [1]. This technique, to which many famous opticians for objectives have resorted, is so sensitive that the objective can confidently be assumed faultless in practice when viewing extrafocal images does not turn up any appreciable aberrations. Some idea of the quality of a photographic objective can also be deduced by photographing stars in very stationary pictures. Since the image on the photographic plate is not the diffraction pattern of the star at the moment, but the sum of the individual momentary effects, air turbulence will make the image of the star on the plate larger than the instantaneous diffraction patterns, and this is why, in examining a photographic objective, defects /4 can be overlooked which would easily be detected in a visual telescope of corresponding size through observation of stars.

Neither the techniques mentioned above nor the Foucault knife-edge method usually employed by opticians permit more than a qualitative determination of the flaws in an objective. In order to compare the objectives of different observatories, their defects must be determined quantitatively, just like other defects in astronomical instruments: collimation errors, the varying thickness of axle journals, etc. It is true that it is less useful to know the defects in objectives than to know e.g. the thickness of the axle journals in a transit, in the sense that the results of observations would be correctable if the errors were known. However, if an objective's errors were known numerically, there would then be a basis for an impartial judgment on whether the objective satisfied the requirements demanded of a good lens, and that can be corrected if needed. Moreover, if the errors in the objective are known, the worst parts can be covered and its performance enhanced in this way. As one example of the importance of studying the defects in any objective, the 80-cm objective of the large photographic telescope in Potsdam has been tested. Hartmann has given a detailed description of this testing [2]. This is a good illustration of opticians and astronomers cooperating to make

*Numbers in the margin indicate pagination in the foreign text.

great improvements in an originally very defective objective. A characteristic example of just how incorrect an assessment of the quality of an objective can be without numerical information on its defects is supplied by the 34-cm objective of the smaller photographic telescope of the same observatory, which has been studied precisely by Wilsing [3]. In this /5
instrument, which had been praised as "an excellent optical product" [3, p. 5], the zonal aberrations make the brightness in the center of the diffraction pattern much less than that in the center of a picture supplied by a flawless objective of corresponding size, while the diameter of the diffraction disk for this objective is somewhat smaller than that for an ideal objective.

The most noticeable of the defects of an objective is chromatic aberration, a defect which cannot be eliminated by grinding, since it is inherent in the nature of the glass. These days, the refractive power of a glass at different wavelengths is determined very precisely before it is used in the manufacture of an objective, so that chromatic aberration can be corrected for any two arbitrary wavelengths to the degree permitted by the glasses employed. The remainder of the chromatic aberration, the so-called secondary spectrum, can be determined by the method reported by Vogel with the aid of a spectroscope. Nowadays, a large error at the apex of the color curve can only be due to major errors in the radii of the surfaces of the objective, errors which can naturally be avoided in careful work.

The situation is different for errors due to inhomogeneities in the lens glass, and to discrepancies between the actual surfaces and the mathematically calculated shapes -- for lenses, usually spherical surfaces. Such errors appear as zonal aberrations, including spherical aberration and astigmatism. All the efforts of opticians are aimed at minimizing these errors. Astigmatic errors are usually vanishingly small, at least in rather small objectives. However, substantial zonal aberrations can occur in /6
both small and large objectives and mirrors. It is therefore of particular importance that there be precise methods by which zonal aberrations can be determined quantitatively.

Numerical determinations of shape defects (zonal aberrations and astigmatism) of objectives were not carried out in observatories until Hartmann invented his famous method of extrafocal images [4]. The main idea of this method is as follows. A disk is placed in front of the objective. There are many small holes in the disk, dividing the light into thin beams. Either micrometrically or photographically, the position of this beam is determined on two planes perpendicular to the axis of the objective, one of the planes being closer than the focus, and the other beyond it. The zonal aberrations and the astigmatism

are determined from the measurements. Usually, the measurements are taken photographically, since this minimizes the actual work at the telescope, and the results are more precise than those of visual measurements. Another factor is that the light beams coming from different points on the objective can be photographed at the same time, so that any motion of the telescope affects all images in the same manner.

Apart from its good points, however, Hartmann's method has a drawback which must always be recalled when it is to be employed. Namely, the smaller the holes, the lower the accuracy of the measurements in general, since reducing the size of the holes increases the diameters of the corresponding diffraction patterns, and this naturally reduces the precision of the measurements. Moreover, even a slight irregularity in the shape of the holes /7 and any air bubbles in the objective induce irregularities in the diffraction pattern thus detrimentally affecting the measurements [5]. On the other hand, the holes cannot be too large, because then they could not be made impervious enough and it would no longer be certain that the objective could be held errorlessly on a region of the size of the hole. In studying an objective 8 cm in diameter, Hartmann used holes only 4 mm in diameter [5]. The diameters of the corresponding diffraction patterns were on the order of one arc minute. It is clear that the precision of such patterns is many times smaller than the alignment accuracy of a pattern generated by the full aperture.

With very large objectives, the situation is quite different. In this case, the holes can be several centimeters in diameter, and the precision is then not much less than the accuracy in using the objective with full aperture. The unsteadiness of the images and certain other factors prevent measuring accuracy from rising very much as the aperture is enlarged, as long as the aperture is already several centimeters. Therefore, the larger the objective, the smaller the role played by the unfortunate circumstance mentioned above.

2. As observed previously, zonal aberrations are generally much more noticeable than astigmatic errors. The former are usually expressed by giving focal lengths for different zones of the objective, reduced by a mean focal length. The zonal aberrations can be graphically illustrated by plotting the zones on a horizontal axis and the focal-length differences /8 on a vertical axis. Hartmann has published extraordinarily valuable material on modern objectives [2], presenting the zonal aberrations of several objectives in both numerical and graphic form.

If the focal-length deviations are known, it is easy to calculate the distribution of light determined by geometrical optics in any arbitrary plane near the focus and at right angles to the optical axis. The plane in which the concentration of the light is greatest can be considered the focal plane. The smaller the area in which the light concentrates in the focal plane, the better the objective is from the viewpoint of geometrical optics. If the mean value of the lateral deviations of all light rays in the focal plane is divided by the mean focal length and the quotient multiplied by $\left|\frac{200000}{\pi}\right|$, a number T is obtained which has come into use as a measure of the quality of an objective, as a so-called technical constant. This parameter is a suggestion of Lehmann [6]. T is approximately the mean radius of the geometrical image, expressed in arc seconds. In [5], Hartmann also calculated the value of T for all the lenses he inspected.

Nevertheless, caution is advisable in assessing objectives on the basis of focal-length curves and the constant T. It must be recalled that geometrical optics ignores the phenomenon of diffraction. If the defects in an objective are so large that their effects far surpass those of diffraction, the distribution of light in the focal plane can be determined quite correctly by geometrical optics. However, the defects in astronomical /9
objectives ought to be so small that the distribution of the light in the image will be mainly determined by diffraction and not by zonal aberrations, because only then is it worth employing the strongest magnifications with an objective. The distribution of the light must then be calculated from diffraction theory, since geometrical optics can lead to highly erroneous results, as will be shown later in examples.

The technical lens constant based on diffraction theory was defined by Strehl [7]. He proposes that the standard for the quality of an objective be the brightness of the midpoint of the diffraction pattern produced by the objective divided by the brightness of the midpoint of a diffraction pattern produced by an ideal objective of the same type. It would be hard to find a more appropriate reliable quantity as a standard of quality for an objective. Unfortunately, Strehl's constant is not as widely used as it should be. This is probably due to the fact that it is considered tedious to calculate it. The greater popularity of the constant T may also be due to its simple interpretation as a measure of the size of the geometrical image. This may perhaps ignore the fact that light rays in the sense employed in geometrical optics do not exist and T can also be assigned a physical interpretation.

3. The primary purpose of the present work is to describe methods of determining defects in objectives, methods which

will be free of the drawback of Hartmann's method -- i.e. that the precision decreases when the size of the holes is reduced. The new methods will therefore make it possible to obtain /10
greater accuracy than in Hartmann's method, whenever permitted by the pictures, and this fact will be demonstrated by direct observations. In the same way, the discrepancies between the light front and a sphere will be determined without integration. These discrepancies must be calculated when the distribution of light near the focus is to be determined on the basis of diffraction theory. The methods to be described are particularly well suited for studying visual objectives, and I have visually examined all the objectives used as examples, but this does not prevent these methods from being used on photographic objectives as well. A suitable method is also given for testing visual telescopes equipped with neither an ocular micrometer nor cross-hairs.

The methods to be described are based on observations of diffraction patterns produced by the interference of light rays passing through two, three, or even four holes. In Hartmann's method, a light ray passing through a given hole generates its own diffraction pattern independently of the other light rays. In the literature, I have found an article in which the joint diffraction pattern of two holes was used to study optical surfaces. Namely, Michelson [8] appears to have used the method of two holes as long ago as 1918 to determine the errors of a lens and a mirror in the laboratory. However, his method cannot be successfully employed in practice in observatories for several reasons, which I will give later. In optical workshops as well, the method developed by the author of the present work ought to /11
be easier to use and more accurate than that of Michelson.

The last section of my treatise deals with the technical constants of lenses. First, a proposed method for more efficient calculation of Lehmann's constant is derived, and then it is shown that the mean deviation of the light front from the surface of a sphere is just as good a practical standard for the quality of an objective as Strehl's constant. The discussion will be illustrated by several typical examples. Finally, the suitability of the Lehmann and Strehl constants as standards of quality for objectives will be analyzed, the formulas derived will be applied to several objectives, the zonal aberrations of which I have found in the literature, and the refinishing of objectives will be treated.

II. The New Methods /12

Basic Idea of the Methods

4. The wave front of light arriving from an infinitely distant point, such as a fixed star, is a plane. Passing through a flawless objective, the wave front is converted to a sphere, the center of which is at the focus of the objective. In actuality, of course, all objectives are more or less flawed, and thus the light front differs more or less from the ideal surface, the sphere. The problem is now to discuss methods of determining these discrepancies.

In Fig. 1, the solid curve is the light front and the dotted line is a spherical surface differing only slightly from the light front. O is the center of the sphere. The normal to the surface drawn at point P of the light front intersects at point Q the plane through point O and perpendicular to the optical axis.

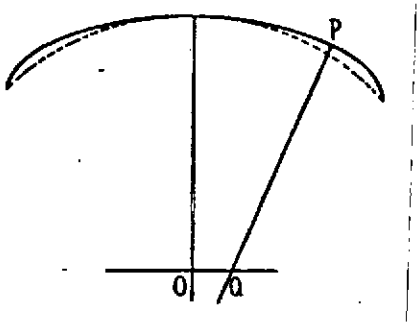

Fig. 1.

Hartmann's method involves determining the position of point Q with the aid of extrafocal images, i.e. determining the direction of the tangent plane to the light front at point P. In the introduction, it was pointed out that diffraction makes it much more difficult to carry out this determination. In fact, the existence of such a difficulty would be immediately evident even if we knew little of the real /13 nature of light, since experimentally, it is impossible to determine the tangent of an arbitrary curve or the tangent plane of a surface. On the other hand, we can determine the position of the chord to a curve or a surface or the position of a plane passing through three points on a curved surface.

To study a light front, we then find natural methods by looking for the position of a chord of the surface or a plane passing through three points instead of a tangent line or plane. We achieve this goal by placing a screen with two or three holes in it in front of the objective, and allowing the light rays coming from different holes to interfere with one another. Let us assume that there are two small holes in the screen through which two points on the light front have been determined. In that case, the well-known interference pattern formed by parallel bright bands is produced in the focal plane. The

central bright band is equally distant from the two points on the wave front. By measuring the position of the central interference band, the direction of the chord connecting the two points on the wave front can be determined.

By using a screen with three small holes at the vertices of a triangle, an interference pattern composed of bright points is obtained. If the position of the central point, which is /14
equally distant from the three points on the wave front determined by the holes, is measured, the direction of the normal to the plane passing through the three points in question on the wave front can be determined.

We arrive at other methods when we attempt to determine the curvature of the wave front in the same way as radii of curvature are measured with the spherometer. If the spherometer has three adjacent feet, of which one can be extended and retracted measurably, the radius of a circular arc can be determined. Usually, however, the spherometer has three fixed feet forming an equilateral triangle and a fourth foot at the midpoint of the triangle, measurements being carried out for the latter. We obtain a method for measuring the curvature of a wave front which is analogous to the first spherometer model by employing a screen containing three colinear small holes. An interference pattern, again formed by bright parallel bands, is projected on a movable plane, and the interference pattern changes when the distance of the movable plane to the objective is changed. One of the bands passes through the center of the circle drawn through the points on the wave front determined by the holes. By shifting the movable plane, the position of this bright band[1] is discovered, and thus the radius of the circle determined. On the other hand, if a screen with three holes at the vertices of an equilateral triangle and a fourth hole at the midpoint of the triangle is used, an interference pattern formed by bright points is obtained, and the pattern varies when the movable plane is shifted. One of the bright points is situated at the center of the sphere passing through the points on the wave front deter- /15
mined by the holes. By shifting the movable plane, the position of this point[1] is ascertained, and the radius of the sphere determined. This method is therefore reminiscent of the measurements with a customary 4-foot spherometer.

The Two-Hole Method

5. Figure 2 depicts a meridian section through a light front and a sphere differing very little from the front, namely the reference sphere. The center of the sphere is 0 and its

[1]Later on, it will be explained how this band or point is distinguished from the other ones.

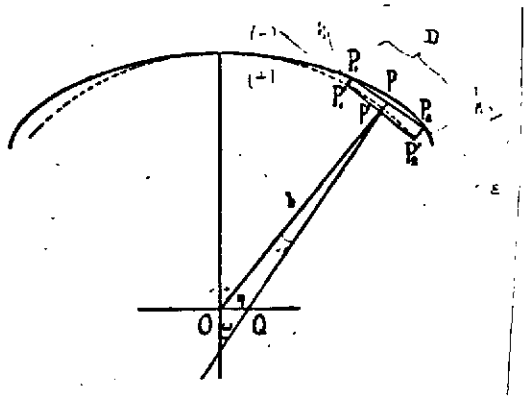

Fig. 2.

radius is b. The points P_1 and P_2 are two points on the light front and P_1' and P_2' are the points on the reference sphere closest to P_1 and P_2 respectively. We term the distances $P_1'P_1 = h_1$ and $P_2'P_2 = h_2$ the deviations of the light front, taking these deviations to be positive in the case in which the light front is behind the reference sphere at the points in question, relative to the direction of propagation of the light. Let D be the length of the chord P_1P_2.

Assume that the deviation h_1 is known. We can determine /16 the deviation h_2 if we know the angle ε between the chords P_1P_2 and $P_1'P_2'$. Let us imagine that the deviations are small. We will consider ε positive when h_2 is greater than h_1, as depicted in Fig. 2. Then

$$h_2 = h_1 + \varepsilon D. \tag{1}$$

The angle ε between the chords is equal to the angle between the central normals PQ and P'O of the chords. We can determine this angle if we know the distance η from O to the intersection Q of the normal PQ and the plane passing through point O and perpendicular to the optical axis, as well as the angle ω which this normal makes with the optical axis. η will be positive if the point Q lies to the right of the optical axis, as in the diagram, and negative if it is to the left of the optical axis. Hence

$$\varepsilon = \frac{\eta \cos \omega}{b} \tag{2}$$

and, applying Eq. (1),

$$h_2 = h_1 + \frac{D}{b} \eta \cos \omega. \tag{3}$$

In practice, it can usually be assumed that $\cos \omega = 1$.

This is the basic idea by which the measurements will be carried out in practice. In the immediate vicinity of the objective, either in front of it or behind it, a screen is placed in which small holes have been made at points P_1 and P_2.

The form of the interference pattern produced by the holes is well known from physics texts. We first assume that the holes are infinitely small in all dimensions, and that the light is monochromatic at the wavelength λ. On any plane extending in /17 the direction of the chord P_1P_2, a figure is formed which consists of very many bright and dark lines, and which is symmetric with respect to the normal plane of the chord P_1P_2. The line of intersection of this normal plane and the image plane will be bright since it is an axis of symmetry of the figure. The spacing of the lines is $b\lambda/D$.

Since, in reality, the holes are finite, the lines can be perceived only near the focus, and the number of lines diminishes as the size of the holes increases. Moreover, if the light is not monochromatic, the lines develop into spectra, so that only a few lines can be seen due to the superposition of spectra of different orders.

Determining the position of the central band -- a measurement which can be carried out either visually by means of a micrometer or photographically -- simultaneously determines the position of the point Q. For the point O, any point as close as possible to the focus in the plane of motion of the micrometer hairline or on the photographic plate can be chosen. The difference $h_2 - h_1$ is determined with the aid of Eq. (3).

We then displace the screen laterally, so that the hole P_1 arrives at the point previously occupied by P_2, and P_2 comes to a new point where the deviation of the light front is h_3. If we again measure the distance of the central bright band from the point O, we obtain the difference $h_3 - h_2$. Continuing the observations in this fashion, we obtain the equations

$$\left.\begin{aligned} h_2 &= h_1 + \frac{D}{b}\eta_1, \\ h_3 &= h_2 + \frac{D}{b}\eta_2, \\ h_4 &= h_3 + \frac{D}{b}\eta_3, \\ &- - - - -. \end{aligned}\right| \qquad (4)$$

We can e.g. write $h_1 = 0$. Then, from the equations in (4), we /18 obtain h_2, h_3, h_4, ...

By this method, the deviations of a light front from the sphere with center at O can be determined. The distance of the crosshairs or of the photographic plate from the objective is thus indicative of the radius of the reference sphere, and

the point from which the distances η are calculated determines the direction of the axis of the reference sphere. The deviations of the light front from any other sphere, differing only slightly from the reference sphere employed first, can be calculated easily, as will be shown later, from the deviations h_1, h_2, h_3, ...

The shape of the holes in the screen could of course be arbitrary, as long as the dimensions of the holes were sufficiently small in all directions, but naturally the holes will be regular, e.g. round or rectangular. Since the astigmatic errors will in general be small in comparison to the zonal aberrations, it is best, when determining zonal aberrations, to make the holes rectangular, with the long side perpendicular to the line connecting the holes, in order to obtain as much light as possible.

The two-hole method can naturally be used for determining factors other than the zonal aberrations. With this method, the direction of any arbitrary chord connecting two points on a light front can be discovered. The entire light front can be "leveled" by the two-hole method, in which case it is best to first ascertain the deviations of just a few points on the surface, and then starting from these, to determine the deviations of a sufficient number of intervening points. The entire measuring technique is highly reminiscent of the precision leveling of a large area of land.

Three-Hole Method /19

6. As previously mentioned, the position of the plane passing through three points on a light front can be determined by using a screen with three holes. For the sake of symmetry, of course, it is best to make the holes equally large and at equal distances from one another. The form of the diffraction pattern in the vicinity of the focus can be calculated in the following manner, assuming that the holes are infinitely small and that the light is monochromatic.

Let P_1, P_2, and P_3 be three points at the vertices of an equilateral triangle on a light front, and suppose that the holes of the screen are located at these points (Fig. 3). We employ a skew coordinate system, with the origin at the midpoint of the triangle $P_1P_2P_3$, the x-axis through the point P_1, the y-axis through the point P_2, and z-axis perpendicular to the plane $P_1P_2P_3$, the positive direction being that toward the image. Let the distance of point P from the origin be r. We consider the distribution of light in a plane E parallel to the xy-plane. Let b be the distance of the intersection of this plane and the z-axis from the point P.

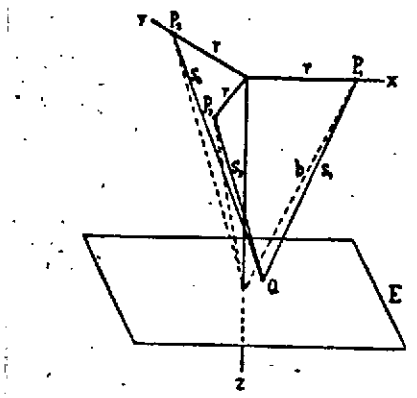

Fig. 3.

The distance s of a point Q(ξ,η,ζ) in the E-plane from one of the points P(x,y,0) is obtained from the equation /20

$$s^2 = (x-\xi)^2 + (y-\eta)^2 - (x-\xi)(y-\eta) + \zeta^2.$$

Since P lies on the light front,

$$b^2 = x^2 + y^2 - xy + \zeta^2$$

and hence

$$s^2 = b^2 + (y-2x)\xi + (x-2y)\eta + \xi^2 + \eta^2 - \xi\eta.$$

Assume that ξ and ζ are very small, so that

$$s = b + \frac{y-2x}{2b}\xi + \frac{x-2y}{2b}\eta.$$

Therefore, the distances from the point Q to the points $P_1(r,0,0)$, $P_2(0,r,0)$, and $P_3(-r,-r,0)$ respectively are

$$s_1 = b - \frac{r}{b}\xi + \frac{r}{2b}\eta,$$

$$s_2 = b + \frac{r}{2b}\xi - \frac{r}{b}\eta,$$

$$s_3 = b + \frac{r}{2b}\xi + \frac{r}{2b}\eta.$$

Let t be time, λ the wavelength of the light, and T the period. The resultant oscillation of light arriving at point Q from the points P_1, P_2, and P_3 is proportional to the expression

$$V = \sin 2\pi\left(\frac{t}{T} - \frac{s_1}{\lambda}\right) + \sin 2\pi\left(\frac{t}{T} - \frac{s_2}{\lambda}\right) + \sin 2\pi\left(\frac{t}{T} - \frac{s_3}{\lambda}\right).$$

Substituting in the expressions for the distances s_1, s_2, and s_3, we obtain, by the addition theorem:

$$V = C\sin 2\pi\left(\frac{t}{T} - \frac{b}{\lambda}\right) - S\cos 2\pi\left(\frac{t}{T} - \frac{b}{\lambda}\right),$$

where

$$C = \cos(-2\xi' + \eta') + \cos(\xi' - 2\eta') + \cos(\xi' + \eta'),$$
$$S = \sin(-2\xi' + \eta') + \sin(\xi' - 2\eta') + \sin(\xi' + \eta'),$$

$$\xi' = \frac{\pi r}{\lambda b}\xi, \quad \eta' = \frac{\pi r}{\lambda b}\eta. \tag{5}$$

/21

Finally, if

$$C = M\cos\varphi, \quad S = M\sin\varphi;$$

then

$$V = M\sin\left[2\pi\left(\frac{t}{T} - \frac{b}{\lambda}\right) - \varphi\right]; \quad M^2 = C^2 + S^2.$$

The intensity I of the light is proportional to the kinetic energy of the oscillation; therefore M^2 can be taken as a measure of the intensity of the light.

Carrying out the calculations, we find

$$I = M^2 = 3 + 2\cos(3\xi' - 3\eta') + 2\cos 3\xi' + 2\cos 3\eta'. \tag{6}$$

It is easy to see that I reaches its maximum value of 9 when

$$\xi' = n_1\frac{2\pi}{3}, \quad \eta' = n_2\frac{2\pi}{3} \quad (n_1, n_2 = 0, \pm 1, \pm 2, \cdots) \tag{7}$$

or

$$\xi = n_1\frac{2\lambda b}{3r}, \quad \eta = n_2\frac{2\lambda b}{3r}. \tag{8}$$

Hence, the light maxima are oriented in the manner depicted in Fig. 4. At the intersection point of the z-axis and the movable plane, a point equidistant from the points P, there is naturally a maximum. The surrounding maxima form a regular hexagon, and outside the latter is a new hexagon the points of which form equilateral triangles with the points of the first hexagon, etc.

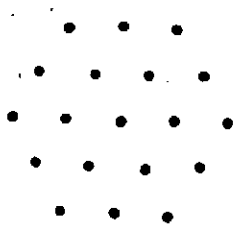

Fig. 4.

The intensity of the light is zero /22 at the midpoints of the triangles formed by the maxima. The distribution of the light can be graphically illustrated by computing curves of equal light intensity. Figure 5 shows the curves of equal light intensity surrounding a maximum point, the intensity of the light changing by half a size class in going from one curve to the next, so that the ratio of light intensities for points on successive curves is 1.585. These curves correspond to the values I = (9), 5.679, 3.583, 2.261, 1.426, 0.900, ...

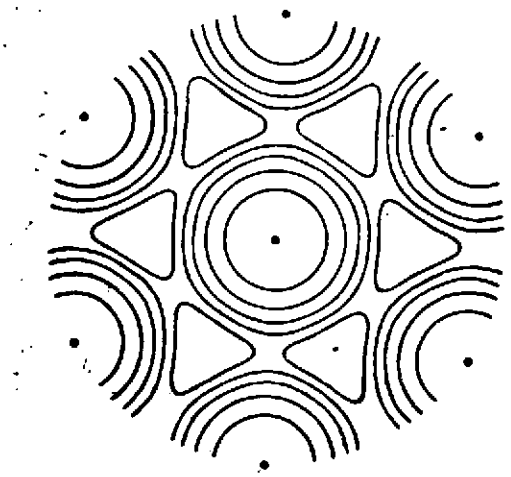

Fig. 5.

Just as in the two-hole method, enlarging the holes in the three-hole method reduces the number of light points, and when the light is not monochromatic, there is just a collection of colored series of points around the central point, no matter how small the holes are made.

In studying the wave front, only the position of the central light point is of interest. By determining its position in the /23 movable plane relative to the axis of the reference sphere, thus involving a measurement of two coordinates, the deviations h_1, h_2, and h_3 of the points P_1, P_2, and P_3 from the reference sphere can be determined in relation to each other. By shifting the screen in suitable fashion, the light front can be studied at a sufficient number of points. The three-hole method is particularly suitable for determining astigmatic errors, as will be explained later.

Three-Slit Method

7. Above, it was briefly mentioned that using a screen with three successive holes makes it possible to determine the radius of the circle passing through the points corresponding to the holes on the light front. We now examine this method more closely, by first making the holes infinitesimally small and the light monochromatic.

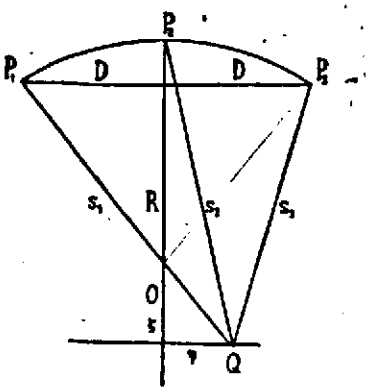

Fig. 6.

Because of the screen, the light can propagate only from the points P_1, P_2, and P_3 on the light front (Fig. 6). O is the center of the circle passing through the points P_1, P_2, and P_3. Let the radius of the circle be R, and let the distance of the points P_1 and P_3 from the line P_2O be D. In studying the distribution of the light, we can restrict ourselves to the plane $P_1P_2P_3O$, since the curves of equal intensity in the vicinity of this plane are lines at right angles to this plane, as is easy to see. We calculate the intensity of light at the point Q, at a distance η from the line P_2O, while the distance from P_2 to the normal to P_2O passing through Q is R + ζ. Then, we easily obtain the following expansions for the distances $P_1Q = s_1$, $P_2Q = s_2$, and $P_3Q = s_3$: /24

$$s_1 = R + \zeta + \frac{D}{R}\eta - \frac{D^2}{2R^2}\zeta + \cdots = s_2 + \frac{D}{R}\eta - \frac{D^2}{2R^2}\zeta + \cdots,$$
$$s_2 = R + \zeta + \cdots,$$
$$s_3 = R + \zeta - \frac{D}{R}\eta - \frac{D^2}{2R^2}\zeta + \cdots = s_2 - \frac{D}{R}\eta - \frac{D^2}{2R^2}\zeta + \cdots.$$

Let the holes P_1 and P_3 be equally large, and let P_2 be k times as large as the first two. The oscillatory velocity of the light at point Q is then proportional to the expression

$$V = \sin 2\pi\left(\frac{t}{T} - \frac{s_1}{\lambda}\right) + k \sin 2\pi\left(\frac{t}{T} - \frac{s_2}{\lambda}\right) + \sin 2\pi\left(\frac{t}{T} - \frac{s_3}{\lambda}\right).$$

The intensity I of the light is calculated in the same way as in the previous method. By carrying out the calculations, we find

$$I = k^2 + 4k\cos\frac{\pi}{\lambda}\left(\frac{D}{R}\right)^2\zeta\cos\frac{2\pi}{\lambda}\frac{D}{R}\eta + 4\cos^2\frac{2\pi}{\lambda}\frac{D}{R}\eta$$
$$= k^2\sin^2\frac{\pi}{\lambda}\left(\frac{D}{R}\right)^2\zeta + \left[k\cos\frac{\pi}{\lambda}\left(\frac{D}{R}\right)^2\zeta + 2\cos\frac{2\pi}{\lambda}\frac{D}{R}\eta\right]^2. \qquad (9)$$

Using the symbols

$$\eta' = \frac{2\pi D}{\lambda R}\eta, \quad \zeta' = \frac{\pi D^2}{\lambda R^2}\zeta \qquad (10)$$

we obtain /25

$$I = k^2 + 4k\cos\zeta'\cos\eta' + 4\cos^2\eta' = k^2\sin^2\zeta' + (k\cos\zeta' + 2\cos\eta')^2. \quad (11)$$

I is therefore a periodic function of both ζ' and η'. Both periods are 2π.

First consider ζ' constant. If $|k\cos\zeta'| < 2$, I reaches its maximum at the points $\eta' = 0, \pm\pi, \pm2\pi, \pm3\pi, \ldots$ and its minimum at the points at which $k\cos\zeta' + 2\cos\eta' = 0$. On the other hand, if $|k\cos\zeta'| \geq 2$, I has its maxima and minima alternatingly at the points $\eta' = \ldots, -2\pi, -\pi, 0, +\pi, +2\pi, \ldots$. For every plane at right angles to the line P_2O, there will be a banded diffraction pattern, which changes as the distance from the plane to the point P_2 is varied.

Now consider the extreme values

$$\eta' = 0, \quad I_0 = k^2 + 4 + 4k\cos\zeta', \qquad \eta' = \pi, \quad I_1 = k^2 + 4 - 4k\cos\zeta' \quad (12)$$

as ζ' is varied. When $\zeta' = 0$, I_0 is a maximum and I_1 is a minimum. As $|\zeta'|$ increases, I_0 decreases and I_1 increases until they are equally large, at $\zeta' = \pm\pi/2$. At these points, I_0 and I_1 are changing most rapidly. As $|\zeta'|$ continues to increase, I_1 becomes larger than I_0. When ζ' is sufficiently close to the values $\pm\pi/2$, I_0 and I_1 are both maxima when $k > 2$.

From the above mathematical analysis, the best way to determine the radius R of curvature can be deduced. With a high-magnification ocular, the diffraction pattern is observed on both sides of the plane $\zeta' = 0$. First, the ocular is e.g. inserted so far that the interference bands, which are initially of different intensities, become equally bright. Then, the ocular /26 is withdrawn until the bands are again equally bright. Halfway between these positions of the ocular is the position at which one sees the plane $\zeta' = 0$. Since I_0 and I_1 are changing fastest at $\zeta' = \pm\pi/2$, it is clear that this measurement is much more accurate than trying to recognize directly the position of the $\zeta' = 0$ plane by looking for the point at which one interference line (I_0) reaches its maximum, and the other (I_1) its minimum brightness.

Since the holes are in reality finite, the number of interference lines will be limited, and the interference pattern will disappear completely when the movable plane is withdrawn far

enough from the point O, so that only the extrafocal images induced by the separate holes can be seen. By exploiting this fact, one can discover whether the movable plane under investigation is $\zeta' = 0$ or one of the planes $\zeta' = 2n\pi$ ($n = \pm 1, \pm 2, \ldots$). If the light employed is not monochromatic, this will also limit the extent of the interference phenomenon in all directions.

Let us first determine the value which k must assume in order to be able to carry out the observations as accurately as possible. The faster the difference $I_0 - I_1$ varies in relation to the mean light intensity $(I_0 + I_1)/2$ of the band, the easier it will be to detect the plane in which I_0 and I_1 are equally great. Hence, as a sensitivity criterion for the method, let us consider the expression

$$K = \left| \frac{\frac{d}{d\zeta'}(I_0 - I_1)}{\frac{1}{2}(I_0 + I_1)} \right|_{|\zeta'| = \frac{\pi}{2}} = \frac{8k}{k^2 + 4} \qquad (13)$$

When $k = 2$, K achieves its maximum value of 2. The method is then most sensitive when the center hole is twice as large as the outer ones.

When the holes are of equal size, i.e. $k = 1$, then $K = 8/5$,/27 and the accuracy is therefore not appreciably smaller than in the theoretically most favorable case. For certain reasons, e.g. because it is desirable to always view the same surface sections when the screen is shifted, it ought to be best to make all holes the same size and shape in practice.

This method is particularly well suited for determining zonal aberrations. When the radius of the circle passing through the points P_1, P_2, and P_3 on the wave front is determined, an equation is obtained for the deviations of the wave front at these points. If the screen is then shifted, and the radius of curvature is determined once more, an equation is found for the deviations of the points P_2, P_3, and P_4, etc. If arbitrary values are assigned to the deviations of three points on the wave front, the remaining deviations are obtained from the equations determined by measurement. In practice, it is most convenient to make the holes in the form of narrow rectangles, and for this reason I have termed the method the three-slit method, in order to distinguish it from the three-hole method previously described.

Four-Hole Method

8. By using a screen containing three holes of equal size forming an equilateral triangle and a fourth hole in the middle

of the first three, one acquires a method with which the curvature of the light front can be determined in the same way that the curvature of a spherical surface is measured with a conventional spherometer.

In calculating the diffraction pattern, we proceed in the same way as before, and again assume the light to be monochromatic and the holes to be infinitesimally small, so that the light can propagate only from the points P_1, P_2, P_3, and P_4 on the light front, of which P_1, P_2, and P_3 form an equilateral triangle and P_4 is equidistant from the points P_1, P_2 and P_3. Let O be the center of the sphere passing through the points P, and let R be the radius of the sphere. We will employ a skew coordinate system, the origin of which is the point P_4. The z-axis coincides with the line P_4O, the xy-plane is perpendicular to the z-axis, the xz-plane passes through the point P_1, and the yz-plane passes through the point P_2. Let the distance of the points P_1, P_2, and P_3 from the z-axis be r. Let the holes P_1, P_2, and P_3 be equally large, and let the hole P_4 be k times as large as the first three. /28

Let us calculate the intensity of the light at a point $Q(\xi,\eta,R+\zeta)$ near the focus. For the distances $P_1Q = s_1$, $P_2Q = s_2$, $P_3Q = s_3$, and $P_4Q = s_4$, we obtain the following expansions:

$$\left.\begin{aligned} s_1 &= R+\zeta-\frac{r}{R}\xi+\frac{r}{2R}\eta-\frac{r^2}{2R^2}\zeta+\cdots,\\ s_2 &= R+\zeta+\frac{r}{2R}\xi-\frac{r}{R}\eta-\frac{r^2}{2R^2}\zeta+\cdots,\\ s_3 &= R+\zeta+\frac{r}{2R}\xi+\frac{r}{2R}\eta-\frac{r^2}{2R^2}\zeta+\cdots,\\ s_4 &= R+\zeta+\cdots. \end{aligned}\right|$$

The oscillatory velocity at the point Q is proportional to the expression

$$\left.\begin{aligned} V = \sin 2\pi\left(\frac{t}{T}-\frac{s_1}{\lambda}\right)+\sin 2\pi\left(\frac{t}{T}-\frac{s_2}{\lambda}\right)+\sin 2\pi\left(\frac{t}{T}-\frac{s_3}{\lambda}\right)+\\ +k\sin 2\pi\left(\frac{t}{T}-\frac{s_4}{\lambda}\right). \end{aligned}\right|$$

The intensity I of the light is calculated as in the previous cases. Let

$$\left.\xi'=\frac{\pi r}{\lambda R}\xi,\quad \eta'=\frac{\pi r}{\lambda R}\eta,\quad \zeta'=\frac{\pi r^2}{\lambda R^2}\zeta,\right| \qquad (14)$$

Then

/29

$$I = k^2 + 3 + 2k\left[\cos(-2\xi' + \eta' - \zeta') + \cos(\xi' - 2\eta' - \zeta') + \cos(\xi' + \eta' - \zeta')\right] + 2\left[\cos(3\xi' - 3\eta') + \cos 3\xi' + \cos 3\eta'\right]. \tag{15}$$

I is therefore a periodic function of all the variables, and the length of the periods is 2π.

Consider the distribution of light in the plane $z = R + \zeta$ and for the time being, take ζ' to be constant. I acquires its extreme values at the points

$$\xi' = n_1 \frac{2\pi}{3}, \quad \eta' = n_2 \frac{2\pi}{3} \quad (n_1, n_2 = 0, \pm 1, \pm 2, \cdots),$$

and these extreme values are all maxima when $k < 6$ and ζ' is sufficiently small. If $k < 3$, the extreme values are maxima no matter what the value of ζ'. There are no other maxima.

The maxima therefore fall at the same points as in the three-hole method, but they are not of equal intensity, but can be divided into the following three classes

$$\begin{cases} (1) \quad \xi' = (2n_1 + n_2)\frac{2\pi}{3}, \quad \eta' = (n_1 + 2n_2)\frac{2\pi}{3}, \\ \qquad\qquad I_1 = k^2 + 9 + 6k\cos\zeta', \\ (2) \quad \xi' = (2n_1 + n_2 + 1)\frac{2\pi}{3}, \quad \eta' = (n_1 + 2n_2 + 1)\frac{2\pi}{3}, \\ \qquad\qquad I_2 = k^2 + 9 + 6k\cos\left(\frac{2\pi}{3} + \zeta'\right), \\ (3) \quad \xi' = (2n_1 + n_2 + 2)\frac{2\pi}{3}, \quad \eta' = (n_1 + 2n_2 + 2)\frac{2\pi}{3}, \\ \qquad\qquad I_3 = k^2 + 9 + 6k\cos\left(\frac{2\pi}{3} - \zeta'\right). \end{cases} \tag{16}$$

The distribution of the maximum points in the movable plane is visible in Fig. 7.

The maximum point $\zeta' = 0$, $\eta' = 0$ belonging to Class (1) is the central point of the figure. It is surrounded by a regular hexagon of maxima belonging in alternation to Class (2) and Class (3).

With the aid of the maxima (2) and (3), the position of the plane $\zeta' = 0$ can be determined precisely. From the above formulas, it can be seen that $I_2 = I_3$ when $\zeta' = 0$, and in the vicinity of the plane $\zeta' = 0$, $I_3 > I_2$ when $\zeta' > 0$, and $I_3 < I_2$ /30

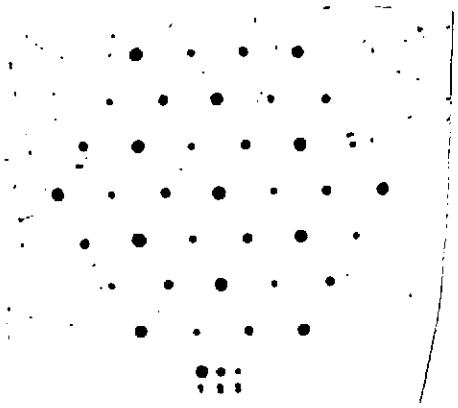

Fig. 7.

when $\zeta' < 0$. In practice, the plane $\zeta' = 0$ is determined by inserting and withdrawing a strongly magnifying ocular and observing when the maxima (2) and (3) surrounding the central point are of equal intensity. This position of the ocular corresponds to the plane $\zeta' = 0$, assuming that no error of an entire period has been made, where $\zeta' = \pm 2\pi, \pm 4\pi, \ldots$.

In actuality, the holes are finite, and this restricts the extent of the interference pattern in all directions. By inserting or withdrawing the ocular far enough, the joint interference pattern formed by the holes can be made to disappear, leaving four separate diffraction patterns. If this circumstance is exploited, one can ascertain whether a plane in question is $\zeta' = 0$ or one of the planes $\zeta' = \pm 2\pi, \pm 4\pi, \ldots$.

Again, we look for the value k at which the method is as sensitive as possible. As a sensitivity criterion, we can employ the expression

$$K = \left| \frac{\frac{d}{d\zeta'}(I_3 - I_2)}{\frac{1}{2}(I_3 + I_2)} \right|_{\zeta'=0} = \frac{6\sqrt{3}k}{k^2 - 3k + 9} \qquad (17)$$

If k = 3, K attains its maximum value of $2\sqrt{3}$. This /31
method is therefore most sensitive when the center hole is just as large as all the surrounding ones put together. If the holes are all of the same size, i.e. k = 1, then $K = 8\sqrt{3}/7$. Although this changes the accuracy quite a bit, it is still probably best to make all holes the same size in practice.

The four-hole method is particularly suitable for accurate focusing of telescopes. The central hole is placed at the center of the objective and the remaining holes near its edge. The method can also be used to determine zonal aberrations. However, because of the unsteadiness of the images, the four-hole method is only usable with exceptionally good images for large objectives.

Theory of the Methods When the Holes Are Finite

9. In deriving the formulas, the holes have so far been assumed to be infinitesimally small. We will now determine the

light distribution in the diffraction pattern for the two-hole method under the assumption that the holes are finite. We will attempt to ascertain the errors which might arise if the holes were identified with their midpoints in determining the shape of the wave front using the two-hole method.

We will first determine the form of the diffraction pattern produced by two equal holes L_1 and L_2 in the focal plane oriented in the same directions, when the light front is assumed to be a sphere and the light monochromatic at wavelength λ. Let the radius of the sphere be b, and the separation of the "centers of gravity" of the holes D. As the origin of an orthogonal coordinate system, we choose the focus O. As the z-axis we take the central normal of the line connecting the centers of the holes. Let the y-axis be parallel to this line, positive toward the hole L_2. Let the x-axis be perpendicular to the yz-plane. /32

The distance s between the point $Q(\xi,\eta,0)$ in the movable plane and the point P(x,y,z) on the light front is obtained from the equation

$$s^2 = (x-\xi)^2 + (y-\eta)^2 + z^2 = b^2 - 2x\xi - 2y\eta + \xi^2 + \eta^2.$$

Very close to the origin, it is sufficiently accurate to write

$$s = b - \frac{x\xi}{b} - \frac{y\eta}{b}.$$

Since the wave front is just a very small portion of the surface of a sphere, the area of the surface element on the wave front can be taken to be dx dy. The resultant oscillation at the point Q is proportional to the expression

$$\iint_{(L_1 L_2)} \sin 2\pi\left(\frac{t}{T} - \frac{s}{\lambda}\right) dx\,dy,$$

where the integration is performed over both holes. The intensity of the light at point Q is calculated as before. We employ the symbols

$$C = \iint_{(L_1 L_2)} \cos\frac{2\pi}{\lambda b}(\xi x + \eta y)\,dx\,dy,$$

$$S = \iint_{(L_1 L_2)} \sin\frac{2\pi}{\lambda b}(\xi x + \eta y)\,dx\,dy.$$

The intensity of the light in the movable plane is then proportional to the expression

$$I = C^2 + S^2.$$

If we set y = -D/2 + y' in integrating over the first hole and y = +D/2 + y' in integrating over the second hole, we obtain the same limits for both integrals. By simplifying, we find

$$C = 2\cos\frac{\pi D\eta}{\lambda b}\cdot C_1, \qquad S = 2\cos\frac{\pi D\eta}{\lambda b}\cdot S_1, \qquad /33$$

taking the integrals

$$C_1 = \iint_L \cos\frac{2\pi}{\lambda b}(\xi x + \eta y')\,dx\,dy', \qquad S_1 = \iint_L \sin\frac{2\pi}{\lambda b}(\xi x + \eta y')\,dx\,dy' \qquad (18)$$

over a single hole. We thus obtain

$$I = 4\cos^2\frac{\pi D\eta}{\lambda b}\cdot(C_1^2 + S_1^2), \qquad (19)$$

where the expression $C_1^2 + S_1^2$ is the light intensity of the diffraction pattern of one hole.

From these formulas, it is evident that the diffraction pattern produced by two congruent holes is similar to the one generated by a single hole, on which bright and dark lines are drawn at right angles to the line connecting the holes. In practice, only the central disc of the diffraction pattern and the lines situated on it can be seen clearly. The distance between dark lines is $\lambda b/D$, and the distance between the bright lines is roughly the same. The smaller the holes in comparison with the distance between them, the larger the number of lines on the central disc of the diffraction pattern produced by one hole, and the greater the regularity of the light distribution along and close to the central line. The above statements also apply to a great extent even when the holes differ somewhat. A precise mathematical analysis of the matter would take too much room, however.

The above discussion implies that the two-hole method has an important advantage over the one-hole method (Hartmann's), namely that irregularities in the shape of the holes and air bubbles in the objective have very little effect on the distribution of light on the central line, the only one concerned in the measurements, while in Hartmann's method, even a very slight irregularity in the shape of the holes makes the diffraction pattern irregular and observation uncertain. /34

When the holes are rectangles, the integration is very easy. Let the lengths of the sides of the rectangle in the x and y directions be γ and δ respectively. Then

$$C_1 = \int_{-\frac{1}{2}\delta}^{+\frac{1}{2}\delta}\int_{-\frac{1}{2}\gamma}^{+\frac{1}{2}\gamma} \cos\frac{2\pi}{\lambda b}(\xi x + \eta y')\,dx\,dy' = \left(\frac{\lambda b}{\pi}\right)^2 \frac{\sin\frac{\pi\gamma\xi}{\lambda b}\sin\frac{\pi\delta\eta}{\lambda b}}{\xi\eta},$$

$$S_1 = \int_{-\frac{1}{2}\delta}^{+\frac{1}{2}\delta}\int_{-\frac{1}{2}\gamma}^{+\frac{1}{2}\gamma} \sin\frac{2\pi}{\lambda b}(\xi x + \eta y')\,dx\,dy' = 0, \qquad (20)$$

$$C_1^2 + S_1^2 = (\gamma\delta)^2\left(\frac{\sin\frac{\pi\gamma\xi}{\lambda b}}{\frac{\pi\gamma\xi}{\lambda b}}\right)^2\left(\frac{\sin\frac{\pi\delta\eta}{\lambda b}}{\frac{\pi\delta\eta}{\lambda b}}\right)^2.$$

We will not examine this formula in detail (cf. [9]). We observe only that the points at which the light intensity is zero form congruent rectangles. The light intensity on the y-axis is zero first at a distance $\lambda b/\delta$ from the origin. Earlier, it was mentioned that in the diffraction pattern produced by two holes, the separation of similar lines is $\lambda b/D$. The number of lines on the central disk of the diffraction pattern produced by a rectangular hole therefore increases in the same ratio as D/δ. /35

10. So far, it has been assumed that the wave front is precisely spherical. In that case, the maximum of the light in the central line is always on the x-axis, as long as the holes are rectangular, and the distribution of the light on both sides of the x-axis is symmetric with respect to the latter. Of course, this symmetry is retained even when the wave front is not a sphere, as long as the deviations are symmetric with respect to the xz-plane. In other cases, it is likely that the maximum line of the central interference band is displaced by a certain amount from the x-axis, and it would no longer be immediately evident that the calculations could be carried out as in the case when the holes were infinitesimally small. We

now assume that the deviations of the wave front are of a relatively general form, and we determine their effects on the maximum line of the central band. For the sake of completeness, we also allow for differences in light intensity over the wave front. Such differences do exist, at least for refracting telescopes, since the thickness of the objective increases toward the center. Nevertheless, near a hole, we assume the light intensity to be constant.

We employ the same type of coordinate system as before. The z-axis is therefore the central normal of the segment connecting the midpoints of the rectangle. As the origin, we choose an arbitrary point on the z-axis, which can be viewed as an approximate focus. The deviations of the wave front are calculated from the sphere with center at the origin and passing through the midpoints of the holes. In general, the sides of the rectangles parallel to the y-axis are very small, so that in practice, it is sufficient to express the deviations of the wave /36 front at the holes L_1 and L_2 by the formulas

$$\left.\begin{aligned} h_1 &= \alpha_1 y' + \psi_1(x, y'), \\ h_2 &= \alpha_2 y' + \psi_2(x, y'), \end{aligned}\right|$$

where the two functions ψ_1 and ψ_2 of both variables are assumed to be even functions of the variable y'. Moreover, we assume that h_1 and h_2 are small compared to the light wave near the rectangles.

The distance between the point (ξ,η) near the origin in the xy-plane and the point (x,y') on the parts L_1 or L_2 of the wave front can be approximately expressed by the formulas

$$\left.\begin{aligned} s_1 &= b + \frac{D\eta}{2b} - \frac{\eta}{b} y' - \frac{\xi}{b} x + h_1, \\ s_2 &= b - \frac{D\eta}{2b} - \frac{\eta}{b} y' - \frac{\xi}{b} x + h_2. \end{aligned}\right|$$

Assume that the light intensities on the parts L_1 and L_2 of the wave front are in the ratio $\rho_1:\rho_2$. Then, the light intensity in the movable plane is proportional to the expression

$$I = C^2 + S^2,$$

where

$$C=\iint_{L_1}\varrho_1\cos\frac{2\pi}{\lambda}\left[+\frac{D\eta}{2b}+\left(\alpha_1-\frac{\eta}{b}\right)y'-\frac{\xi}{b}x+\psi_1\right]dx\,dy'$$
$$+\iint_{L_2}\varrho_2\cos\frac{2\pi}{\lambda}\left[-\frac{D\eta}{2b}+\left(\alpha_2-\frac{\eta}{b}\right)y'-\frac{\xi}{b}x+\psi_2\right]dx\,dy',$$
$$S=\iint_{L_1}\varrho_1\sin\frac{2\pi}{\lambda}\left[+\frac{D\eta}{2b}+\left(\alpha_1-\frac{\eta}{b}\right)y'-\frac{\xi}{b}x+\psi_1\right]dx\,dy'$$
$$+\iint_{L_2}\varrho_2\sin\frac{2\pi}{\lambda}\left[-\frac{D\eta}{2b}+\left(\alpha_2-\frac{\eta}{b}\right)y'-\frac{\xi}{b}x+\psi_2\right]dx\,dy'.$$

Since we intend only to discover the position of the maximum line of the central band, and since we need to know the latter only in the immediate vicinity of the y-axis, both ξ and η as well as, by what has been said previously, the arguments of the trigonometric functions in the integrands are very small, so that we can omit powers higher than the square in the series expansion of the trigonometric functions. We therefore obtain: /37

$$C=\iint_{L_1}\varrho_1\left\{1-\frac{2\pi^2}{\lambda^2}\left[+\frac{D\eta}{2b}+\left(\alpha_1-\frac{\eta}{b}\right)y'-\frac{\xi}{b}x+\psi_1\right]^2\right\}dx\,dy'$$
$$+\iint_{L_2}\varrho_2\left\{1-\frac{2\pi^2}{\lambda^2}\left[-\frac{D\eta}{2b}+\left(\alpha_2-\frac{\eta}{b}\right)y'-\frac{\xi}{b}x+\psi_2\right]^2\right\}dx\,dy',$$
$$S=\iint_{L_1}\varrho_1\frac{2\pi}{\lambda}\left[+\frac{D\eta}{2b}+\left(\alpha_1-\frac{\eta}{b}\right)y'-\frac{\xi}{b}x+\psi_1\right]dx\,dy'$$
$$+\iint_{L_2}\varrho_2\frac{2\pi}{\lambda}\left[-\frac{D\eta}{2b}+\left(\alpha_2-\frac{\eta}{b}\right)y'-\frac{\xi}{b}x+\psi_2\right]dx\,dy'.$$

When we do the integrations, the x-integration extending between the limits $-\gamma/2$ and $+\gamma/2$, and the y-integration between the limits $-\delta/2$ and $+\delta/2$, we find

$$C=(\varrho_1+\varrho_2)\gamma\delta+\varepsilon(\xi)+\left(\frac{\pi}{\lambda}\right)^2\left[\frac{1}{3}(\varrho_1\alpha_1+\varrho_2\alpha_2)\gamma\delta^3+\right.$$
$$\left.+2D\left(-\varrho_1\iint_{L_1}\psi_1\,dx\,dy'+\varrho_2\iint_{L_2}\psi_2\,dx\,dy'\right)\right]\frac{\eta}{b}-$$
$$-\left(\frac{\pi}{\lambda}\right)^2(\varrho_1+\varrho_2)\gamma\delta\left(\frac{1}{2}D^2+\frac{1}{6}\delta^2\right)\left(\frac{\eta}{b}\right)^2,$$
$$S=\frac{\pi}{\lambda}\left[2\left(\varrho_1\iint_{L_1}\psi_1\,dx\,dy'+\varrho_2\iint_{L_2}\psi_2\,dx\,dy'\right)+(\varrho_1-\varrho_2)D\gamma\delta\frac{\eta}{b}\right],$$

where $\varepsilon(\xi)$ contains terms independent of η and small with respect to the main term. Furthermore,

$$I = C^2 + S^2 = (\varrho_1 + \varrho_2)^2 (\gamma\delta)^2 + \varepsilon_1(\xi) +$$
$$+ \left(\frac{\pi}{\lambda}\right)^2 \gamma\delta \left[\frac{2}{3}(\varrho_1 + \varrho_2)(\varrho_1\alpha_1 + \varrho_2\alpha_2)\gamma\delta^3 + 8\varrho_1\varrho_2 D\left(-\iint\limits_{L_1} \psi_1\, dx\, dy' + \right.\right.$$
$$\left.\left. + \iint\limits_{L_2} \psi_2\, dx\, dy'\right)\right]\frac{\eta}{b} - \left(\frac{\pi}{\lambda}\right)^2 (\gamma\delta)^2 \left[4\varrho_1\varrho_2 D^2 + \frac{1}{3}(\varrho_1 + \varrho_2)^2 \delta^2\right]\left(\frac{\eta}{b}\right)^2 + \cdots$$

where $\varepsilon_1(\xi)$ again contains the small terms independent of η. /38

In order to learn the value of η at which I attains its maximum, we write $dI/d\eta = 0$. If we expand and solve this equation, we obtain

$$\frac{\eta}{b} = \frac{\frac{1}{3}(\varrho_1 + \varrho_2)(\varrho_1\alpha_1 + \varrho_2\alpha_2)\delta^2 + 4\varrho_1\varrho_2 \frac{D}{\gamma\delta}\left(-\iint\limits_{L_1} \psi_1\, dx\, dy' + \iint\limits_{L_2} \psi_2\, dx\, dy'\right)}{4\varrho_1\varrho_2 D^2 + \frac{1}{3}(\varrho_1 + \varrho_2)^2 \delta^2}.$$

This expression can be written in the form

$$\frac{\eta}{b} = \frac{\alpha_1 + \alpha_2 + \frac{\varrho_2 - \varrho_1}{\varrho_2 + \varrho_1}(\alpha_2 - \alpha_1)}{6\left(\frac{D}{\delta}\right)^2 \left[1 - \left(\frac{\varrho_2 - \varrho_1}{\varrho_2 + \varrho_1}\right)^2\right] + 2} + \frac{\bar{h}_2 - \bar{h}_1}{D\left[1 + \frac{\frac{1}{3}\left(\frac{\delta}{D}\right)^2}{1 - \left(\frac{\varrho_2 - \varrho_1}{\varrho_2 + \varrho_1}\right)^2}\right]}$$

by using the symbols

$$\bar{h}_1 = \frac{1}{\gamma\delta}\iint\limits_{L_1} \psi_1\, dx\, dy' = \frac{1}{\gamma\delta}\iint\limits_{L_1} h_1\, dx\, dy',$$
$$\bar{h}_2 = \frac{1}{\gamma\delta}\iint\limits_{L_2} \psi_2\, dx\, dy' = \frac{1}{\gamma\delta}\iint\limits_{L_2} h_2\, dx\, dy'. \qquad (21)$$

hence, $\bar{h}_1$ and $\bar{h}_2$ are the mean values of the deviations of the wave front in the regions L_1 and L_2 respectively.

Since, in reality, ρ_2 and ρ_1 are approximately of the same size, it is sufficiently precise to write

$$\frac{\eta}{b} = \frac{\eta'}{b} + \frac{\eta''}{b} + \frac{\eta'''}{b}, \qquad (22)$$

where

$$\frac{\eta'}{b} = \frac{\alpha_1 + \alpha_2}{6\left(\frac{D}{\delta}\right)^2 + 2}, \quad \frac{\eta''}{b} = \frac{\frac{\varrho_2 - \varrho_1}{\varrho_2 + \varrho_1}(\alpha_2 - \alpha_1)}{6\left(\frac{D}{\delta}\right)^2 + 2}, \quad \frac{\eta'''}{b} = \frac{\bar{h}_2 - \bar{h}_1}{D\left[1 + \frac{1}{3}\left(\frac{\delta}{D}\right)^2\right]}. \qquad (23)$$

To start with, consider the first term η'/b of the correction expression. In usable telescopes, $\alpha_1 + \alpha_2$ would not amount /39
to very many seconds even if the most unfavorable points on the wave front were selected and D were chosen accordingly. Since, for the most part, the wave front has a relatively simple shape (very often, the residual spherical aberration is the most important constituent of the deviations), $\alpha_1 + \alpha_2$ can reach the greatest possible value only when D is relatively large. In that case, however, D/δ is also large, because one is trying to make δ as small as possible, and η'/b is therefore small because of the large denominator $6(D/\delta)^2 + 2$. If, for example, $D/\delta = 4$, $\eta'/b = (\alpha_1 + \alpha_2)/98$. Making D/δ smaller does make the denominator in the expression for η'/b smaller as well, but in general it also makes $\alpha_1 + \alpha_2$ smaller. One of the smallest values coming into consideration is $D/\delta = 2$, so that $\eta'/b = (\alpha_1 + \alpha_2)/26$. If e.g. $\alpha_1 + \alpha_2 = 1"$, then $\eta'/b = 0.04"$.

This implies that the influence of the correction η' in ordinary cases is very insignificant. It can become appreciable only if the deviations of the wave front are very large. In such a case, however, there is generally no reason to measure the errors with such great absolute precision as when studying good objectives. Nevertheless, there is one case in which it may be desirable to determine large deviations with great absolute precision, namely when a parabolic mirror with a short focal length is being studied with the aid of an artificial star placed at the center of curvature. Even in this case, however, the correction η' is not taken into account. For one thing, the deviations increase relatively slowly from the center toward the edge, since a regular spherical aberration is involved. Second, it is easy to provide the artifical star with such a luminous intensity that the slits can be made very narrow, without impairing the accuracy of the observations, and this makes D/δ /40
sufficiently large. In general, the observations can be arranged so that in practice, $\eta' = 0$.

Now consider the term η''/b. In objectives, ρ_1 and ρ_2 are somewhat different, since the middle of an objective is thicker than its edges. For such a large objective as that of the Lick Observatory, this difference is only 15 mm, and the corresponding absorption of the glass is at most 6%, even for light with chemical effects (cf. the absorption table for optical glasses in [10]). Recalling that the distance between the sets in practice is only a fraction of half the aperture of the objective, it is easy to see that the influence of changes in absorption is very small. In reflecting telescopes, ρ_1 and ρ_2 can be different only when there are spots on the reflector due to faulty silver-coating. For example, assume that $\rho_2:\rho_1 = 105:95$, i.e. that $(\rho_2-\rho_1)/(\rho_2+\rho_1) = 1/20$, and $D/\delta = 2$. Then $\eta''/b = (\alpha_2 - \alpha_1)/520$. Without further arguments, it can be said that η'' is vanishingly small in practice.

Likewise, it is usually safe to write $\eta''' = 0$. Approximately,

$$\frac{\eta'''}{b} = \frac{\bar{h}_2 - \bar{h}_1}{D}. \qquad (24)$$

Comparing this formula with (3), we can make the following statement: by the two-hole method, the mean value of the deviations of the parts of the wave front corresponding to the holes can be determined.

As previously stated, this mean value can be replaced by the deviation in the middle of the hole. At any rate, the calculations can be carried out in first approximation under this assumption, and the accuracy subsequently improved if it should prove necessary. Enhancing the accuracy comes into consideration in the determination of zonal aberrations when the slits are made relatively long in order to achieve sufficient light intensity, and when there is a depression or elevation in the center of the wave front in a small area. /41

In the above discussion, it was assumed that the holes are congruent rectangles. If the holes are of different size and irregular at the edges, so that they deviate to some extent from the rectangular shape, this has the same effect, in first approximation, as a different $\rho_1 : \rho_2$ ratio, and therefore does not induce any appreciable change in the value of η. Moreover, a hypothetical influence due to holes of different sizes can be eliminated by rotating the screen by 180°.

It should be kept in mind that the above theory was not formulated for completeness, since the higher-order terms were thrown out in deriving the formulas, and since only the position of the maximum line is calculated, without studying the distribution of light even in its vicinity. For instance, it is conceivable that when the light is not distributed symmetrically on both sides of the maximum line, the alignment also is not precisely on the maximum line, but systematically somewhat to the side of it. Of course, this error cannot be calculated theoretically, and therefore we have contented ourselves with the above simple theory. After all, its purpose was not to derive formulas by which the errors could be corrected, but to estimate the order of magnitude of the errors and then to show that the errors are vanishingly small in practice. This is particularly true for the corrections η' and η''. As for the correction η''', the form in which it was previously expressed in words appears so natural that it could have actually been guessed even without calculations. /42

A study similar to the one just conducted for the two-hole method could of course be performed for the other methods as well,

and the results would doubtlessly be similar. However, we do not consider it worthwhile deriving the corresponding formulas, especially since the calculations become more complicated when more holes are included. We observe only that the result obtained for the two-hole method -- i.e. that the mean value for the deviations of the points of the wave front for each hole are determined by the observations -- is easily seen to be valid for all methods.

III. Applications /43

11. In order to illustrate the practical application of the method which I have described for studying objectives, I will now give a report on the examination of three telescopes of the Helsinki Observatory and a parabolic mirror which I ground. At the same time, I will make some observations of a general nature on the organization of the observations in different cases, on error sources, on precision, etc.

The particular instruments of the Observatory are the portable transit, the old Utzschneider-Fraunhofer refractor, and the large transit. In investigating the optics of these instruments, I employed the two-slit and three-hole methods, since these are generally the best to use when the instrument is stable and is equipped with an ocular micrometer. It would also have been interesting to examine the largest instrument in the Observatory, the astrograph, but there was no suitable opportunity to do so, because it was tied up by photographic projects.

As an illustration of an application of the three-slit method, I will describe only observations made at home while I was grinding a parabolic mirror 17.5 cm in diameter. I have checked the applicability of the four-hole method only for small objectives, but did attain quite satisfactory results. In this /44 treatise, I will content myself with just this remark.

At the conclusion of this Chapter, I will make some remarks on Michelson's method and I will mention some modifications in my methods.

Application of the Two-Slit Method to the Small Transit

12. The portable transit (Repsoldt, 1886) has a bent telescope, so that the images are affected both by the errors of the objective and those of the prism. The objective aperture is 7 cm and the focal length 75 cm. The instrument is equipped with a very good ocular micrometer which can be turned through 90°. It can therefore be viewed as a typical example of a small instrument usable for precise measurements.

In studying the objective, it is generally better to use an artificial star instead of a real one as the light source. Among the advantages of the former are: an artificial star can easily be made bright enough so that observations can be made without difficulty even when the slits in the screen are very small. Of course, observations can also be made when the sky is cloudy, and they will be more precise than when real stars are utilized, assuming that the artificial star is not too far away. The observations and calculations are simpler when an

artificial star is used, because the star does not move. The light from an artificial star can also be made monochromatic, and this will certainly yield more accurate measurements than when nonmonochromatic light is employed. Moreover, the chromatic aberration can be determined precisely by varying the wavelength.

I attached the artificial star to a stone pillar which was about 50 m to the east of the transit and carried a sighting mark. In place of the mark, I made a straight slit a few tenths of a millimeter wide, which could be turned into the vertical or horizontal directions as desired. Behind the slit, I placed a 50-candlepower frosted electric lamp, when I employed a linear light source, and a bright 50-candlepower, so-called 1/2-watt lamp when I required a point light source. I placed the filament of the latter lamp at right angles to the slit. In both methods, the interference lines were clearly visible, although the slits in the screens were only 2 mm wide and 6 mm long. /45

The screens I produced as follows (Fig. 8).

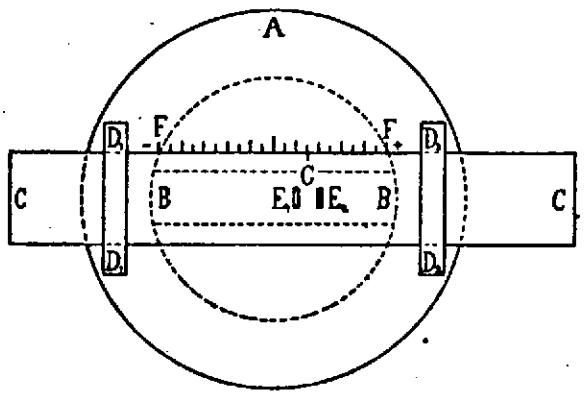

Fig. 8.

A round cardboard disk A was fastened in front of the objective. In the disk was a hole BB, the length of which was equal to the diameter of the objective. A sheet CC, made of heavy drawing paper, and containing the slits E_1 and E_2 could be moved back and forth beneath the paper strips D_1D_1 and D_2D_2. Thus, CC formed a movable screen. The position of the slits relative to the center of the objective was read off the scale FF with the aid of the index mark G. The scale had 20 divisions numbered from -10 to +10. The spacing between two successive lines was 3.3 mm. /46

Since, in the center of the hypotenuse surface of the prism, there was a depression for field illumination, the observations had to be organized so that the slit never fell in the center of the objective. In Fig. 9, the points lying on the diameter of the objective for which the deviations of the wave front were determined are marked. The extreme points (-10, +10) were 33 mm from the center of the objective or 2 mm from its edge.

Fig. 9.

The distance between two successive points was 1^p = 3.3 mm. By using a screen in which the separation of the slits was D_4 = = 4^p = 13.2 mm, the deviations of the wave front were determined at the points -6, -2, +2, and +6, the deviations at the points -10 and +10 being assumed to be zero. Based on these observed deviations, the deviations of the intervening points -8, -4, +4, and +8 were found using a screen with $D_2 = 2^p$ = 6.6 mm. Finally, the deviations at -9, -7, -5, -3, +3, +5, +7, and +9 were found with a screen with $D_1 = 1^p$ = 3.3 mm. In the latter screen, the slits were about 1.7 mm wide. With the aid of screen D_4, therefore, the first-order points were determined, followed by the second-order and third-order points using the other screens and the results with the first one.

Assume that the horizontal diameter was the one to be investigated. The movable hairline of the micrometer was set vertically, and the linear slit of the light source was made precisely vertical, as well as the slits in the screen. The /47
positive reading of the scale FF was set on the side of the optical axis toward which the reading of the micrometer increased. The observations were carried out in the following order. The screen D_4 was first placed so that the slits arrived at the points -10 and -6. The index mark G was then opposite the -8 line on the scale. For the sake of brevity, we will say that the position of the screen was -8. The central interference band was aligned twice with the movable hairline. Next, the observations were made in the positions -4, 0, +4, and +8, and then the observations were repeated in the reverse sequence. The observations were continued with the other screens in the same fashion, i.e. in positions -9, -7, -5, -3, +3, +5, +7, and +9 and back again with screen D_2, and in positions -9.5, -8.5, ..., -2.5, + 2.5, ..., +9.5 and back again with screen D_1. Finally, a second series of observations was made with screen D_4. The magnification of the telescope was 120 for all observations. In observing the sighting mark, the value of one screw revolution was 55.60".

13. In Tables I-IV, I present the observations I made on the evening of March 3, 1921 to determine the errors along the horizontal diameter of the objective, the artificial star being situated at the center of the field of vision.

TABLE I.

$D_1 = 4^P = 13.2$ mm

y	u'	u''	u'''	u''''	u
−8	$17^R.156$	$17^R.161$	$17^R.155$	$17^R.159$	$17^R.158$
- 4	230	230	231	221	228
0	200	196	200	199	199
+4	184	188	188	180	185
+8	220	224	222	223	222

TABLE II.

/48

$D_1 = 2^P = 6.6$ mm

y	u'	u''	u'''	u''''	u
−9	$17^R.093$	$17^R.100$	$17^R.102$	$17^R.094$	$17^R.097$
−7	184	170	178	170	176
−5	219	211	229	215	218
−3	205	195	201	203	201
+3	182	170	168	179	175
+5	170	178	164	180	173
+7	226	221	204	210	215
+9	236	232	230	228	232

TABLE III.

$D_1 = 1^P = 3.3$ mm

y	u'	u''	u'''	u''''	u
−9.5	$17^R.069$	$17^R.069$	$17^R.065$	$17^R.060$	$17^R.066$
−8.5	114	144	112	121	123
−7.5	168	155	154	144	155
−6.5	180	181	169	196	182
−5.5	200	202	197	205	201
−4.5	235	235	242	228	235
−3.5	230	236	212	225	226
−2.5	194	178	191	165	182
+2.5	170	166	158	158	163
+3.5	185	200	192	189	192
+4.5	164	174	164	170	168
+5.5	166	160	162	174	166
+6.5	200	215	195	195	201
+7.5	224	209	219	223	219
+8.5	230	225	230	229	228
+9.5	232	248	250	255	246

TABLE IV. /49

$D_4 = 4^P = 13.2$ mm

y	u'	u"	u"'	u""	u
−8	$17^R.150$	$17^R.151$	$17^R.140$	$17^R.147$	$17^R.147$
−4	216	217	216	222	218
0	199	199	199	199	199
+4	176	180	185	185	182
+8	225	227	229	225	226

The position y of the screen is indicated in the first column. u' and u" are the alignments when the screen is shifted in the positive direction, and u"' and u"" are the corresponding alignments when the screen is shifted in the negative direction. The last column contains the mean value u of the different readings.

On two evenings, March 3 and 9, 1921, I made a total of 16 series of observations of the above type with screen D_4, some to investigate the horizontal diameter and some to investigate the vertical one. Sometimes the artificial star was at the center of the field of vision, and sometimes to one side. From all these observations, I calculated the mean error ε of an alignment in a different way. For simplicity's sake, I computed it with the aid of the average error. The mean error of the differences u' − u" and u"' − u"" is $\varepsilon\sqrt{2}$. From this material, I obtained $\varepsilon = \pm 0^R.00222 = \pm 0.123"$. From the differences $(u' + u")/2 - (u"' + u"")/2$, one finds $\varepsilon = \pm 0^R.00309 = \pm 0.172"$, i.e. a significantly larger value which can be explained by possible changes in the instrument, in exact adjustment of the screen, etc. It is interesting that from the differences u' − u"' one obtains $\varepsilon = \pm 0^R.00325 = \pm 0.181"$ and from the differences u" = u"" a significantly smaller value, namely ε = /50
$= \pm 0^R.00259 = \pm 0.144"$. One possible source of this difference might be a small change produced in the instrument when the screen is shifted, a difference which is gradually neutralized and therefore acts principally on the early alignments. For simplicity, we give all alignments the same weight and therefore consider the mean value $(u' + u" + u"' + u"")/2$ as the final value. By the second mode of calculation, its mean error is found to be $\varepsilon_u = \varepsilon/2 = \pm 0^R.00154 = \pm 0.086"$ or in linear units ±0.31 μm; the screw rotation is 0.2 mm.

In eight series of observations conducted with screen D_2, I obtained as the mean error of an alignment $\varepsilon = \pm 0^R.00452 =$ $= \pm 0.251"$ from the differences u' − u" and u"' − u""; $\varepsilon =$ $= \pm 0.00528 = \pm 0.294"$ from the differences $(u' + u")/2 - (u"' + u"")/2$.

With the aid of the latter value of ε, the mean error of the mean value is found to be $\varepsilon_u = \pm 0^R.00264 = \pm 0.147"$. From the two series carried out with screen D_1, I obtained through the two modes of calculation described above $\varepsilon = \pm 0^R.0082 = \pm 0.46"$ or $\varepsilon = \pm 0^R.0107 = \pm 0.59"$ as the mean error of an alignment, and from the latter value $\varepsilon_u = \pm 0^R.0054 = \pm 0.30"$.

These figures show that the actual alignment error is inversely proportional to the spacing D between the slits, as would have been anticipated. Namely, 0.123":0.251":0.46" = 1/4: :1/2:1/1, approximately. In the mean errors ε_u as well, the same law holds for the observations made with screens D_2 and D_1, but the ε_u corresponding to screen D_4 is already relatively somewhat larger. This too is expected, since the motions of the instruments and other errors independent of the distance between the slits have relatively greater effects on the observations carried out with screen D_4 than on the other observations.

In his method of extrafocal images, Hartmann [11] assumed /51 that the mean error in measuring the distance between two images was about $\varepsilon = 0.008$ mm if the images were reasonably good, and perhaps $\varepsilon = 0.003$ mm if they were very good. The first value agrees with the results of Lehmann [12]. In order to obtain the alignment accuracy of an image, the figures must be divided by $\sqrt{2}$. If these figures are compared with the mean errors I have given, it can be seen that the precision obtained with the two-slit method is many times greater than that achieved by the Hartmann method. It should also be observed that Hartmann, in his studies of objectives with an artificial star, used monochromatic light, while I employed just the nonmonochromatic light delivered by an ordinary electrical bulb. For this reason, when the screen was shifted to one side, the distribution of the colors was not quite symmetric with respect to the central interference band because of the secondary spectrum. If monochromatic light had been used, the accuracy would certainly have been even greater.

14. The deviations of the wave front were calculated with the aid of formula (3). If, in this formula, we set $\cos\omega = 1$, we then obtain

$$h_2 - h_1 = D\eta/b$$

Now $\eta/b = \rho(u - \bar{u})$, where ρ is the value in radians corresponding to one screw revolution and $\bar{u}$ is a micrometer reading to be determined later. Hence, from the measurements taken with the screen D_4, we obtain the equations

$$
\begin{aligned}
h_{-8} - h_{-10} &= D_4\,\varrho\,(u_{-8} - \bar{u}),\\
h_{-4} - h_{-8} &= D_4\,\varrho\,(u_{-4} - \bar{u}),\\
h_{0} - h_{-4} &= D_4\,\varrho\,(u_{0} - \bar{u}),\\
h_{4} - h_{0} &= D_4\,\varrho\,(u_{4} - \bar{u}),\\
h_{10} - h_{8} &= D_4\,\varrho\,(u_{8} - \bar{u}).
\end{aligned}
\qquad (25)
$$

We set $h_{-10} = h_{10} = 0$; we then obtain from the above equations /52

$$
\bar{u} = \frac{1}{5}(u_{-8} + u_{-4} + u_0 + u_4 + u_8). \qquad (26)
$$

The calculation for the first series of observations is reproduced in Table V. h' is the deviation obtained from the first series, and h" that from the second series, while h is the mean value of the two.

TABLE V.

$D_4 = 4^p = 13.2$ mm; $D_4\varrho = 3.56 \cdot 10^{-3}$

y	u	$10^3(u-\bar{u})$	$D_4\varrho(u-\bar{u})$	h'	h''	h
			nm	nm	nm	nm
−10				0	0	0
−6	$17^R.158$	−40.4	−144	−144	−169	−156
−2	228	+29.6	+105	−39	−85	−62
+2	199	+0.6	+2	−37	−69	−53
+6	185	−13.4	−48	−85	−113	−99
+10	222	+23.6	+84	−1	0	0

$\bar{u} = 17^R.1984$

h' and h" differ sharply. The following calculation shows that the deviations are not due to observation errors. We calculate e.g. the mean error $\varepsilon_{h_{-2}}$ of the deviation h_{-2} obtained from a series of observations. For this purpose, we express h_{-2} explicitly in terms of the observed quantities u. Accordingly, /53 we employ the previously calculated value $\varepsilon_u = \pm 0^R.00154$ as the mean error of u. We find

$$
h_{-8} = \frac{1}{5} D_4\,\varrho\,(3u_{-8} + 3u_{-4} - 2u_0 - 2u_4 - 2u_8)
$$

and hence

$$
\varepsilon_{h_{-8}} = \frac{\sqrt{30}}{5} D_4\,\varrho\,\varepsilon_u = \pm 6.0 \quad \text{nm}
$$

Furthermore, $\varepsilon_{h_{+2}} = \varepsilon_{h_{-2}}$ and $\varepsilon_{h_{\pm 6}} = \sqrt{20} D_4 \rho \varepsilon_u / 5 = \pm 5.2$ nm. From the mean errors, it can be seen that the differences h' - h" are real. The explanation is that the first series of observations was taken as soon as the pavilion was opened, so that the temperature of the instrument was somewhat higher than that of the open air. The position of the movable plane changed as the temperature varied.

From observations which I made to investigate the vertical diameter of the objective with the screen D_4, I obtained

TABLE VI.

y	h'	h"	h
	nm	nm	nm
-10	0	0	0
-6	-233	-235	-234
-2	-270	-278	-274
+2	-300	-314	-307
+6	-273	-278	-276
+10	0	0	0

The differences h' - h" have the same sign here as in the observations on the horizontal diameter, but the magnitude of the differences is of the order of magnitude of the observation errors. It is also evident from the results that the curvature of the wave front in the vertical direction is quite different from that in the horizontal direction. We will return to this point later. /54

15. Exploiting the values obtained with the screen D_4, we now wish to determine the deviations of the wave front for the intervening points with the screens D_2 and D_1. Before we describe these calculations, we investigate the form of the wave front using only the observations made with screens D_2 and D_1. Since no uniform series of observations could be carried out with these screens because of the illuminating prism, no individual deviations h could be determined from these observations, but the mean values $h_y^0 = (h_{-y} + h_y)/2$ could be.

From the measurements undertaken with screen D_2, we obtain

$$
\begin{aligned}
h_{-8} - h_{-10} &= D_2 \varrho (u_{-9} - \bar{u}), \\
h_{-6} - h_{-8} &= D_2 \varrho (u_{-7} - \bar{u}), \\
&\text{— — — — — — — —}
\end{aligned}
\qquad (27)
$$

and from the latter

$$
\begin{aligned}
h_8^0 - h_{10}^0 &= \tfrac{1}{2} D_2 \varrho (u_{-9} - u_9), \\
h_6^0 - h_8^0 &= \tfrac{1}{2} D_2 \varrho (u_{-7} - u_7), \\
h_4^0 - h_6^0 &= \tfrac{1}{2} D_2 \varrho (u_{-5} - u_5), \\
h_2^0 - h_4^0 &= \tfrac{1}{2} D_2 \varrho (u_{-3} - u_3).
\end{aligned}
\qquad (28)
$$

If we write $h_{10}^0 = 0$, we can obtain h_8^0, h_6^0, h_4^0, and h_2^0 from these equations. As the mean error of h_2^0, we obtain $\varepsilon_{h_2^0} = \sqrt{2} D_2 \rho \varepsilon_u = \pm 6.7$ nm, assuming that $\varepsilon_u = \pm 0^R.00264$.

From the observations made with screen D_1, we obtain in the same way

$$
\begin{aligned}
h_9^0 - h_{10}^0 &= \tfrac{1}{2} D_1 \varrho (u_{-9\frac{1}{2}} - u_{9\frac{1}{2}}), \\
h_8^0 - h_9^0 &= \tfrac{1}{2} D_1 \varrho (u_{-8\frac{1}{2}} - u_{8\frac{1}{2}}), \\
&\text{— — — — — — — —} \\
h_2^0 - h_3^0 &= \tfrac{1}{2} D_1 \varrho (u_{-2\frac{1}{2}} - u_{2\frac{1}{2}})
\end{aligned}
\qquad (29)
$$

/55

and $\varepsilon_{h_2^0} = 2 D_1 \rho \varepsilon_u = \pm 9.6$ nm, assuming $\varepsilon_u = \pm 0^R.0054$. For purposes of comparison, it should be noted that $\varepsilon_{h_2^0} = \pm D_4 \rho \varepsilon_u = \pm 5.5$ nm is obtained from the observations made with screen D_4, assuming that $\varepsilon_u = \pm 0^R.00154$.

If we carry out the calculations for the observations with these formulas, we obtain the results collected in Table VII. They are recorded in the table in the same order as that in which the observations were made. The observations made with screen D_4 are also included.

TABLE VII.

h^0_y

	Horizontal Diameter				Vertical Diameter			
y	(D_4)	(D_2)	(D_1)	(D_3)	(D_4)	(D_2)	(D_1)	(D_3)
	nm	nm	nm	nm	nm	nm	nm	nm
10	0	0	0	0	0	0	0	0
9			−80				−106	
8		−120	−127			−170	−178	
7			−156				−225	
6	−114	−155	−164	−141	−253	−262	−262	−256
5			−148				−304	
4		−115	−119			−310	−321	
3			−104				−328	
2	−38	−92	−96	−77	−285	−298	−314	−296

Hence, there appears to be a small systematic difference between the results obtained with the different screens in the measurements of the two diameters. It is not hard to see /56 that the errors due to the finiteness of the slits are vanishingly small. The cause of the systematic differences is probably an effect of the secondary spectrum. Namely, the central interference band is not symmetric with respect to the colors, except when the slits are symmetric with respect to the center of the objective. The asymmetry increases linearly as the screen is moved toward the edge. Since changing the screen modifies the thickness and separation of the interference bands, it is probable that systematic alignment errors, which grow roughly linearly with y, are produced when different screens are employed. Upon reflection, we can see that the effects of such systematic errors would be the same as those produced by shifting the movable plane. Hence, they will have no great influence on the form of the zonal aberrations.

We will now show how the observations made with screens D_2 and D_1 are used to determine new points between the points -10, -6, ... found with screen D_4. From the observations made with screen D_2, we easily obtain

$$\begin{aligned} h_{-8} &= \tfrac{1}{2}(h_{-10} + h_{-6}) + \tfrac{1}{2} D_2 \varrho (u_{-9} - u_{-7}), \\ h_{-4} &= \tfrac{1}{2}(h_{-6} + h_{-2}) + \tfrac{1}{2} D_2 \varrho (u_{-5} - u_{-3}), \\ &\text{— — — — — — — — — — — —.} \end{aligned} \qquad (30)$$

The mean error in the deviations h_{-8}, h_{-4}, ... resulting from the observations with the screen D_2 is $(\sqrt{2}/2)D_2\rho\varepsilon_u = \pm 3.3$ nm, if $\varepsilon_u = \pm 0^R.00264$.

With screen D_1, we obtain in the same way

$$\begin{aligned} h_{-9} &= \tfrac{1}{2}(h_{-10} + h_{-8}) + \tfrac{1}{2} D_1 \varrho (u_{-9\frac{1}{2}} - u_{-8\frac{1}{2}}), \\ h_{-7} &= \tfrac{1}{2}(h_{-8} + h_{-6}) + \tfrac{1}{2} D_1 \varrho (u_{-7\frac{1}{2}} - u_{-6\frac{1}{2}}), \\ &\text{— — — — — — — — — — — —}. \end{aligned} \qquad (31)$$

The mean error for the deviations h_{-9}, h_{-7}, ... resulting from the observations with screen D_1 is $(\sqrt{2}/2)D_1\rho\varepsilon_u = \pm 3.4$ nm, if $\varepsilon_u = \pm 0^R.0054$. /57

As we have just seen, there is a systematic difference between the observations made with different screens. We now investigate the magnitude of the errors which would result if we employed the formulas derived above without reducing the observations made with screens D_2 and D_1 to the same system as the observations made with screen D_4. When the horizontal diameter is studied, the difference between the values h_2^0 found with screens D_4 and D_2 is equal to -34 nm. For simplicity, we assume that this difference corresponds to the center of the objective. This difference is produced when the entire diameter, i.e. 20^p, is measured independently with both screens. If, by means of the screen D_2, new points are determined half way between the points found with the screen D_4, only a fifth of the diameter, i.e. 4^p, is taken into account. The systematic correction is then, as is easily seen, -34/25 nm = -1.4 nm, and this can be neglected. In observations on the vertical diameter, the systematic difference is much smaller. Finally, when determining new points using the screen D_1, only 1/10 of the entire diameter is taken into account, so that the systematic correction to be applied to the new points would be only 1/100 of the systematic difference which would be produced near the center of the objective if the entire diameter was investigated independently with screens D_4 and D_1. By neglecting the small systematic corrections, we obtain the deviations in Table VIII from formulas (30) and (31).

We have already emphasized the great differences between the deviations on the horizontal diameter and those on the vertical diameter. Therefore, the objective-prism system is highly astigmatic. The above observations are not, however, well suited for a precise determination of the magnitude of the astigmatism, since the time during which the observations along

TABLE VIII. /58

	Horizontal Diameter			Vertical Diameter		
y	h_{-y}	h_{+y}	h_y^0	h_{-y}	h_{+y}	h_0
	nm	nm	nm	nm	nm	nm
10	0	0	0	0	0	0
9	−99	−40	−70	−83	−118	−100
8	−148	−64	−106	−153	−181	−167
7	−163	−89	−126	−199	−234	−216
6	−156	−99	−128	−234	−276	−255
5	−141	−85	−113	−269	−317	−293
4	−94	−74	−84	−288	−319	−304
3	−58	−76	−67	−290	−325	−308
2	−62	−53	−58	−274	−307	−290

the horizontal and vertical diameters were made was about an hour, so that a change in temperature could have had an appreciable effect on the curvature of the wave front. Therefore, I determined the astigmatism later by means of special observations. Another feature attracting attention is the asymmetry in the deviations of the wave front relative to the center of the objective, an aberration known by the name of coma. This aberration will also be treated in more detail later.

16. We now consider the actual zonal aberrations. The deviations of the wave front calculated so far depend on the position of the movable plane. They can be made invariant under /59 displacements of the movable plane by determining the reference sphere in such a fashion that the corresponding deviations will also be zero at a third point. If possible, the center of the objective is chosen as this point. Since, with the present objective, the center is out of the question, the reference sphere is determined so that $h_2^0 = (h_{-2} + h_2)/2 = 0$.

Let the distance from the movable plane to the second principal plane of the objective during the measurements be b. If the center of the reference sphere lies in the movable plane, let the deviation from the reference sphere of the point y on the meridian section of the wave front be h. We now shift the center of the reference sphere outward from the objective by a distance Δb. If we assume that the point of the reference sphere on the optical axis remains unchanged, it is easy to

deduce that the deviation h increases roughly by $-y^2\Delta b/2b^2$ because of the displacement of the center of the reference sphere. The deviation of the point y on the outermost zone of the objective increases by $-y_0^2\Delta b/2b^2$. Since the specified deviation will continue to be equal to zero, we add $y_0^2\Delta b/2b^2$ to all the deviations, and thus obtain the following formula for the change in the deviation at point y.

$$\Delta h = \frac{\Delta b}{2b^2}(y_0^2 - y^2). \qquad (32)$$

From the observations along the horizontal diameter, we obtained $h_2^0 = -58$ nm. To make this deviation zero and to keep h_{10}^0 equal to zero, the term

$$+58\,\frac{10^2 - y^2}{10^2 - 2^2} = +0.604\,(100 - y^2)$$

/60

is to be subtracted from the deviations. Likewise,

$$+290\,\frac{10^2 - y^2}{10^2 - 2^2} = +3.020\,(100 - y^2).$$

is to be subtracted from the deviations for the vertical diameter. These reductions are applied to the deviations $h_y^0 = (h_{-y} + h_y)/2$. The resulting sums, which we designate z_y, are the actual zonal aberrations.

Table IX shows the zonal aberrations calculated from the values for h_y^0 in the preceding table in columns (D_4, D_2, D_1). Of these, only the measurements made with screen D_4 were involved in the determination of z_6.

The observations made with screens D_2 and D_1 can also be employed independently for determining zonal aberrations. For this purpose, we need only to apply the reductions to the values /61 in columns (D_2) and (D_1) in Table VII. The resulting zonal aberrations are found in columns (D_2) and (D_1) in Table IX.

The zonal aberration z_6 was determined independently with all three screens. We calculate its mean error in each of the three cases. For this task, we express z_6 explicitly in terms of the observed quantity u. For example, for D_4, we find

TABLE IX.

z_y

	Horizontal Diameter			Vertical Diameter		
y	$(D_4D_2D_1)$	(D_2)	(D_1)	$(D_4D_2D_1)$	(D_2)	(D_1)
	nm	nm	nm	nm	nm	nm
10	0	0	0	0	0	0
9	−59		−61	−43		−44
8	−84	−86	−91	−58	−58	−60
7	−95		−105	−62		−58
6	−89	−94	−100	−62	−63	−53
5	−68		−73	−67		−59
4	−33	−34	−35	−50	−49	−46
3	−12		−13	−33		−30
2	0	0	0	0	0	0

$$z_6 = \frac{1}{6} D_4 \varrho \, (u_{-6} - 2u_{-4} + 2u_4 - u_6).$$

The mean error of z_6 is consequently

$$\varepsilon_{z_6} = \frac{\sqrt{10}}{6} D_4 \varrho \varepsilon_u = \pm 2.9 \text{ nm}.$$

Likewise, in case D_2, we obtain

$$\varepsilon_{z_6} = \frac{\sqrt{5}}{3} D_2 \varrho \varepsilon_u = \pm 3.5 \text{ nm}$$

and in the case D_1

$$\varepsilon_{z_6} = \frac{\sqrt{10}}{3} D_1 \varrho \varepsilon_u = \pm 5.1 \text{ nm}$$

In each of the cases, the values of ε_u mentioned on pp. 33-34 were used.

If we compare the values obtained for the zonal aberrations with different screens, we notice that the deviations can be explained by random observation errors. We take the values in column $(D_4D_2D_1)$ as the final values.

There is an appreciable difference between the zonal aberrations obtained from measurements along the horizontal and vertical diameters. It seems very likely that this difference, like the marked astigmatism, is due to the prism and not to the objective. In order to clarify this situation, on March 9, 1921 I determined the deviations along the horizontal and vertical diameters using screens D_4 and D_2, after first screwing out the objective by 90°. Then I made new observations, after having screwed the objective back in. Table X contains the zonal aberrations obtained from these measurements. /62

TABLE X.

z_y

	Objective 90°		Objective 0°	
y	Horiz.	Vertic.	Horiz.	Vertic.
	nm	nm	nm	nm
10	0	0	0	0
8	−80	−67	−90	−55
6	−75	−67	−85	−57
4	−26	−54	−27	−48
2	0	0	0	0

From the table, it is evident that the difference between the zonal aberrations obtained from observations along the horizontal and vertical diameters are primarily due to the prism. Nevertheless, there appears to be a certain difference attributable to the objective.

We can express the magnitude of the astigmatism by the formula

$$a = h_2^0(\text{horiz.}) - h_2^0(\text{vertic.}).$$

I obtained the following values for this expression.

TABLE XI. /63

	Objective 90°		Objective 0°	
	Horiz.	Vertic.	Horiz.	Vertic.
	nm	nm	nm	nm
h_2^0	+114	−55	−106	−290
a	+169		+184	

Within the limits of observational errors, therefore, the astigmatism did not change when the objective was screwed out. Hence, the primary cause of the astigmatism must be sought in the prism.

On April 7, I again determined the astigmatism, using screen D_4. From two measurements on the vertical and horizontal diameters, I obtained a = +194 nm. We calculate the displacement of the movable plane corresponding to this value. We substitute $y_0 = 10^p$, $y = 2^p$, $b = 230^p$ (= 761 mm) in formula (32). We find $\Delta b = 1103$ $\Delta h = +0.207$ mm. According to the observations on the horizontal diameter, the movable plane therefore lies 0.207 mm closer to the objective than indicated by observations along the vertical diameter.

17. We now consider the asymmetry of the wave front. At a distance y from the center, its magnitude is determined by the expression $c_y = (h_y - h_{-y})/2$, which we call the coma. From the following measurements along the horizontal diameter taken on March 9, it can be seen that the coma depends on the position of the star in the field of vision. The position of the star is indicated by the micrometer readings u given at the top of the table.

TABLE XII. /64

y	$u = 5^R.1$		$u = 16^R.9$		$u = 30^R.6$	
	h_y	c_y	h_y	c_y	h_y	c_y
	nm	nm	nm	nm	nm	nm
−10	0		0		0	
−8	−206		−170		−80	
−6	−264		−185		−107	
−4	−199		−125		−75	
−2	−129		−111		−77	
+2	—	—	−102	+4	−110	−16
+4	−114	+42	−114	+6	−135	−30
+6	−84	+90	−128	+28	−184	−38
+8	−50	+78	−90	+40	−141	−30
+10	0	0	0	0	0	0

We wish to express the magnitude of the asymmetry of the wave front by a single number, so that, among the numbers c_y, we choose the central one, i.e. c_6. The following table contains

the values c_6 which I found from my observations with screen D_4 on March 16 for the horizontal diameter and on March 21 for the vertical one.

TABLE XIII.

	Horizontal Direction						Vertical Direction					
Micr. Reading u .	2.8	11.5	17.4	24.3	31.3	34.4	2.7	8.1	16.8	25.5	32.6	
Obs., c_6 . . .	+100	+60	+26	−6	−36	−53	+2	−6	−26	−53	−65	
Calc. c_6 .	+100	+58	+30	−4	−38	−53	+5	−8	−29	−49	−66	
Obs.-Calc..	0	+2	−4	−2	+2	0	−3	+2	+3	−4	+1	

The following linear formulas represent the observed c_6 very well. ε_{c_6} is the mean error of an observation calculated calculated from the remaining errors.

Horizontal direction $c_6 = 114 - 4.85\ u$, $\varepsilon_{c_6} = \pm 2.6$ nm. /65

Vertical direction $c_6 = 11 - 2.36\ u$, $\varepsilon_{c_6} = \pm 3.6$ nm.

On the other hand, we obtain $\varepsilon_{c_6} = (\sqrt{30}/10) D_4 \rho \varepsilon_u = 0.00195 \varepsilon_u$. If, in this equation, we substitute the mean value of the mean errors given above, i.e. $\varepsilon_{c_6} = \pm 3.1$ nm, we obtain $\varepsilon_u = \pm 0^R.00159$, i.e. roughly the same value as found on p. 33. I should also remark that in the coma observations, I made only two alignments instead of four at each position of the screen.

From the above formulas, we find that the position at which the coma is equal to zero is not in the center of the field of vision. According to the formula for the horizontal direction, $c_6 = 0$ when $u = 23^R.5$, and according to the formula for the vertical direction, when $u = 4^R.7$. On the other hand, the center of the crosshairs is roughly 18^R. These numbers mean that the optical system is poorly centered. The fact that there is any coma at all in this optical system, a coma changing linearly with u, shows that the sine condition is not satisfied in the objective-prism system. The only peculiar feature is that the coefficient of u in the formulas for the coma obtained from observations along the horizontal and vertical diameters is quite different. Effects in the prism must be responsible for this effect. I did not investigate this behavior any further.

In early 1922, I removed the prism and examined its faces with the aid of Newton's rings. I employed a glass slide, having

previously determined the deviations of its surfaces from the plane. According to my observations, the hypotenuse face of the prism is a convex spherical surface with a radius of 1.66 km. This explains the high astigmatism of the optical system. Namely, this curvature on the hypotenuse face corresponds to an astigmatism of a = +153 nm according to my calculations, i.e. /66 roughly the same as that which I found on p. 43 by the two-slit method.

As mentioned earlier, the light source in my observations was an ordinary electrical bulb. The effective wavelength λ of the light can be determined by measuring the spacing of the interference strips. Let $u_2 - u_1$ be the distance between two successive interference bands, expressed in terms of screw revolutions. Then $\lambda = D\rho(u_2 - u_1)$. With screen D_4, I obtained by measuring the separation of the bands -- first with the central band -- λ = 569 nm, with screen D_2, λ = 555 nm, and with a grating in which the separation of the slits was 1^p, λ = 577 nm.

Application of the Three-Hole Method to the Small Transit

I used the three-hole method only for investigating astigmatism. In the screen (Fig. 10), there were 12 round holes 0, 30, 60, ... roughly 4 mm in diameter spaced around a circle of radius 30 mm with its center at the center P of the objective. /67 Outside the circle, there was a concentric circle of similar holes 15, 45, 75, ..., which formed equilateral triangles with the first set of points, as can be seen from the diagram. The sides are 15.54 mm long. The hole 0 was arranged so that it was directly above the center of the objective. A second disk, which could be rotated about the point P, was placed on the screen. There was a triangular aperture in this disk, so that when the disk was in the appropriate position, light could pass only through the holes 0, 15, 30 or 30, 45, 60 etc.

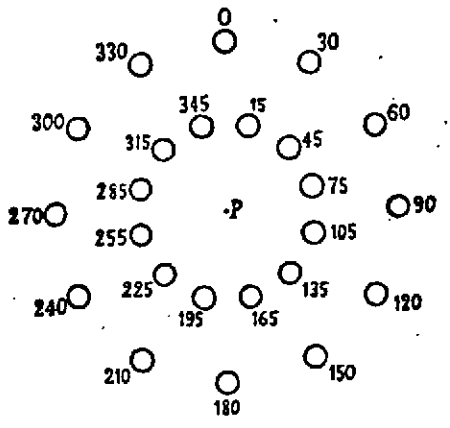

Fig. 10.

The observations were made as follows. A point-like artificial star was used. The ocular micrometer was first adjusted so that measurements could be taken in the vertical direction. The disk was rotated so that light passed through holes 0, 15, 30. The central point of the interference pattern

was aligned with the movable hairline. Let the micrometer reading be u'_{15}. The disk was then turned until holes 30, 45, 60 were simultaneously visible. A new alignment was carried out, the micrometer reading of which we designate u'_{45}. Continuing, an entire revolution is made in this way. Then, the observations are made all over again in the reverse direction, resulting in the readings u". The final reading is taken to be the mean value $u = (u' + u'')/2$.

Then, the ocular micrometer was turned through 90°, so that measurements could be taken in the horizontal direction. The observations were made as above. To distinguish them from the preceding ones, we now designate the micrometer readings v and employ the same indices as above.

In Table XIV, I reproduce the entire series of observations which I made on March 15, 1921 to determine astigmatic aberrations. /68 The position of the disk is designated by α.

TABLE XIV.

	Measurement in Vertical Direction			Measurement in Horizontal Direction		
α	u'	u''	u	v'	v''	v
15°	$16^R.860$	$16^R.866$	$16^R.863$	$17^R.022$	$17^R.023$	$17^R.022$
45	853	860	856	025	025	025
75	821	825	823	045	050	048
105	805	804	804	040	049	044
135	784	782	783	034	035	034
165	775	774	774	020	021	020
195	785	781	783	035	040	038
225	798	794	796	038	035	036
255	814	810	812	030	028	029
285	820	821	820	020	020	020
315	846	849	848	029	023	026
345	868	868	868	036	038	037
			$\bar{u} = 16\,819$			$\bar{v} = 17\,032$

On April 15, I made a similar series of observations. From these series, I obtained $\pm 0^R.0032 = \pm 0.18"$ as the mean error of an alignment by using the differences u' - u" and v' - v" and $\varepsilon = \pm 0^R.0023 = \pm 0.13"$ as the mean error of the means u and v,

or in linear units, ±0.46 nm. The alignment accuracy is therefore roughly the same as in the two-slit method using screen D_4.

19. We now show how the deviations h_0, h_{30}, h_{60}, ... of the wave front for the points 0, 30, 60, ... can be calculated from the observations. As the center of the reference sphere, we choose the point in the movable plane corresponding to the average micrometer readings $\bar{u}$ and $\bar{v}$. To designate the positions of the holes, we use an orthogonal coordinate system with the origin at the point P, with the x-axis upward, and with the y-axis to the right. Let the coordinates of the two holes in the screen be (x_1,y_1) and (x_2,y_2) and let the deviations of the wave front at these points be h_1 and h_2 respectively. Let D be the distance between the holes and, as before, let ρ be the value of a screw revolution in radians. If we imagine that we first proceed from the point (x_1,y_1) of the wave front in the direction of the x-axis along the light front to the point (x_2,y_1) and from here to the point (x_2,y_2) along the y-axis, we obtain by applying the basic formula of the two-slit method twice in succession: /69

$$h_2 - h_1 = \varrho\,(x_2 - x_1)\,(u - \bar{u}) + \varrho\,(y_2 - y_1)\,(v - \bar{v}). \qquad (33)$$

Applying this formula at points 0, 30, 60, ..., we obtain the formulas

$$\begin{aligned}
h_{30} - h_0 &= -D\varrho \sin 15^\circ\,(u_{15} - \bar{u}) + D\varrho \cos 15^\circ\,(v_{15} - \bar{v}),\\
h_{60} - h_{30} &= -D\varrho \sin 45^\circ\,(u_{45} - \bar{u}) + D\varrho \cos 45^\circ\,(v_{45} - \bar{v}),\\
&\cdots\cdots\cdots\cdots\cdots\cdots\cdots\cdots\cdots\cdots\\
h_{360} - h_{330} &= -D\varrho \sin 345^\circ\,(u_{345} - \bar{u}) + D\varrho \cos 345^\circ\,(v_{345} - \bar{v}),
\end{aligned} \qquad (34)$$

where

$$D\rho = 0.00419.$$

Because of the observation errors, it is only in exceptional cases that $h_{360} = h_0$. The correction for the terminal error $h_{360} - h_0$ is distributed uniformly over the deviations h of the intervening points, and the corrected deviations are designated by h'. The mean error of the differences $h_{30} - h_0$, $h_{60} - h_{30}$, ... is $D\rho\varepsilon$ and hence the mean terminal error is $\sqrt{12}D\rho\varepsilon = \pm 33$ nm, assuming that $\varepsilon = \pm 0^R.0023$.

The calculations for the above observations are shown in Table XV. In the table, $h_0 = 0$.

TABLE XV. /70

α		$10^3(u-\bar{u})$	$10^3(v-\bar{v})$	$-D_\varrho(u-\bar{u})\sin\alpha$	$D_\varrho(v-\bar{v})\cos\alpha$	$h_{\alpha+15}-h_{\alpha-15}$	h	$-\frac{\alpha}{360}(h_{360}-h_0)$	h'
				nm	nm	nm	nm	nm	nm
15°	0°	+44	−10	−48	−40	−88	0	0	0
45	30	+37	−7	−110	−21	−131	−88	+1	−87
75	60	+4	+16	−16	+17	+1	−219	+1	−218
105	90	−15	+12	+61	−13	+48	−218	+2	−216
135	120	−36	+2	+107	−6	+101	−170	+2	−168
165	150	−45	−12	+49	+49	+98	−69	+3	−66
195	180	−36	+6	−39	−24	−63	+29	+4	+33
225	210	−23	+4	−68	−12	−80	−34	+4	−30
255	240	−7	−3	−28	+3	−25	−114	+5	−109
285	270	+1	−12	+4	−13	−9	−139	+5	−134
315	300	+29	−6	+86	−18	+68	−148	+6	−142
345	330	+49	+5	+53	+20	+73	−80	+6	−74
	360						−7	+7	0

In my second series of observations, the terminal error was +4 nm.

To the deviations h', we can attach the linear correction term Ax + By + C, because this just shifts the center of the reference sphere in the movable plane to another position, and increases all deviations by the constant C. We can then choose that expression so that none of the points in question on the wave front acquire a preferred position. We content ourselves with supplementing the corrections h' by linear corrections so that the deviations at points 0 and 180 are zero, and the deviations at points 90 and 270 are equal. The new deviations we designate h^0. In Table XVI, this calculation is carried out /71 for observations which I took as examples. The table also includes results of a series of observations made 1 month later in normal form, and the mean value of the two series.

From the table, it can be seen that the maximum curvature of the wave front is located on the horizontal axis and the minimum curvature on the vertical axis. The astigmatism is

$$a=\frac{1}{2}(h_0^0+h_{180}^0)-\frac{1}{2}(h_{90}^0+h_{270}^0)=+187 \text{ nm}$$

TABLE XVI.

$h^0 - h' = -16.5(1-\cos\alpha) + 41\sin\alpha$			18/21	18/21	Mean	$-187\sin^2\alpha$	$h^0 + 187\sin^2\alpha$
α	h'	$h^0 - h'$	h^0	h^0	h^0		
	nm	nm	nm	nm	nm	nm	nm
0°	0	0	0	0	0	0	0
30	−87	+18	−69	−85	−77	−47	−30
60	−218	+27	−191	−191	−191	−140	−51
90	−216	+25	−191	−182	−187	−187	0
120	−168	+10	−158	−187	−172	−140	−32
150	−66	−11	−77	−86	−82	−47	−35
180	+33	−33	0	0	0	0	0
210	−30	−51	−81	−79	−80	−47	−33
240	−109	−60	−169	−174	−172	−140	−32
270	−134	−57	−191	−183	−187	−187	0
300	−142	−43	−185	−187	−186	−140	−46
330	−74	−22	−96	−110	−103	−47	−56
360	0	0	0	0	0	0	0

The mean error of the value of a obtained from the series of observations is $(\sqrt{3}/2)D\rho\varepsilon = \pm 8.4$ nm, if $\varepsilon = \pm 0^R.0023$. However, this astigmatism parameter cannot be compared directly with the value of a = +194 nm obtained on p. 44, since these points on the wave front do not lie exactly in the same zone. The astigmatism of +187 nm corresponds to the focal difference of +0.241 mm. /72

If the astigmatism were entirely due to the spherical shape of the hypotenuse face of the prism, h^0 would be proportional to the expression $\sin^2\alpha$. The expression $-187\sin^2\alpha$ listed in the seventh column of the table has the same values at points 0, 90, 180, 270 as the deviations of the wave front. The last column shows that the differences between the observed values of h^0 and those calculated by the formula exhibit a rather regular behavior. I did not attempt to discover the source of these regular deviations. I only wish to remark that the wave front must have further deviations beyond the pure astigmatism proportional to the expression $\sin^2\alpha$, since this optical system is poorly centered, as the previous investigation of the coma indicated.

The Old Utzschneider-Fraunhofer Refractor

20. The diameter of the objective is 17.5 cm, and its focal length is 288 cm. The instrument is equipped with a position filar micrometer, and one screw revolution corresponds to 23.33" in stellar observations.

I first attempted to determine the zonal aberrations of the objective by the two-slit method, observing the pole star on several evenings. The distance of the outermost observed zone from the center of the objective was 75 mm. I did not place any slits close to the edge, since the field illumination mirror at one sighting angle would have obstructed the passage of the light. One scale division on the screen was 1^p = 6.25 mm, so that the distance from the outermost zone to the center was 12^p. Primarily, I used two screens in which the spacing of the slits was $D_4 = 4^p$ = 25 mm and $D_2 = 2^p$ = 12.5 mm. The width /73
of the slits in the former was 8 mm and in the latter 6.5 mm. In both cases, the slits were 30 mm long. I made a few experiments with a screen with slits $D_1 = 1^p$ = 6.25 mm apart and only 3.5 mm wide. However, with such small slits, the star was very difficult to perceive. The field illumination in the instrument is very weak. Magnifications between 120 and 300 were used in the observations.

For many years, the refractor has been used exclusively as a training instrument, and its mounting is no longer in good condition. Although the greatest caution was taken in moving the screen and in turning the micrometer screw, there were occasionally major shifts in the position of the telescope, so that a whole series of observations had to be thrown out. The observations were always organized so that the first and last alignments were made with the screen in the same position, so that I would be able to tell whether the instrument had moved appreciably in the course of the observations. Because of the unsteadiness of the instrument, the measurements taken as part of its inspection were naturally not as accurate as those which would have been obtained in examining a first-class instrument.

Using the pole star, I determined the zonal aberrations in three directions, at the angles of sight 0°, 60°, and 120°, corresponding to the readings P = 108°, 168°, and 228° on the position compass. Suppose that an observation was to be made with screen D_2. The star was positioned in the field of vision so that it would pass roughly through the center of the field of vision after about 4 min. The screen was placed at position -11, the movable hairline near the image of the star, and the transit of the central interference band through /74
the movable hairline was observed by the chronometer. Then an observation was made in each of the positions -9, -7, ..., +11, followed by the same observations in the reverse order. One series of observations lasted about 8 min. The screen was moved by an assistant. In studying the P = 108° diameter, the star moved along the movable hairline, so the observation was naturally carried out by turning the micrometer screw. Using screen D_4, I made observations twice back and forth without interruption.

The calculations for the observations were performed as follows. During the brief period of time occupied by the observation, the motion of the pole star perpendicular to the movable hairline can be represented by the expression

$$u' = a + bt + ct^2,$$

where u' is the micrometer reading corresponding to the pole star, t the time from a moment near the middle of the observations, and a, b, and c constants. If u' is subtracted from the observed micrometer readings, the remainders differ among themselves by amounts which depend only on the deviations of the wave front and the observation errors. In practice, I allowed for the motion of the pole star only by calculating theoretically the effect of the term ct^2, and derived the linear expression a + bt from the first and last observations made with the screen in the given position. Finally, I took the mean values, designated by u, of the reduced micrometer readings corresponding to the same positions of the screen.

The final values of u are ascertained from two individual observations when screen D_2 is used and from four when screen D_4 is used. Therefore, the mean error ε of an alignment can be calculated from the deviations of the different observations. /75
On March 23 and 26, 1921, I made a total of eight series of observations with screen D_4, and obtained $\varepsilon = \pm 0^R.0137 = \pm 0.32"$ as the mean error of an alignment. From six series of observations with screen D_2 on March 18 and 26, I obtained $\varepsilon = \pm 0^R.0119 = \pm 0.28"$. The accuracy achieved with the two screens can be viewed as identical on the basis of these observations. We use the value $\varepsilon = \pm 0^R.0128 = \pm 0.30"$ for both screens. As the mean error of the values u, we find in this respect $\varepsilon_u = \pm 0^R.0090 = \pm 0.21"$ or ± 2.9 μm in linear units, in observations with screen D_2; when screen D_4 was used, $\varepsilon_u = \pm 0^R.0064 = \pm 0.15"$ or ± 2.1 μm in linear units.

The deviations of the wave front were calculated from the mean values u in the same way as for the objective aberrations of the small transit. Now, we can naturally determine the deviation of the wave front in the center of the objective as well. From the observations with screen D_4, we obtain the zonal aberrations e.g. from the formulas

$$\left.\begin{aligned} h_{12}^0 &= 0, \\ h_8^0 &= h_{12}^0 + \tfrac{1}{2} D_4 \varrho\,(u_{-10} - u_{10}), \\ h_4^0 &= h_8^0 + \tfrac{1}{2} D_4 \varrho\,(u_{-6} - u_6), \\ h_0^0 &= h_4^0 + \tfrac{1}{2} D_4 \varrho\,(u_{-2} - u_2), \end{aligned}\right\} \qquad (35)$$

$$
\begin{aligned}
z_{12} &= 0,\\
z_8 &= h_8^0 - \tfrac{5}{9} h_0^0,\\
z_4 &= h_4^0 - \tfrac{8}{9} h_0^0,\\
z_0 &= 0,
\end{aligned}
\qquad (36)
$$

as long as we don't wish to first determine all deviations h_y /76 separately by using formulas corresponding to (25) and (26).

Tables XVII and XVIII contain the zonal aberrations of the objective which I determined on the above days with the aid of the pole star. Since no appreciable differences were found among the zonal aberrations determined at various angles of sight in any of the series of observations, I took the mean values separately of the observations with the two screens. The mean errors listed under the mean values were calculated from the remaining errors, and the mean error of a zonal-aberration observation was found from the same numbers and is listed in the rows labeled ε_Z (afterward). The mean error ε_Z (before), on the other hand, was obtained via the following formulas from the mean error ε_u assumed in the paragraph preceding the previous one.

$$
\begin{aligned}
&D_4 = 4^p;\quad \varepsilon_{z_8} = \varepsilon_{z_4} = \frac{\sqrt{33}}{9} D_4 \varrho \varepsilon_u = 0.638\, D_4 \varrho \varepsilon_u.\\
&D_2 = 2^p;\quad \varepsilon_{z_{10}} = \varepsilon_{z_2} = \frac{\sqrt{615}}{36} D_2 \varrho \varepsilon_u = 0.689\, D_2 \varrho \varepsilon_u,\\
&\qquad\qquad \varepsilon_{z_6} = \varepsilon_{z_4} = \frac{\sqrt{1056}}{36} D_2 \varrho \varepsilon_u = 0.903\, D_2 \varrho \varepsilon_u,\\
&\qquad\qquad \varepsilon_{z_8} = \frac{\sqrt{1215}}{36} D_2 \varrho \varepsilon_u = 0.968\, D_2 \varrho \varepsilon_u.
\end{aligned}
\qquad (37)
$$

The mean errors of the observations made with screen D_2 before and after correction agree very well, while the mean error from the deviations of the final results of the observations made with screen D_4 is smaller than that obtained before the correction.

Since the slits in the screen were relatively long -- 30 mm -- we cannot immediately assume that the average deviations of the parts of the wave front corresponding to the slits will be the same as the deviations of the wave front at the midpoints /78 of the slits (cf. p. 26). Based on the curve which I had drawn in accordance with the zonal aberrations obtained with screen D_2, I calculated the differences:

h in the center of the slit, minus the average value of h

TABLE XVII.

z_y

$D_4 = 4^p = 25$ mm; $z_{12} = z_0 = 0$

Date	P	$y = 8$	$y = 4$
		nm	nm
11/3 21	108°	- 62	−26
»		−54	−34
»		−59	−43
»		−48	−34
20/3 21		−62	−33
23/3 21	168°	−54	−54
29/3 21		−52	−36
31/3 21	228°	−60	−41
Mean		−56	−38
Mean error		±1.8	±3.0
	ε_z (aft.)	±5.1	±8.4
	ε_z (bef.)	±11.5	±11.5

TABLE XVIII.

z_y

$D_4 = 2^p = 12.5$ mm; $z_{12} = z_0 = 0$

Date	P	$y = 10$	$y = 8$	$y = 6$	$y = 4$	$y = 2$
		nm	nm	nm	nm	nm
11/3 21	108°	−82	−81	−72	−49	−14
20/3 21		−64	−60	−32	−14	+1
»		−68	−72	−50	−35	−10
»	168°	−60	−61	−68	−56	−13
18/3 21	228°	−53	−63	−52	−40	−22
26/3 21		−58	−53	−52	−47	−10
Mean		−64	−65	−54	−40	−11
Mean error		±4.1	±4.0	±5.8	±6.0	±3.1
	ε_z (aft.)	±10.1	±9.9	±14.3	±14.7	±7.5
	ε_z (bef.)	±8.7	±11.5	±12.3	±11.5	±8.7

and found values of -5, -2, 0, +1, +2, +5, +5 nm for this difference at the points y = 12, 10, 8, ... If these values are reduced so that the corrections at the points y = 12 and y = 0 are equal to zero, the zonal aberrations then take the corrections 0, 0, -1, -2, -2, 0, 0 nm, and they can be neglected.

21. Besides using the pole star, I also determined the aberrations of the objective using an artificial star. I employed a point-like light source throughout. I produced this source in the manner described previously. The light source was in the window of a building 260 m away from the objective. The spacing of the slits in the screens was the same as before, i.e. D_4 = = 25 mm and D_2 = 12.5 mm. Moreover, I determined the zonal aberrations for the edge of the objective with the screen D_1 = = 6.25 mm. In all the screens, the slits were only 3 mm wide and 15 mm long. The interference bands were quite clearly visible. In observing the artificial star, the angular value of one screw revolution was 1^R = 23.07".

I determined the deviations of the wave front along the diameters of the objective corresponding to the readings P = 0°, 30°, 60°, ... of the position compass. The screen was shifted from the negative end of the diameter to the positive end and back, and an alignment was made after each displacement of the screen. Each u was then the mean value of two alignments. From the difference between the alignments associated with the same position of the screen, I calculated the mean error in an alignment. From the six series of observations conducted with screen D_2 on April 9, and from the 12 conducted on April 11, I obtained $\varepsilon = \pm 0^R.0119 = \pm 0.27"$ as the mean error of an alignment, and from the 12 on April 10 with screen D_4, $\varepsilon = \pm 0^R.0088 = \pm 0.20"$. The mean error of the mean value u is therefore $\varepsilon_u = \pm 0^R.0084 = \pm 0.19"$ for screen D_2 and $\varepsilon_u = \pm 0^R.0062 = \pm 0.14"$ for screen D_4. /79

The precision of the observations is therefore greater than for those with the pole star, but appreciably less than that for observations which I made in studying the small transit with screen D = 13.2 mm. The lower precision in comparison with the latter observations was due not only to the unsteadiness of the refractory but also to the fact that the artificial star used in studying the refractor was not as stationary as that used in studying the small transit. In traveling from the artificial star to the refractor, the light crossed a building not far above its roof. The building was heated by day, and this exerted an unfavorable influence on the images. One reason for the fact that the precision obtained with screen D_2 was substantially less than that with screen D_4 was obviously that the series of observations with the first screen were twice as long as those

with the latter, so that the motions of the instrument were greater in the former series. In some series, there was a clearly systematic behavior to the differences between alignments corresponding to the same position of the screen, a behavior originating in the motion of the instrument. A series of observations in which this difference amounted to almost 2" was repeated.

Table XIX contains the zonal aberrations calculated from the observations with screen D_2. I have placed the zonal aberrations obtained from measurements along a given diameter in one group, and put the mean values in the last row of the group. The values in the first row of each group are from the observations on April 9, and the remaining ones were found from the observations on April 11. The diameters $P = \alpha$ and $P = \alpha + 180°$ are naturally the same, so that the zonal aberrations corresponding to them can be directly compared with one another. /80

At the bottom of the table are found the mean error ε_z (aft.) of a zonal-aberration observation derived from the deviations of the individual observations, the resulting mean error ε_M of the individual group means and the mean error ε_z (bef.) of a zonal-aberration observation calculated from the values of ε_u mentioned previously. ε_z (aft.) and ε_z (bef.) are essentially identical. The final rows contain the mean value of all observations, its mean error, derived from the remaining deviations of the individual group means, and the same mean error derived from the mean errors ε_M. Judging from the mean errors, it is likely that the differences between the zonal aberrations obtained from the measurements along different diameters are real.

The corresponding results of the observations made with screen D_4 on April 10 are collected in Table XX. If the results of the two tables are compared, it is evident that the greatest differences between the zonal aberrations obtained from the various diameters in the two tables head in the same direction (see e.g. $P = 150°$). Between the values z_8 for the two screens, there is a difference which heads in the same direction as in the pole-star observations.

As the final zonal aberrations z_8 and z_4, I take the mean values from the results with both screens, and I derive the zonal aberrations of the remaining points from the results obtained with screen D_2, by interpolating the systematic reduction based on the zonal aberrations z_8 and z_4.

TABLE XIX.

z_y

$D_1 = 2^P = 12.5$ mm; $z_{12} = z_0 = 0$

P	$y=10$	$y=8$	$y=6$	$y=4$	$y=2$
	nm	nm	nm	nm	nm
0°	−59	−48	−46	−40	−16
0	−46	−49	−42	−55	−25
180	−58	−60	−49	−37	−6
Mean	−54	−52	−46	−44	−16
30	−54	−70	−54	−40	−33
30	−60	−60	−52	−38	−12
210	−58	−64	−70	−53	−21
Mean	−57	−65	−59	−44	−22
60	−33	−40	−44	−34	0
60	−57	−67	−60	−60	−24
240	−39	−38	−43	−38	−3
Mean	−43	−48	−49	−44	−9
90	−56	−66	−46	−48	−25
90	−55	−72	−52	−42	−10
270	−62	−72	−66	−44	−16
Mean	−58	−70	−55	−45	−17
120	−60	−62	−30	−15	+4
120	−71	−76	−46	−42	−28
300	−67	−72	−61	−48	−18
Mean	−66	−70	−46	−35	−14
150	−64	−66	−78	−76	−30
150	−67	−76	−78	−76	−26
330	−72	−87	−84	−71	−20
Mean	−68	−76	−80	−74	−25
ε_M	±3.9	±5.3	±5.6	±6.2	±6.3
ε_z (aft.)	±6.8	±9.2	±9.7	±10.7	±11.0
ε_z bef.)	±8.1	±10.6	±11.4	±10.6	±8.1
Gen. Mean	−58	−64	−56	−48	−17
Mean Error	±3.7	±4.8	±5.3	±5.5	±2.3
Mean Error from ε_M	±1.6	±2.2	±2.3	±2.5	±2.6

TABLE XX.

/81

z_y

$D_4 = 4^P = 25$ mm; $z_{12} = z_0 = 0$

P	$y=8$	$y=4$
	nm	nm
0	−39	−48
180	−58	−50
Mean	−48	−49
30	−63	−58
210	−40	−44
Mean	−52	−51
60	−58	−64
240	−43	−25
Mean	−50	−44
90	−46	−34
270	−45	−39
Mean	−46	−36
120	−50	−22
300	−46	−36
Mean	−48	−29
150	−66	−58
330	−78	−63
Mean	−72	−60
ε_u	±7.3	±9.0
ε_z (aft.)	±10.3	±12.8
ε_z bef.)	±11.1	±11.1
Gen. Mean	−53	−45
Mean Error	±4.0	±4.5
Mean Error from ε_u	±3.0	±3.7

/82

Hence, we take the values

z = 0, -55, -59, -53, -47, -17, 0 nm

as the final zonal aberrations at the points y = 12, 10, ...

From the measurements taken with screen $D_1 = 6.25$ mm at the periphery of the objective, I determined (using the above-mentioned fundamental values) zonal aberrations for the zone $y = 11$ and also for the zone $y = 13^p = 81.25$ mm near the edge of the objective. From my observations on April 22 for diameters $P = 0°, 30°, \ldots, 330°$, I obtained $z_{11} = -44$ nm, $z_{13} = +73$ nm. In these observations, the mean error of an alignment was $\pm 0^R.018 = \pm 0.42''$. The zonal aberrations of the refractor are depicted graphically in the table at the conclusion of the treatise.

22. In this connection, I mention a general formula by which the mean error of the zonal aberration for the zone half way between the center and the edge of an objective can be determined. Let us assume that the separation of the slits is 1/n times the radius of the outermost zone. Let n be an integer. Then, the mean error is

$$\varepsilon_{z_{\frac{1}{2}n}} = \frac{\sqrt{10}}{8\sqrt{n}} nD\varrho\varepsilon_u. \qquad (38)$$

Here, nD is the radius of the outermost zone.

Let us examine how accuracy varies when the spacing of the slits is modified. When the distance between the slits is very small, we can consider the alignment error to be proportional to the number n (cf. p. 34), so that $\varepsilon_u = n\varepsilon_0$, where ε_0 is a constant. Then,

$$\varepsilon_{z_{\frac{1}{2}n}} = \frac{\sqrt{10}}{8}\sqrt{n}\cdot nD\varrho\varepsilon_0. \qquad (39)$$

Accuracy therefore rises as the distance between the slits increases. Continuing to increase the distance between the slits, we find that the increase in alignment accuracy gradually comes to a halt, until the accuracy is essentially independent of the spacing of the slits beyond a specific limit. From formula (38) we find that the accuracy of the zonal-aberration determination decreases while the distance between the slits increases. However, if we allow for the fact that the number of observations which can be made in a given period of time is proportional to the distance between the slits, we arrive at the result that the mean error $\varepsilon_{z_{\frac{1}{2}n}}$ is independent of the spacing of the slits, as long as a given amount of time independent of the length of the series is employed for each observation. Utilizing a fine slit spacing has one thing in its favor, namely that the zonal aberrations at several points can be determined at the same time.

/83

In general, the maximum alignment accuracy ought to be achieved when the distance between the slits is still relatively small. In studying medium-sized telescopes, there is no point in making the distance between the slits more than about 3-4 cm. If the separation of the slits is about 1/6 or 1/8 of the radius of the outermost zone, the values obtained will already furnish the basis for a zonal-aberration curve, presuming that the wave front has a simple configuration. Extra points are most useful for the peripheral zones, because there the variations in the wave front are usually large.

23. I now mention briefly the results of my coma studies. From observations which I made in determining zonal aberrations, I found that the wave front did not exhibit any appreciable asymmetry, as long as the image was in the center of the field of vision. On April 12, I determined with screen D_2 the coma from observations along diameters P = 0°, 90°, 180°, 270°, while the artificial star was situated at the edges of the field of vision at micrometer readings u = 6^R and 54^R. The results are found in Table XXI. /84

TABLE XXI.

$c_y = \frac{1}{2}(h_y - h_{-y})$

$c_{11} = c_0 = 0.$

P	u	y = 10	y = 8	y = 6	y = 4	y = 2
		nm	nm	nm	nm	nm
0	54^R	−22	−10	−11	−8	−6
	6^R	+5	−2	+8	+13	+11
	Diff.	−27	−8	−19	−21	−17
180	54^R	+8	−1	−12	+12	+6
	6^R	+17	+36	+30	+27	+12
	Diff.	−9	−37	−42	−15	−6
270	54^R	+10	−2	−6	−3	−2
	6^R	+34	+15	+18	−2	−6
	Diff.	−24	−17	−24	−1	+4
90	54^R	−6	−0	−4	+4	+14
	6^R	−4	−6	+5	+5	+6
	Diff	−2	+6	−9	−1	+8
Mean . Diff.		−16	−14	−24	−10	−3
Mean error		±6	±9	±7	±5	±6

From the table, it can be seen that the image is almost coma-free over the entire field of vision. It is well known that the Fraunhofer objective design is close to that design in which the sine condition is satisfied.

By measuring the separation of the interference bands, I obtained as the effective wavelength of the light source λ = /85
= 572 nm with aperture D_4, λ = 573 nm with aperture D_2, and λ = 584 nm with a grating in which the slit spacing was 6.25 mm.

24. Using the three-hole method, I studied the astigmatism of the objective by determining the aberrations of the wave front in a zone of radius 75 mm. The measurements were taken in the same fashion as in the investigation of the small transit, but the number of holes was twice as large so that the aberration of the wave front was determined at 24 points in that zone. The distance between adjacent holes was 19.57 mm, and the holes were 5 mm in diameter.

I will mention only the final results of the four series of observations made on April 20, 1921. From differences in the alignments made with the same aperture position, I found the mean error of an alighnment to be $\pm 0^R.0.138 = \pm 0.32''$, which means that the mean error of each u and v is $\varepsilon = \pm 0^R.0098 = \pm 0.23''$. According to this mean error, the mean final error of a series of observations would be $\sqrt{24}D\rho\varepsilon = \pm 105$ nm. In fact, the final errors are +26, -46, -72, and +79 nm, and therefore much smaller. The aberrations of the wave front are shown in Table XXII.

The fourth column of the table contains the mean values of the aberrations at points lying along a given diameter. These can be approximated by the formula

$$h = -34 + 39 \cos 2(P + 12^\circ),$$

and these calculated values are entered in the fifth column. The last column contains the differences between the values of the preceding two columns.

TABLE XXII. /86

P	h_P	$h_{P+180°}$	Mean	h	Diff.
	nm	nm	nm	nm	nm
0°	0	0	0	+2	−2
15	−13	−3	−8	−11	+3
30	−31	−29	−30	−30	0
45	−66	−47	−56	−50	−6
60	−69	−66	−68	−66	−2
75	−67	−62	−64	−73	+9
90	−82	−82	−82	−70	−12
105	−69	−24	−46	−57	+11
120	−66	−10	−38	−38	0
135	−50	0	−25	−18	−7
150	−40	+22	−9	−2	−7
165	−10	+40	+15	+5	+10

The mean value $(h_P + h_{P+180°})/2$ can also be determined by the two-slit method from the observations along various diameters. I calculated these mean values from the observations made to determine zonal aberrations, and found almost the same astigmatism properties as I had found earlier with the three-hole method. However, the latter method is preferable in studying astigmatism for easily understandable reasons.

The Large Transit

25. In this instrument as well, the objective is a product of Utzschneider & Fraunhofer. Its diameter is 16 cm and its focal length 240 cm. The instrument was used in its time to observe the Helsinki zone of the A.G. Catalogue. The objective was considered good.

On April 19, 1921, I determined the zonal aberrations of /87
the objective by the two-slit method, observing the pole star in inferior culmination. The slits in the screen were 30 mm long and 6.25 mm wide, and their centers were 12.5 mm apart. The outermost observed zone was 75 mm from the optical axis. I studied only the horizontal diameter of the objective. The screen was shifted back and forth three times, so that a total of six alignments were made in each position of the screen. The mean error of an alignment was ±0.42". From the observations, I obtained the following zonal aberrations.

TABLE XXIII.

Zone radius y in mm . . .	75	62.5	50	37.5	25	12.5	0
Zonal aberration z_w in nm . . .	0	−58	−93	−86	−73	−27	0
Mean error		±7	±9	±10	±9	±7	

The mean errors are derived from the mean error of an alignment.

Application of the Three-Slit Method

26. At home, I studied small objectives and the parabolic mirror I had ground myself, using almost exclusively the three-slit method, since this method does not require that the [illegible] investigation apparatus be extremely steady, a property hard to achieve in an ordinary living room. As an example, I will take the parabolic mirror which I ground for the "Ursa" astronomical society. The mirror was 17.5 cm in diameter. I used an artificial star placed close to the center of curvature of the mirror. The focal length of the mirror was 120 cm. In the /88 investigation, the mirror was unsilvered.

The investigation apparatus is depicted schematically in Fig. 11.

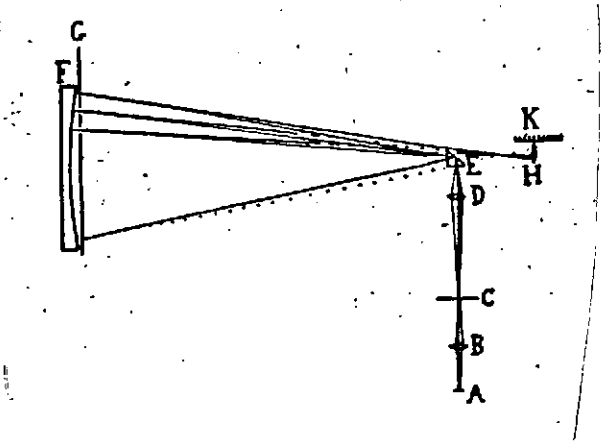

Fig. 11.

A is the light source (the filament of an electric bulb), and B a microscope objective which projects the image of A into the 0.1-mm hole in the screen C. The microscope objective D reduces the resulting point image, and the prism E reflects the light beam toward the mirror F under investigation, in front of which is a movable screen G with three slits in it. Reflected by the mirror, the light beam passes the prism E and generates an image near the center of curvature of the mirror. This image is viewed with the powerful ocular H the motion of which in the direction of the optical axis is read off the scale K divided into millimeters.

The slits in the screen were 25 mm long and 5 mm wide, and the midpoints of adjacent slits were D = 20 mm apart. Accordingly, the distance between adjacent marks on the scale showing the position of the screen G was 1^p = 20 mm. The outermost investi- /89 gated zone was 80 mm from the optical axis.

The observations were made as follows. The screen was placed so that the slits were situated at the points -4, -3, and -2. For the sake of brevity, we say that the position of the screen was -3. An observation was made (see p. 15), obtaining the readings w' and w" on the scale of the ocular. Next, observations were made with the screen in positions -2, -1, 0, 1, 2, and 3. To save time, I have made such simple observations when grinding mirrors. Table XXIV contains my observations on December 17, 1921. w is the mean value of the readings w' and w", and $w_y^0 = (w_y + w_{-y})/2$.

TABLE XXIV.

y	w'	w''	w	w^0
	mm	mm	mm	mm
−3	54.4	63.2	58.80	59.00
−2	54.3	62.6	58.45	58.22
−1	51.5	59.8	55.65	55.68
0	49.2	58.1	53.65	53.65
+1	51.2	60.2	55.70	
+2	53.4	62.6	58.00	
+3	54.8	63.6	59.20	

27. Let b be the approximate distance between the image and the mirror, and let $\bar{w}$ be the average position of the ocular, and let us imagine that the center of the reference sphere is located in the corresponding movable plane. We use the symbols

$$\Delta h_{y+\frac{1}{2}} = h_{y+1} - h_y,$$
$$\Delta^2 h_y = \Delta h_{y+\frac{1}{2}} - \Delta h_{y-\frac{1}{2}} = h_{y+1} - 2h_y + h_{y-1}. \qquad (40)$$

It is then easy to find the following basic formula /90

$$\Delta^2 h_y = \left(\frac{D}{b}\right)^2 (w_y - \bar{w}). \qquad (41)$$

The calculations can be done e.g. as follows. First, we take $h_{-4} = h_{-3} = 0$. Using formulas (40) and (41), we determine the remaining deviations h_{-2}, h_{-1}, ..., h_4. By attaching a suitable expression $\alpha + \beta y + \gamma y^2$ to the deviations, changing only the reference sphere, we arrange that $h_{-4} = h_0 = h_4 = 0$.

Also, $\bar{w}$ and $\Delta h_{-3\frac{1}{2}}$ can be determined in advance so that $h_{-4} = h_0 = h_4 = 0$. One then makes use of the formulas

$$\left.\begin{aligned} \bar{w} &= \tfrac{1}{16}(w_{-3} + 2w_{-2} + 3w_{-1} + 4w_0 + 3w_1 + 2w_2 + w_3), \\ \Delta^2 h_y &= \left(\frac{D}{b}\right)^2 (w_y - \bar{w}), \\ \Delta h_{-3\frac{1}{2}} &= -\tfrac{1}{4}(3\Delta^2 h_{-3} + 2\Delta^2 h_{-2} + \Delta^2 h_{-1}), \\ h_{-4} &= 0. \end{aligned}\right\} \qquad (42)$$

By means of formulas (40), the remaining deviations are obtained, as well as two controls, since $h_0 = h_4 = 0$.

If we desire only the zonal aberrations, we take the mean values $w_y^0 = (w_y + w_{-y})/2$ and then use the formulas (42) and (40), substituting $w_y = w_{-y} = w_y^0$ in them everywhere. In our example, the calculation of the zonal aberrations is organized as follows (see Table XXV).

TABLE XXV.

y	w^0		$w^0 - \bar{w}$	$\Delta^2 h$		Δh	h	Red.	z
	mm		mm	nm		nm	nm	nm	nm
4							0	0	0
						−18			
3	59.00	9.00	+2.78	+178	+534		−189	+183	−6
						−11			
2	58.22	16.44	+2.00	+128	+256		−200	+139	−61
						+117			
1	55.68	17.04	−0.54	−34	−34		−83	+44	−39
						+83			
0	53.65	7.30	−2.57	−164			0	0	0
		49.78			+756				

$\bar{w} = 56.22$ $\qquad \Delta h_{-3\frac{1}{2}} = -189$

The artificial star was a = 2300 mm from the mirror, while the image was b = 2500 mm away. In order to find the deviations of the wave front when the star is at an infinite distance, the reduction

$$\frac{1}{8abF}y^2(y_0^2-y^2) \qquad (43)$$

is to be applied to the deviations h, where F is the focal length of the mirror and y_0 the radius of the outermost zone. Taking this reduction into account, we obtain the zonal aberrations listed in the last column of the table. The deviations of the surface of the mirror from a paraboloid are exactly equal to half the numbers z. /91

28. I will now devote a few words to the precision of the observations. From several series of observations which I made in grinding the mirror mentioned in the example and another mirror of equal size, I calculated the differences w" - w' and then the mean error of a w from their deviations from the mean value. I found $\varepsilon_w = \pm 0.17$ mm. For the mean error of the zonal aberrations, I derived the following formulas:

$$\begin{aligned} \varepsilon_{z_3} &= \frac{\sqrt{91}}{16}\left(\frac{D}{b}\right)^2\varepsilon_w, \\ \varepsilon_{z_2} &= \frac{\sqrt{112}}{16}\left(\frac{D}{b}\right)^2\varepsilon_w, \\ \varepsilon_{z_1} &= \frac{\sqrt{43}}{16}\left(\frac{D}{b}\right)^2\varepsilon_w. \end{aligned} \qquad (44)$$

Taking $\varepsilon_w = \pm 0.17$ mm, we obtain $\varepsilon_{z_3} = \pm 6$ nm, $\varepsilon_{z_2} = \pm 7$ nm, $\varepsilon_{z_1} = \pm 4$ nm. The accuracy is therefore quite satisfactory. /92

In the general case in which D is 1/n of the radius of the outermost zone, where n is an integer, the mean error $\varepsilon_{z_{\frac{1}{2}n}}$ of the zonal aberration for the zone halfway between the center and the edge of the objective is obtained from the following formula, which I will not derive here for the sake of brevity.

$$\varepsilon_{z_{\frac{1}{2}n}} = \frac{1}{8}\sqrt{\frac{n(n^2+5)}{3}}\left(\frac{D}{b}\right)^2\varepsilon_w. \qquad (45)$$

If D is small, $(D/b)^2\varepsilon_w$ can be viewed as roughly constant. I observed this in the experiments, and it seemed natural after some reflection. From (45), one then finds that n should be as small as possible and hence D as large as possible in order that $z_{\frac{1}{2}n}$ be determined as precisely as possible. If D increases,

so does $(D/b)^2\varepsilon_w$, albeit gradually, and finally a limit is reached after which ε_w no longer diminishes appreciably. Then, the accuracy of the zonal-aberration determination decreases while D increases. The most favorable value of D must be determined empirically. In studying the 17.5-cm mirror mentioned in the example, the aberration of zone y = 40 mm would have been somewhat more accurately determined with screen D = 40 mm than with screen D = 20 mm, but in view of the fact that the latter screen would still have to have been used to interpolate the aberrations of zones y = 60 mm and y = 20 mm, requiring substantially more time for the observations, I contented myself with using just screen D = 20 mm.

From the difference w" - w' (p. 63), the effective wavelength of the light source can be determined by means of the formula (cf. pp. 14-15)

$$\lambda = \left(\frac{D}{b}\right)^2 (w'' - w') \qquad (46)$$

/93

From several observations with screen D = 20 mm, I obtained the mean value w" - w' = 8.83 mm, corresponding to λ = 565 nm.

I also carried out some experiments using the three-slit method with a star as the light source, and the method proved quite usable in this case as well. Since the rapid motion of the star is not detrimental, as it would be in the two-slit method, first-magnitude stars can be used as observation targets. In the northern latitudes, for example, Vega and Capella are very suitable for this purpose.

Michelson's Method and Other Applications of the Methods

29. Michelson's method, which was already referred to in the introduction, differs substantially from the two-slit method described above in that Michelson held a slit at the center of the objective during the entire duration of the measurements and gradually shifted the other slit from near the center toward the edge. Both of Michelson's experiments were conducted in the laboratory using monochromatic light and a highly magnifying microscope. In these measurements, the method did prove thoroughly practical, but it is evident that Michelson's method would be beset by many difficulties in observatories, where it is mainly natural or distant artifical stars which are used. It was mentioned on p. /83 that the alignment accuracy eventually quits increasing as the distance between the slits is enlarged, because of air turbulence. This occurs when the slits are several centimeters

/94

apart, and is the reason why the deviations of the peripheral zones are determined most poorly, and why, in fact, the alignment of the central interference band can be impossible because of air turbulence when the peripheral zones of large telescopes are investigated. In refractors, the secondary spectrum also makes it very difficult to distinguish the central interference band from the remaining ones when the separation of the slits is large. In some cases, Michelson's method requires a special ocular microscope, since ordinary magnifications are not good enough for clear observation of the fine interference figure. The circumstance that the size of the interference figure changes with the separation of the slits can induce systematic alignment errors. In this respect as well, my method should be better.

30. I would also like to mention two modifications which I envisage in the two-slit and three-hole methods, so that it will no longer be necessary to keep the instrument stationary except for a short period of time. The basic idea of these modifications is that a second image of the star is obtained in the various methods, and this image is independent of the interference figure generated by the movable screen. I will describe this procedure in the application of the two-slit method; it requires only minor revisions to apply it to the three-hole method as well.

In one modification, the comparison image is produced by means of a small prism, the prism angle of which is so small that the light beam is only deflected by a few tens of arc seconds in passing through it. Assume e.g. that the movable screen is in the horizontal direction. Above or below the movable screen, two slits are made in the strip which holds it, the slits being parallel to the slits on the screen. The prism is fastened to the slits of the strip. In that case, two separate interference figures are visible simultaneously. In each position of the screen, an alignment is made on the central bands of both figures. The telescope must therefore be stationary only for a few seconds. In photographing, both figures are imaged at the same time. It is useful to turn the prism into such a position that the interference figures are as close as possible to being one above the other, since then the observations can be made with a minimum of screw rotation. Using a simple prism naturally suffices in all cases, since the prism angle is so small that the prism does not generate any appreciable spectrum, and moreover, any such spectrum would never make the interference figure asymmetric about the central band as long as the prism has been turned into the given position. In observing the pole star, one can even get along without movable hairlines, either by turning the prism into such a position that the transit of the two images at a fixed hairline takes place in a very short time, or by observing the transits of the bands over two different hairlines. /95

The second procedure uses extrafocal images. As in the first modification, the slits are made in the fixed strip as far as possible from the movable screen. If, in both slit systems, the separation of the slits is small in comparison to the semidiameter of the objective aperture, two independent interference figures are produced in the movable plane, once the movable plane has been pushed inward or outward a suitable distance from the focus. The measurements are then made in the same way as in the first modification. The observations are /96 to be made while the movable plane is inside and then outside the focus. The first section of the calculations is done in the same way as in Hartmann's method. By this method, I determined the zonal aberrations of the 17.5-cm refractor with a short series of observations, and, on the whole, obtained the results given earlier. This modification is not completely satisfactory, however, since the correction term η'' (p. 25) may assume measurable values. In my opinion, the reliability of the method therefore requires detailed study based on suitable experiments.

IV. ASSESSING THE QUALITY OF OBJECTIVES /97

Lehmann's Technical Constant

31. Lehmann's technical constant T is calculated by the well-known formula [13]:

$$T = \frac{200000}{F_0^2} \cdot \frac{\Sigma r^3 |F - F_0|}{\Sigma r}. \qquad (47)$$

For the calculation, the objective is broken up into many zones of equal width. r is the radius of the general zone and F its corresponding focal length. F_0 is an average focal length.

The value of T depends on the value chosen for F_0. It might appear most natural to determine F_0 so that T is minimized. This is the way Fox calculated the technical constant for the large objective of the Yerkes observatory [14]. However, since the F_0 corresponding to the minimum of T cannot be calculated by a simple formula, attempts have been made to determine F_0 in other ways.

In his calculations of the technical constant T for several large objectives, Hartmann employed two different methods to determine F_0 [2, p. 102]. In most cases, the mean value of the /98 focal lengths of the different zones was chosen as F_0. In other cases, however, Hartmann believed that this method would not accurately reflect the correction of an objective, and he chose as the movable plane the plane in which all light beams passing through the objective compress to the smallest area, and which is calculated as follows [2, p. 45].

> "If F_1 and F_2 are the extreme values of the focal length nearest to the edge of the objective, corresponding to radii r_1 and r_2, the smallest geometric scattering disk is obtained at
>
> $$F_0 = \frac{F_1 r_1 + F_2 r_2}{r_1 + r_2}." \qquad (48)$$

These procedures, particularly the latter, were also used later in calculating the technical constant in order to determine the movable plane.

We wish to show the results which will be obtained by these methods for determining the movable plane in two typical cases, namely for pure spherical aberration and for typical zonal aberration.

Let the radius of the objective aperture be R. We use the symbols

$$\varrho = \frac{r}{R}, \quad \Delta = F - F_0', \tag{49}$$

where F_0' is an average value of the focal length.

Pure spherical aberration is represented by the formula

$$\Delta = k_1 \varrho^2, \tag{50}$$

and the following formula expresses the typical zonal aberration at which the central and peripheral beams have the same focal lengths:

$$\Delta = k_2 (\varrho^2 - \varrho^4). \tag{51}$$

If the objective is divided into infinitely many zones, /99
the definition of the technical constant is obtained in the form

$$T = \frac{4 \cdot 10^5}{F_0^2 R^2} \int_0^R r^2 |\Delta - \Delta_0| \, dr \tag{52}$$

or else

$$T = 4 \cdot 10^5 \cdot \frac{R}{F_0^2} \int_0^1 \varrho^2 |\Delta - \Delta_0| \, d\varrho. \tag{53}$$

We now consider the case of pure spherical aberration. We determine Δ_0 at first so that T attains its minimum value T_0. By calculations, with which I will not bother the reader, we find

$$\Delta - \Delta_0 = k_1 \left(\varrho^2 - \sqrt[3]{\tfrac{1}{4}}\right) = k_1 (\varrho^2 - 0.62996),$$

$$T_0 = 80000 \left(1 - \sqrt[3]{\tfrac{1}{4}}\right) \frac{k_1 R}{F_0^2} = 29693 \frac{k_1 R}{F_0^2}. \tag{54}$$

If, on the other hand, the adjustable plane is chosen so that one takes the mean value of the focal lengths of all zones, we find

$$\Delta - \Delta_0 = k_1 \left(\varrho^2 - \tfrac{1}{3}\right).$$

and the corresponding technical constant is

$$T_1 = 42398 \frac{k_1 R}{F_0^2} = 1.43\, T_0.$$

If we calculate Δ_0 by Hartmann's second method, we find

$$\Delta - \Delta_0 = k_1 (\rho^2 - 1),$$
$$T_2 = 53333 \frac{k_1 R}{F_0^2} = 1.80\, T_0.$$

As is evident, both T_1 and T_2 are quite different from T_0. The second method is obviously totally unsuitable in this case, since the differences will then all have the same signs. /100

We perform the same calculations for the case of typical zonal aberration. By the minimum condition, we go through relatively tedious calculations to find

$$\Delta - \Delta_0 = k_2 (\rho^3 - \rho^4 - 0.1933),$$
$$T_0 = 7978 \frac{k_2 R}{F_0^2}. \qquad (55)$$

By Hartmann's first method, we find

$$\Delta - \Delta_0 = k_2 (\rho^3 - \rho^4 - 0.1333),$$
$$T_1 = 9761 \frac{k_2 R}{F_0^2} = 1.22\, T_0,$$

and with the second

$$\Delta - \Delta_0 = k_2 (\rho^3 - \rho^4 - 0.1035)$$
$$T_2 = 11746 \frac{k_2 R}{F_0^2} = 1.47\, T_0.$$

In this case, T_1 and T_2 do not differ as much from T_0 as in the case of pure spherical aberration, but the difference is still considerable.

As mentioned, Hartmann states that his first method is not suitable for determining the movable plane in some cases. From the above calculations, however, we see that Hartmann's second method cannot be used at all in cases like that of pure spherical aberration. By contrast, typical zonal aberration is reminiscent of cases in which Hartmann's second method would be usable. By choosing the most appropriate of these methods for each individual case, it ought to be possible to determine T

properly in many cases, although the resulting values will generally be larger than those calculated from the minimum condition. On the other hand, it is undeniable that it may be difficult to decide which of the two methods to employ in complicated cases, and the result of the calculation will acquire a subjective stamp. Therefore, I think it preferable to give priority to a method of calculation applicable in all cases without yielding highly erroneous results, and in which T does not differ too much from the minimum value of T if this can somehow be accomplished. //101

32. Various ways of determining Δ_0 are contained in the formula

$$\Delta_0 = \frac{\int_0^1 \varrho^n \Delta d\varrho}{\int_0^1 \varrho^n d\varrho} = (n+1)\int_0^1 \varrho^n \Delta d\varrho \quad (n \geq 0). \tag{56}$$

The larger the value of n, the greater the weight given to the peripheral beams.

The case n = 0 is identical with Hartmann's first method.

If n = 3, it is easy to show that we can find the adjustable plane in which the sum of the squares of the lateral deviations of the light beams is minimized. Determining Δ_0 in this way, we will obtain, in the zonal-aberration cases discussed above, values for T differing very little from T_0; namely, for pure spherical aberration we find a technical constant of 1.007 T_0 and for typical zonal aberration 1.047 T_0.

In our examples, the technical constant differs even less from T_0, when n = 2 and Δ_0 is therefore determined by the formula

$$\Delta_0 = 3\int_0^1 \varrho^2 \Delta d\varrho$$

Fox employed this formula in the form of a finite sum in the previously mentioned case, in order to find an approximate value for T_0. By improving it, he then looked for the plane in which T was minimized. However, this minimum was only slightly less than the first approximation to T_0. //102

In the case of pure spherical aberration, we obtain, determining Δ_0 by the last formula

$$\Delta - \Delta_0 = k_1 \left(\varrho^2 - \frac{3}{5}\right),$$
$$T = 29744 \frac{k_1 R}{F_0^2} = 1.005\, T_0$$

and in the case of typical zonal aberration

$$\Delta - \Delta_0 = k_2 (\varrho^2 - \varrho^4 - 0.1714),$$
$$T = 8237 \frac{k_2 R}{F_0^2} = 1.032\, T_0.$$

Practically speaking, the technical constant found in both cases is identical with T_0. It seems very natural that the latter method for determining the adjustable plane would not yield totally erroneous results in more general cases either. Moreover, this method makes calculating the technical constant relatively simple, since the value of the integrand $\rho^2\Delta$ calculated to derive Δ_0 can be employed in calculating T.

Consequently, I propose that the latter method be employed in all cases to calculate the technical constant based on the focal lengths, i.e. that T be calculated by the formulas

$$\Delta_0 = 3 \int_0^1 \varrho^2 \Delta d\varrho,$$
$$T = 4 \cdot 10^5 \cdot \frac{R}{F_0^2} \int_0^1 \varrho^2 |\Delta - \Delta_0| d\varrho. \qquad (57)$$

With the aid of these formulas, I have calculated the value/103 of T over again for the objectives, the technical constants of which Hartmann had reported in his previously cited work, and also for some other objectives, the zonal aberrations of which I was able to discover in the literature. The results are collected in Table XXIX. The most noteworthy change was found for the technical constants of the objectives of Pulkowa and Ottawa, which were, according to the new calculation, less than half the previously calculated values. No great changes were encountered in the constants of the remaining objectives. For some objectives, my value was even larger than the previous one, which can be explained by the fact that I extrapolated the focal-length curves to the edge of the objective, where the deviations are usually the greatest.

Diffraction-Theoretic Technical Constant

33. As mentioned in the Introduction, Strehl thought that a good standard for the quality of an objective was the ratio

between the light intensity at the center of the diffraction pattern produced by the objective and that at the center of a diffraction pattern produced by an aberration-free objective of equal size. Since the brightness of the center of the pattern changes depending on how the telescope is focused, one must attempt to determine the movable plane so that the brightness in the center of the image is as great as possible.

As before, we use h to designate the deviation of the light front from the reference sphere at a distance r from the optical axis and at the azimuth ω. In the center of the reference sphere, the light intensity is proportional to the expression [15]:

$$I = C'^2 + S'^2$$ /104

where

$$C' = \int_0^{2\pi}\int_0^R \cos\frac{2\pi h}{\lambda} r\,dr\,d\omega,$$

$$S' = \int_0^{2\pi}\int_0^R \sin\frac{2\pi h}{\lambda} r\,dr\,d\omega$$

or, setting $q = (r/R)^2 = \rho 2$,

$$C' = \tfrac{1}{2}R^2\int_0^{2\pi}\int_0^1 \cos\frac{2\pi h}{\lambda} dq\,d\omega,$$

$$S' = \tfrac{1}{2}R^2\int_0^{2\pi}\int_0^1 \sin\frac{2\pi h}{\lambda} dq\,d\omega.$$

Assume that the objective has only zonal aberrations. Then, h depends only on q and we obtain

$$C' = \pi R^2\int_0^1 \cos\frac{2\pi h}{\lambda} dq,$$

$$S' = \pi R^2\int_0^1 \sin\frac{2\pi h}{\lambda} dq.$$

For an ideal objective, h = 0, and accordingly

$$C_0' = \pi R^2, \quad S_0' = 0, \quad I_0 = \pi^2 R^4.$$

The technical constant Z corresponding to the definition of Strehl is therefore obtained from the formula

$$Z = \frac{I}{I_0} = C^2 + S^2, \tag{58}$$

where

$$C = \int_0^1 \cos \frac{2\pi h}{\lambda} dq, \qquad S = \int_0^1 \sin \frac{2\pi h}{\lambda} dq. \tag{59}$$

/105

Since the cases occurring in practice seldom have deviations of the wave front which can be represented by simple analytic expressions, the integrals C and S must generally be evaluated by numerical integration. However, in the case that the deviations of the wave front are very small, the calculation of Z can be set up more simply by substituting series expansions for the trigonometric functions in the integrands.

For brevity, let

$$\delta = 2\pi h/\lambda. \tag{60}$$

We obtain

$$C = \int_0^1 \left(1 - \frac{1}{2}\delta^2 + \frac{1}{24}\delta^4 - \frac{1}{720}\delta^6 + \frac{1}{40320}\delta^8 - + \cdots\right) dq,$$

$$S = \int_0^1 \left(\delta - \frac{1}{6}\delta^3 + \frac{1}{120}\delta^5 - \frac{1}{5040}\delta^7 + - \cdots\right) dq.$$

Let

$$\gamma_1 = \int_0^1 \delta\, dq, \quad \gamma_2 = \int_0^1 \delta^2\, dq, \quad \gamma_3 = \int_0^1 \delta^3\, dq, \ldots, \tag{61}$$

Then

$$C = 1 - \frac{1}{2}\gamma_2 + \frac{1}{24}\gamma_4 - \frac{1}{720}\gamma_6 + \frac{1}{40320}\gamma_8 - + \cdots,$$

$$S = \gamma_1 - \frac{1}{6}\gamma_3 + \frac{1}{120}\gamma_5 - \frac{1}{5040}\gamma_7 + - \cdots$$

and

$$Z = 1 + \left(\gamma_1^2 - \gamma_2\right) + \left(\frac{1}{4}\gamma_2^2 - \frac{1}{3}\gamma_1\gamma_3 + \frac{1}{12}\gamma_4\right) + \left(\frac{1}{36}\gamma_3^2 - \frac{1}{24}\gamma_2\gamma_4 + \right.$$
$$+ \frac{1}{60}\gamma_1\gamma_5 - \frac{1}{360}\gamma_6\Big) + \left(\frac{1}{576}\gamma_4^2 - \frac{1}{360}\gamma_3\gamma_5 + \frac{1}{720}\gamma_2\gamma_6 - \right.$$
$$\left. - \frac{1}{2520}\gamma_1\gamma_7 + \frac{1}{20160}\gamma_8\right) + \cdots. \qquad (62)$$

/106

34. Now assume that the deviations of the wave front are so small that the higher-order terms can be neglected. Then

$$Z = 1 - (\gamma_2 - \gamma_1^2) + \cdots.$$

We now determine the reference sphere so that Z is as large as possible, so that

$$\tau = \left(\frac{\lambda}{2\pi}\right)^2 (\gamma_2 - \gamma_1^2) = \int_0^1 h^2\,dq - \left(\int_0^1 h\,dq\right)^2$$

is as small as possible.

A very small change in the reference sphere, without changing the optical axis, turns the deviation h of the wave front into the deviation h', the latter being obtained from the equation

$$h' = h + aq + b,$$

where a and b are constants which depend on the change in the reference sphere.

In that case, τ becomes

$$\tau' = \int_0^1 h'^2\,dq - \left(\int_0^1 h'\,dq\right)^2 =$$
$$= \int_0^1 h^2\,dq - \left(\int_0^1 h\,dq\right)^2 + a\left(2\int_0^1 hq\,dq - \int_0^1 h\,dq\right) + \frac{1}{12}a^2.$$

Therefore, b has no effect on the value of τ', as would have been anticipated. τ' is a minimum when

$$a = 6\left(\int_0^1 h\,dq - 2\int_0^1 hq\,dq\right). \qquad \text{/107}$$

The corresponding minimum of τ' is

$$\tau_0' = \int_0^1 h'^2\,dq - \left(\int_0^1 h'\,dq\right)^2$$
$$= \int_0^1 h^2\,dq - \left(\int_0^1 h\,dq\right)^2 - 3\left(\int_0^1 h\,dq - 2\int_0^1 hq\,dq\right)^2.$$

Substituting

$$h = h' - \int_0^1 h'\,dq = h + aq - \left(\frac{1}{2}a + \int_0^1 h\,dq\right)$$

we find

$$\tau_0' = \int_0^1 h^2\,dq.$$

Hence, τ_0' is the mean value of the squares of the deviations $\bar{h}$ of the wave front. The square root

$$\sqrt{\tau_0'} = \varepsilon$$

we term the mean deviation of the light wave front, analogous to the term "mean error" used in the least-squares method. In reality, the deviations $\bar{h}$ are then the remaining errors obtained when the least-squares method has been used to determine the sphere which best fits the wave front, and ε is the mean remaining error.

We now correct the formulas for calculating the mean deviation. We calculate

$$a = 6\left(\int_0^1 h\,dq - 2\int_0^1 hq\,dq\right),$$

$$h = h + aq - \left(\frac{1}{2}a + \int_0^1 h\,dq\right), \qquad \text{/108} \quad (63)$$

$$\varepsilon^2 = \int_0^1 h^2\,dq$$

i.e.

$$\varepsilon^2 = \int_0^1 h^2 dq - \left(\int_0^1 h dq\right)^2 - 3\left(\int_0^1 h dq - 2\int_0^1 hq\, dq\right)^2. \qquad (64)$$

Finally, when the deviations of the wave front are sufficiently small,

$$Z = 1 - \left(\frac{2\pi}{\lambda}\right)^2 \varepsilon^2. \qquad (65)$$

Hence, if the deviations of the wave front are very small, Z depends only on the mean deviation ε and not at all on the configuration of the wave front. The number ε can be viewed as a standard for the quality of an objective which is just as good as the number Z. When the deviations of the wave front are so large that the higher-order terms in the expression for Z can no longer be neglected, the constant Z can naturally no longer be calculated with the aid of ε by itself, but the mean deviation ε can still be viewed as a standard for the quality of the objective, since in general Z decreases as ε increases.

If the deviations of the wave front are so large that the series expansion of Z does not converge rapidly, it is best to calculate Z by numerical integration using exact formulas. For simplicity, the reference sphere can then be determined as in the calculation of the mean deviation ε[1]. In executing the calculations, one therefore employs the deviations h, or else the deviations h', which would yield an identical result. /109

The reference sphere can also be determined graphically. This is the way Strehl did it [16]. The deviations of the wave front are plotted on the vertical axis and q on the horizontal axis. The surface of the sphere is then represented by a straight line in the diagram. The line which best fits the curve representing the wave front can be drawn quite well by examination. The graphic method can also be used, of course, to do the integrations. Namely, the mean deviation can be calculated rapidly by the graphic procedure.

35. We will first apply our formulas to pure spherical aberration and to typical zonal aberration. The deviations h of the wave front are computed from the focal-length deviations

[1] Of course, this reference sphere is not precisely the same as the sphere which minimizes Z.

Δ using the differential equation

$$\frac{dh}{dr} = \frac{r\Delta}{F^2}, \tag{66}$$

which we can also write in the form

$$\frac{dh}{dq} = \frac{1}{2}\left(\frac{R}{F}\right)^2 \Delta \tag{67}$$

In practice, an average focal length F_0 can be used on the right side of the equation in place of F. We then obtain

$$h = \frac{1}{2}\left(\frac{R}{F_0}\right)^2 \int_0^q \Delta\, dq, \tag{68}$$

if we assume h = 0 in the center of the objective.

In the case of spherical aberration, /110

$$\Delta = k_1 q.$$

By integration, we obtain

$$h = \frac{1}{4} k_1 \left(\frac{R}{F_0}\right)^2 q^2 = x_1 q^2; \quad x_1 = \frac{1}{4} k_1 \left(\frac{R}{F_0}\right)^2. \tag{69}$$

Using the formulas we have derived, we find

$$\begin{aligned} \bar{h} &= x_1\left(q^2 - q + \frac{1}{6}\right), \\ \varepsilon &= \frac{x_1}{6\sqrt{5}} = \left(\frac{R}{F_0}\right)^2 \frac{k_1}{24\sqrt{5}}, \\ Z &= 1 - \frac{1}{180}\left(\frac{2\pi x_1}{\lambda}\right)^2 + \frac{1}{75600}\left(\frac{2\pi x_1}{\lambda}\right)^4 - \frac{1}{60540480}\left(\frac{2\pi x_1}{\lambda}\right)^6 + \cdots \end{aligned} \tag{70}$$

or, when x_1 is expressed in terms of ε,

$$Z_1 = 1 - \left(\frac{2\pi\varepsilon}{\lambda}\right)^2 + \frac{3}{7}\left(\frac{2\pi\varepsilon}{\lambda}\right)^4 - \frac{675}{7007}\left(\frac{2\pi\varepsilon}{\lambda}\right)^6 + \cdots. \tag{71}$$

In the case of typical zonal aberration, we start with the equation

$$\Delta = k_2(q - q^2)$$

and obtain

$$h=\frac{1}{6}x_2\left(\frac{R}{F_0}\right)^2\left(\frac{3}{2}q^2-q^4\right)=x_2\left(\frac{3}{2}q^2-q^3\right);\quad x_2=\frac{1}{6}k_2\left(\frac{R}{F_0}\right)^2,$$

$$h=x_2\left(\frac{1}{20}-\frac{3}{5}q+\frac{3}{2}q^2-q^3\right),$$

$$\varepsilon=\frac{x_2}{20\sqrt{7}}=\left(\frac{R}{F_0}\right)^2\frac{k_2}{120\sqrt{7}}, \tag{72}$$

$$Z=1-\frac{1}{2800}\left(\frac{2\pi x_2}{\lambda}\right)^2+\frac{479}{8408400000}\left(\frac{2\pi x_2}{\lambda}\right)^4-\cdots,$$

$$Z=1-\left(\frac{2\pi\varepsilon}{\lambda}\right)^2+\frac{958}{2145}\left(\frac{2\pi\varepsilon}{\lambda}\right)^4-\cdots.$$

We take one further example, in which the number of zones n can be arbitrarily large. Let

$$h=x_2\cos 2\pi nq \tag{73}$$

We obtain /111

$$\begin{aligned}\bar{h}&=h,\\ \varepsilon&=\frac{x_2}{\sqrt{2}},\\ Z&=\left[J_0\left(\frac{2\pi x_2}{\lambda}\right)\right]^2=\left[J_0\left(\frac{2\sqrt{2}\pi\varepsilon}{\lambda}\right)\right]^2,\end{aligned} \tag{74}$$

where J_0 is the zero-order Bessel function, i.e.

$$J_0(x)=\frac{1}{\pi}\int_0^{\pi}\cos(x\cos\omega)\,d\omega.$$

The series expansion is

$$Z=1-\left(\frac{2\pi\varepsilon}{\lambda}\right)^2+\frac{3}{8}\left(\frac{2\pi\varepsilon}{\lambda}\right)^4-\frac{5}{72}\left(\frac{2\pi\varepsilon}{\lambda}\right)^6+\cdots. \tag{75}$$

Hence, Z is independent of the number n of zones.

Figure 12 depicts the deviations of the wave front in the three cases discussed above. Among the cases with many zones, n = 2 was chosen. The abscissa in the diagram is not q but the radius ρ. For all curves, ε was chosen to have the same value.

In examining the series expansions of Z in terms of ε in these three cases, it can be seen that the corresponding coefficients in the various series do not differ very much, so /112

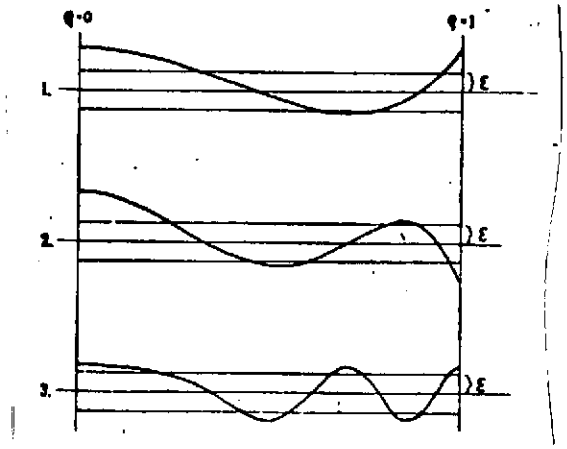

Fig. 12.

that it seems likely that the values of Z corresponding to the same ε in these three cases will also be roughly equal even when ε is rather large. The purpose of Table XXVI is to show how Z varies with ε in my selected examples.

In the first column, ε is expressed in terms of the wavelength of the light. In the next two columns, this number is converted to nanometers, first by assuming λ = 560 nm, i.e. the wavelength of the optically most effective light, and in the second by assuming λ = 430 nm, i.e. the photographically most effective light. The three following columns give Z for the cases of pure spherical aberration (Z_1), typical zonal aberration (Z_2), and the many zones (Z_3). In the last column, Z has been calculated with the aid of the first two terms of the series expansion, i.e.

$$Z_4 = 1 - \left(\frac{2\pi\varepsilon}{\lambda}\right)^2.$$

TABLE XXVI.

$\frac{\varepsilon}{\lambda}$	ε $\lambda = 560$ nm	ε $\lambda = 430$ nm	Z_1	Z_2	Z_3	Z_4
	nm	nm				
0.00	0	0	1.000	1.000	1.000	1.000
0.02	11	9	0.984	0.984	0.984	0.984
0.04	22	17	0.939	0.939	0.938	0.937
0.06	34	26	0.867	0.867	0.865	0.858
0.08	45	34	0.773	0.774	0.770	0.747
0.10	56	43	0.666	0.668	0.660	0.605
0.12	67	52	0.553	0.555	0.541	0.432
0.14	78	60	0.442	0.444	0.421	0.226
0.16	90	69	0.341	0.340	0.308	−0.011
0.18	101	77	0.252	0.247	0.208	−0.279
0.20	112	86	0.181	0.169	0.125	−0.579
0.22	123	95	0.131	0.107	0.062	−0.911
0.24	134	103	0.099	0.061	0.022	−1.274
0.26	146	112	0.084	0.029	0.002	−1.669

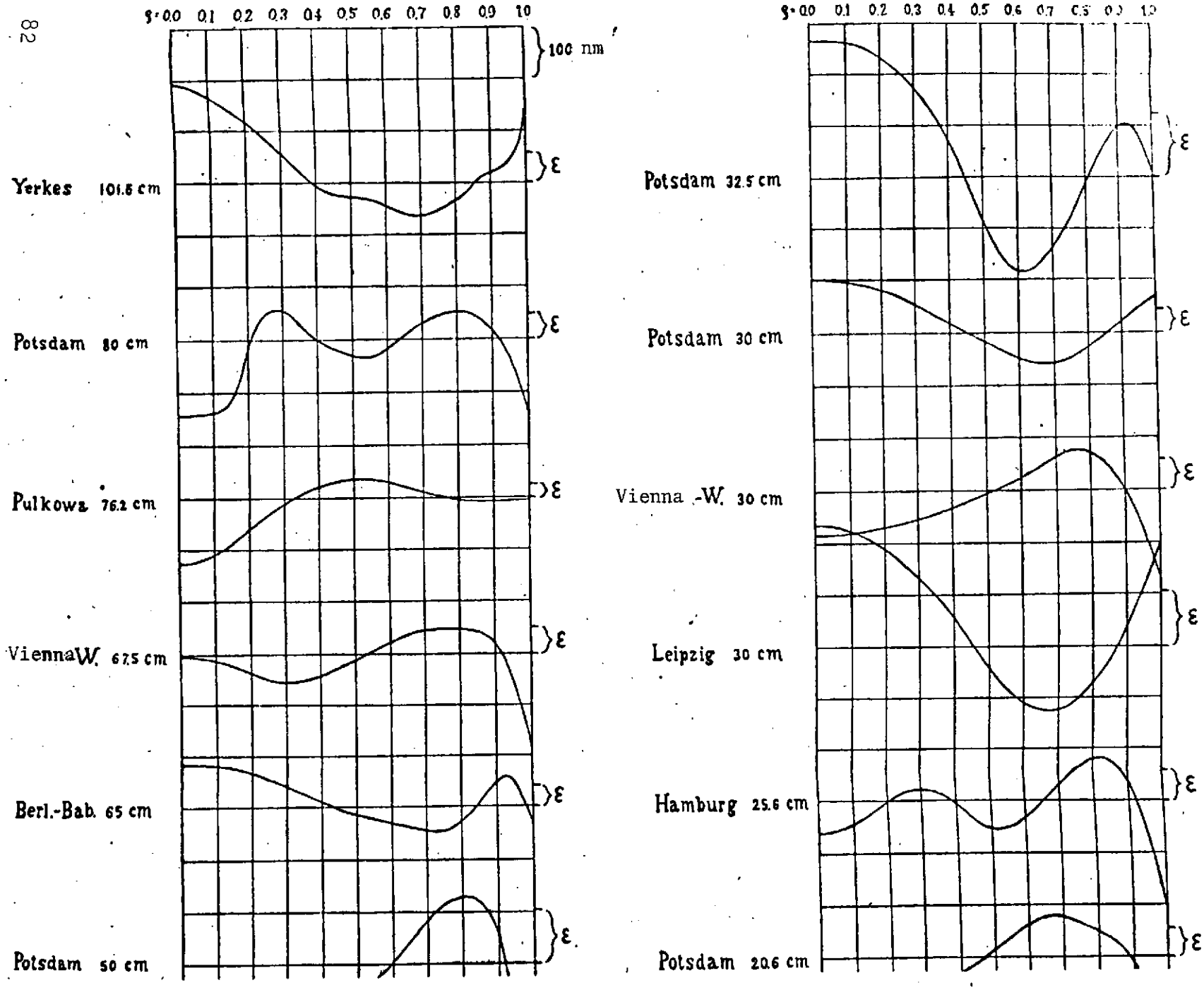
s· 0.0 0.1 0.2 0.3 0.4 0.5 0.6 0.7 0.8 0.9 1.0
100 nm
ε
Yerkes 101.6 cm
Potsdam 80 cm
Pulkowa 76.2 cm
ViennaW. 67.5 cm
Berl.-Bab. 65 cm
Potsdam 50 cm
Potsdam 32.5 cm
Potsdam 30 cm
Vienna -W. 30 cm
Leipzig 30 cm
Hamburg 25.6 cm
Potsdam 20.6 cm

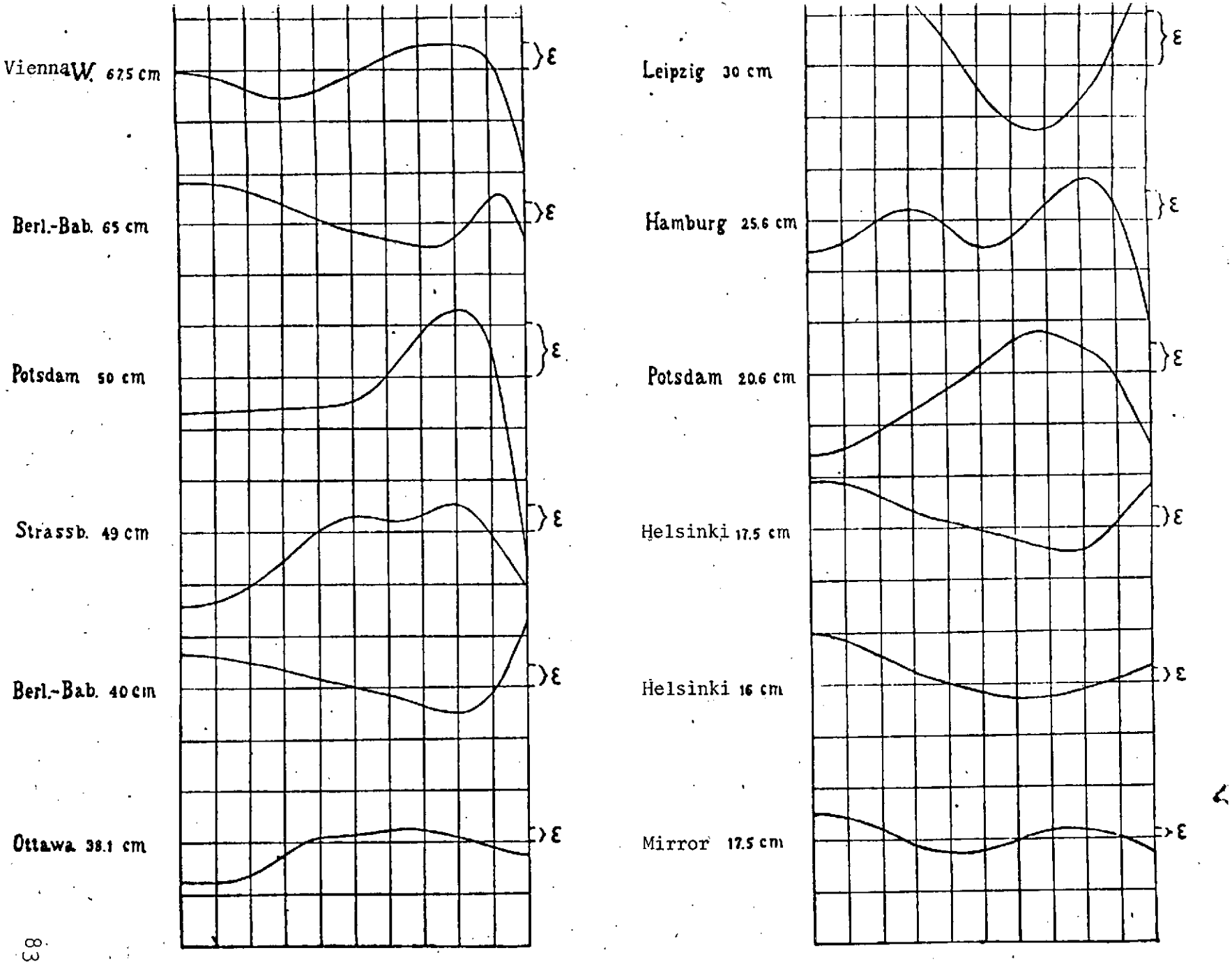
Vienna W. 67.5 cm
Berl.-Bab. 65 cm
Potsdam 50 cm
Strassb. 49 cm
Berl.-Bab. 40 cm
Ottawa 38.1 cm
Leipzig 30 cm
Hamburg 25.6 cm
Potsdam 20.6 cm
Helsinki 17.5 cm
Helsinki 16 cm
Mirror 17.5 cm
ε

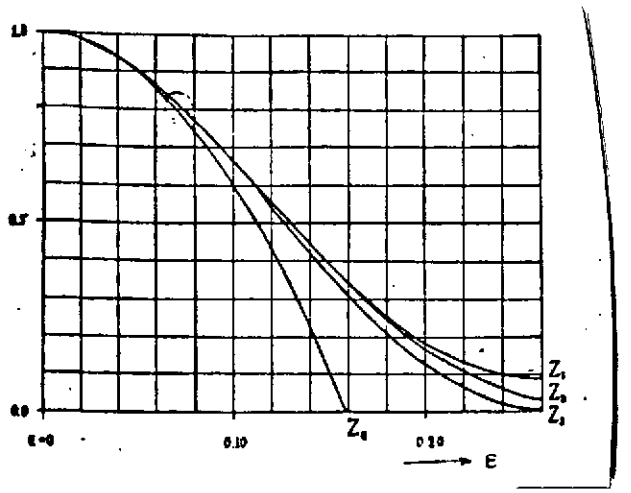

Fig. 13.

Z is depicted as a function of ε in Fig. 13. /113

As can be seen from the diagram, the curves for Z_1, Z_2, and Z_3 do not differ markedly until large values of ε, and are all less than 1. As ε increases, the values of Z decrease, and finally reach a minimum at a specific point. If the computations were continued, it would be observed that the numbers for Z would oscillate while decreasing, the amplitude of the wave converging to zero.

36. As a comparison, we will also calculate how the technical constant T based on the focal lengths depends on ε in these three cases.

In the case of pure spherical aberration,

$$T^{(1)} = 1.589\frac{10^4\varepsilon}{R} \qquad (76)$$

is acquired directly from the previously derived expressions. In the case of typical zonal aberration,

$$T^{(2)} = 2.533\frac{10^4\varepsilon}{R} = 1.594\,T^{(1)}. \qquad (77)$$

With many zones, /114

$$h = x_3\cos 2\pi nq = \varepsilon\sqrt{2}\cos 2\pi nq$$

the focal-length deviations

$$\Delta = 2\left(\frac{F_0}{R}\right)^2\frac{dh}{dq} = -4\sqrt{2}\,\pi\varepsilon\left(\frac{F_0}{R}\right)^2 n\sin 2\pi nq$$
$$= -4\sqrt{2}\,\pi\varepsilon\left(\frac{F_0}{R}\right)^2 n\sin 2\pi n\varrho^2.$$

are obtained.

For simplicity, we take $\Delta_0 = 0$. It is not hard to see that as n increases, the movable plane defined in this way approaches the movable plane in which T attains its minimum. We therefore obtain

$$T^{(3)} = 4 \cdot 10^5 \frac{R}{F_0^2} \int_0^1 \varrho^2 \, |\Delta - \Delta_0| \, d\varrho$$

$$= 16\sqrt{2} \cdot 10^5 \frac{\pi n \varepsilon}{R} \int_0^1 \varrho^2 \, |\sin 2\pi n \varrho^2| \, d\varrho.$$

If we set $v = 2\rho\sqrt{n}$, break up the interval of integration into subintervals determined by the zeros of the integrand, and integrate by parts, we find

$$T^{(3)} = \frac{1}{5}\sqrt{2}\frac{10^6 \varepsilon}{R\sqrt{n}} \{2(\sqrt{2} + \sqrt{4} + \cdots + \sqrt{4n-2}) + \sqrt{4n} +$$
$$+ 2[c(\sqrt{2}) - c(\sqrt{4}) + c(\sqrt{6}) - + \cdots + c(\sqrt{4n-2})] - c(\sqrt{4n})\},$$

where

$$c(v) = \int_0^v \cos\tfrac{\pi}{2} v^2 \, dv$$

is the well-known Fresnel integral, for which tables have been given in many optical works (cf. [17]).

For different values of n, we obtain

$$\begin{aligned} n = 1, \quad & T^{(3)} = 1.527 \frac{10^6 \varepsilon}{R}, \\ n = 2, \quad & T^{(3)} = 3.031 \frac{10^6 \varepsilon}{R} = 2 \cdot 1.516 \frac{10^6 \varepsilon}{R}, \\ n = 3, \quad & T^{(3)} = 4.541 \frac{10^6 \varepsilon}{R} = 3 \cdot 1.514 \frac{10^6 \varepsilon}{R}, \\ n = 4, \quad & T^{(3)} = 6.050 \frac{10^6 \varepsilon}{R} = 4 \cdot 1.512 \frac{10^6 \varepsilon}{R}. \end{aligned} \tag{78}$$

/115

If n is very large, then

$$T^{(3)} = \frac{16}{15}\sqrt{2}\, n \frac{10^6 \varepsilon}{R}\left[1 + \left(\frac{1}{n}\right)\right] = 1.508\, n \frac{10^6 \varepsilon}{R}\left[1 + \left(\frac{1}{n}\right)\right], \tag{79}$$

where

$$\lim_{n=\infty} \left(\frac{1}{n}\right) = 0.$$

From these numerical examples, it is evident that T increases in rough proportion to the number of zones, while ε remains constant. Since, if ε is small, the same values of ε correspond to roughly equal values of Z, this indicates that the technical constants of Strehl and Lehmann can provide a quite contrasting picture of the correctness of the objective.

Assessing Objectives on the Basis of the Technical Constants

37. Starting from well-known facts and our calculations so far, we will now attempt to present the principles on which objectives can be judged. We first assume that there will be high demands made on the objective, as will usually be the case for an astronomical objective.

In a diffraction pattern produced by an ideal objective, the light intensity in the central disk is 84% of the entire light energy passing through the objective [18]. The remainder /116
of the light is distributed over the interference rings, which appear around the central disk. Keeping in mind that the light intensity even at the brightest spot in the first interference ring is only 1/60 of the light intensity at the center of the diffraction pattern, and that the light intensity in the remaining rings drops off sharply, it is clear that observation will deal almost exclusively with the central disk of the diffraction pattern and that its light intensity and diameter will determine the power of the objective. The situation will not be altered as long as the objective has zonal aberrations which are so small that the brightness of the central disk continues to dominate, and provides the actual image. Since the diameter of the central disk depends in a complicated fashion on the zonal aberrations, and, as mentioned previously, is once in a while even smaller than in the diffraction pattern of the ideal objective, the possibility remains that the light intensity of the central disk, compared to the light intensity of the central disk in the pattern produced by an ideal objective of the same type, can be viewed as a standard for the technical perfection of the objective. Since it would generally be tedious to calculate this number, one must content oneself with ascertaining just the brightness of the center of the image, which will be roughly proportional to the intensity of the entire central disk. In this fashion, one arrives at the technical constant Z defined by Strehl.

This shows that an objective will certainly be a good one if Z has a value close to unity, no matter what the form of the light front. For an ideal objective, Z = 1 exactly. An answer to the question of how much less than unity Z can be without the objective losing its ranking as a first-class lens is best sought empirically, namely by determining the constant Z for the largest possible number of modern objectives, the properties of which have been established by thorough examinations. In Table /117
XXIX, I have collected my calculated values of Z for several objectives. For most of the objectives in the table, Z is about 2/3 and above. All these objectives have been considered first-class.

If Z is only a small fraction of unity, only a small fraction of the entire light energy is concentrated in the central disk of

the diffraction pattern, and the remainder is distributed over the surrounding interference rings and makes them noticeably brighter. The central disk therefore loses its dominant position, and the pattern no longer has the form characteristic of a good one. It is clear that the objective is then not good enough for exact observations, e.g. perceiving fine surface details of planets, separating close doubles, etc. In these cases, the magnifications employed with the objective must be weak enough that the central disk of the pattern and the interference rings blur into a single image. Since the quality of the image also depends on the distribution of the light over the interference rings, and Z gives no information about that, the number Z can no longer be considered a standard for comparing objectives with such great aberrations. If the Z of an objective intended for precise observations is very small, however, a more detailed classification is not necessary, and the objective can simply be labeled unsatisfactory. It would not matter whether Z was e.g. 0.01 or 0.05.

Earlier, it was pointed out that the mean deviation ε of the wave front can also be viewed as a standard in judging the quality of an objective. This claim is supported by my three typical examples, which represent very different types of zonal aberrations. In these illustrations, we discovered that a specific value of ε corresponded to roughly identical values of Z in these three different cases. The difference was not /118 appreciable until ε was so large that the corresponding Z was only a small fraction of unity. However, as we have just noted, the precise calculation of Strehl's constant is no longer significant in that case. The mean deviation ε of the wave front therefore proves to be a suitable measure of the perfection of objectives intended for fine observations, for the same reasons as for Strehl's constant Z. Not only is ε much simpler to calculate than Z, a very good approximation to Z can also be obtained from ε with the aid of Table XXVI as long as ε is not too large. Since pure spherical aberration is the most frequent zonal aberration, using the value Z_1 seems like a good idea. Even in the case that ε is large, it is still to a certain extent a suitable measure for the quality of an objective, since understandably, the larger ε, the poorer the objective in general.[2]

---

[2]Nonetheless, it is possible to construct cases in which Z = 1, although ε is large. Such a case is e.g. a wave front formed by two concentric spherical-surface sections, with a phase difference equal to the wavelength of the light. Of course, such a case does not occur in practice unless it is specially arranged.

38. Starting from the diffraction-theoretic constants Z and ε, we now analyze the suitability of Lehmann's constant T as a measure of the quality of an objective. If ε is very small, the quality of the objective is independent of the configuration of the wave front. On the other hand, our examples have shown that T rises roughly linearly with the number of zones if ε is constant. Therefore, T does not deliver a reliable picture of the quality of the objective, and hence is not recommended as a means to classify objectives. It might be entirely /119
possible that two objectives of equal size would acquire zonal aberrations in refinishing giving them the same ε but giving one of them a value of T five times as large as that of the other. Such great differences may well not occur in practice. How different the results from ε and T can be in practice can be seen from the number $RT/10^6\varepsilon$ in Table XXIX. This number is based on the distribution of zonal aberrations to the various zones. It can therefore be considered a constant characterizing the shape of the wave front.

This says that an objective does not necessarily have to be a poor one even if T were relatively large. On the other hand, if T is very small, we can be practically certain that the objective is a first-class one, since if T is sufficiently small, Z is close to unity. In this case, we have assumed that the wave front has no discontinuities.[3]

We now assume we are dealing with an objective which is not intended for purposes which will place great demands on the objective. To this class we may assign photographic objectives /120
for terrestrial pictures, terrestrial telescopes used with weak magnifications, and, among astronomical objectives, at any rate, the objectives of comet-seekers and short-focal-length objectives and mirrors for stellar photographs. Such objectives can be quite usable, even if the constant Z were to be small, and thus

---

[3]If the wave front is made up of two equally large sections of concentric spheres, between which there is a phase difference of one half a wavelength, the geometric focus is located at the center of the spheres, and T = 0, so the objective would be a good one. In actuality, however, interference would reduce the intensity of the light at the center of the spheres to zero, and the maximum Z along the optical axis would be only about 0.1, so that the objective was really a poor one. By dividing a parabolic mirror into two zones of equal size, and covering them with silver layers of different thicknesses, this zonal aberration and others as well similar to it can be produced in practice.

the distribution of the light outside the optical axis as well must be calculated in order to compare such objectives with one another. It is very arduous to carry out such a calculation using diffraction theory [19], so that a retreat to geometrical optics and to its technical constant T would be in order. If the deviations of the wave front are so large that the influence of the diffraction phenomenon can be neglected by comparison with the zonal aberrations, it would naturally be legitimate to use T. In a certain sense, therefore, the parameters Z and T are supplementary, the former working well when the deviations of the wave front are small, and the latter becoming more and more suitable for comparing different objectives as the deviations of the wave front increase.

The constants T and Z differ in another respect as well. Namely, if it is applicable, the former parameter can be used to compare objectives of different sizes, while the constant Z expresses only the ratio of the power of an objective to that of an ideal objective of the same dimensions. Objectives of different sizes can be compared using Z in the following fashion. As as observed earlier at one point, the intensity of light in the central disk of the diffraction pattern can be considered proportional to Z in first approximation. Since the light /121
intensity in the pattern of an ideal objective is proportional to the square of the diameter D of the objective, the intensity in the central disk of the objective is proportional to the expression ZD^2. This expression can also be viewed as a measure of the quality of an objective. For greater convenience, it may be replaced by its square root $D\sqrt{Z}$, which gives the diameter of the ideal lens for which the intensity of the light in the central disk of the pattern is the same as that in the central disk of the pattern of the objective in question. The number $D\sqrt{Z}$ we term the effective diameter of the objective. With this number, it is possible to classify objectives intended for fine measurements but with different dimensions, and in fact, the objectives can be grouped by light intensity, while in the classification by T, if legitimate, the objectives can be grouped by the diameter of the patterns.

Applications

39. The methods described in this report for assessing the quality of objectives were applied to the objectives given in the following summary; I found the zonal aberrations for these objectives in the literature. The figures on most of the objectives mentioned in the list are taken from the publication of Hartmann cited in the Introduction. The only mirror I include is the one I ground myself, since I have encountered hardly any numbers referring to the aberrations of mirrors in the literature.

TABLE XXVII. /122

No.	Observatory	Optician	Type	Diam. D	Focal Length F	F:D	Source
				cm.	cm.		
1	Yerkes	Clark	Vis.	101.6	1935	19.0	Publ. Potsdam 46
2	Potsdam	Steinheil	Phot.	80	1219	15.2	"
3	Pulkovo	Clark	Vis.	76.2	1412	18.5	"
4	Vienna-Währing	Grubb	"	67.5	1036	15.4	"
5	Berlin-Bab.	Zeiss	"	65	1039	16.0	Veröff. Berl.-Bab. III
6	Potsdam	Steinheil	"	50	1256	25.1	Publ. Potsdam 46
7	Strassburg	Merz	"	49	692	14.1	A. N. 202, 4830
8	Berlin-Bab.	Steinheil	Phot.	40	550	13.8	Veröff. Berl.-Bab. III
9	Ottawa	Brashear	Vis.	38.1	570	15.0	Publ. Potsdam 46
10	Potsdam	Steinheil	Phot.	32.5	341	10.6	"
11	Potsdam	Steinheil	Vis.	30	363	12.1	"
12	Vienna-Währing	Clark	"	30	480	16.0	"
13	Leipzig	Reinfelder u. H.	"	30	360	12.0	"
14	Hamburg	Merz	"	25.6	302	11 8	Mitt. Hamb.-Bergedorf 12
15	Potsdam	Grubb	"	20.6	316	15.4	Publ. Potsdam 46
16	Helsinki	Utzschn. u. Fraunh.	"	17 5	288	16.5	This report
17	Helsinki	Utzschn. u. Fraunh.	"	16	240	15.0	"
18	—	Author	Mirror	17.5	121	6.9	"

Except for the three last objectives, all lenses were studied by Hartmann's method, finding the focal-length deviations Δ. The deviations of the light front h are obtained from these values by the formula

$$h = \frac{1}{2}\left(\frac{R}{F}\right)^2 \int_0^q \Delta \, dq$$

by numerical integration. To perform this calculation, I first drew focal-length curves from the given values for Δ. I extrapolated these curves toward the center and toward the edge of the objective, and then took values of Δ corresponding to the zones /123

$$\rho^2 = q = 0.02,\ 0.06,\ 0.10,\ \ldots,\ 0.98$$

from the curves. After that, I did the mechanical integration in simple fashion by calculating the first sum in the deviations Δ and multiplied the resulting numbers by 0.04. In this way, I determined h for the zones q = 0, 0.04, 0.08, ..., 1.00.

From the values found for h, I calculated the mean deviation ε of the wave front by two methods, first directly with formula (64) and second using formulas (63), having first computed the reduced deviations $\bar{h}$. In all mechanical integrations, the integrands were calculated for the zones q = 0.02, 0.06, ..., 0.98. I also found Strehl's constant Z directly from its defining formulas (58) and (59) by mechanical integration. For the visual objectives and the mirror, I took λ = 560 nm as the effective wavelength, and λ = 430 nm for the photographic objectives.

The configuration of the wave front is depicted graphically in the table at the conclusion of the treatise. The abscissa is ρ and the ordinate $\bar{h}$ expressed in nm. Beside each curve, the value of ε is given. The numerical values of the deviations $\bar{h}$ are found in Table XXVIII.

For each of the above objectives, Table XXIX contains 1) the mean deviation ε of the wave front, 2) the value of Strehl's constant Z_1 corresponding to the mean deviation ε in the case of pure spherical aberration, 3) the value of Z calculated from the defining formulas of Strehl's constant, 4) the effective diameter $D\sqrt{Z}$, 5) the Lehmann constant T calculated by formulas (57), 6) the previously reported Lehmann constant T', /125
and 7) the expression $RT/10^6\varepsilon$ based on the form of the zonal-aberration curves.

From the values for Strehl's constant it can be seen that most of the objectives listed in the table are relatively good from the point of view of zonal aberrations. Among the large objectives, the one closest to the ideal is the 38.1-cm objective in Ottawa and the 76.2-cm objective in Pulkowa. The 50-cm Potsdam, the 32.5-cm (phot.) Potsdam and the 30-cm Leipzig objectives have the smallest Strehl's constant. However, it should be kept in mind that the deviations of the wave front for these objectives are already so large that the reference sphere used in calculating the mean deviation can differ appreciably /126
from the reference sphere which maximizes Z. In particular, this is true of the Potsdam 32.5-cm objective. According to the calculations of Wilsing [19, p. 20], the brightness at the center of the diffraction pattern at the focus of this objective is 0.15 of the brightness at the center of an ideal objective of corresponding size.

Comparing the values Z_1 and Z in the table shows that the difference between these two numbers is at most 0.01, as long as the three poor objectives mentioned above are ignored. Our earlier conjecture, namely that ε determines Z for good objectives, is therefore corroborated in practice. The expression given in the final column of the table ($RT/10^6\varepsilon$) can, as previously mentioned, be viewed as a constant reflecting the form

TABLE XXVIII.

h in nm

Obj. / q	1	2	3	4	5	6	7	8	9	10	11	12	13	14	15	16	17	18
0.00	+191	−142	−125	−2	+92	−70	−143	+62	−75	+268	+104	−81	+236	−61	−158	+91	+100	+51
0.02	+145	−121	−90	−20	+79	−66	−121	+55	−74	+251	+94	−76	+213	−30	−133	+81	+73	+34
0.06	+93	+47	−38	−49	+54	−60	−81	+43	−45	+212	+73	−64	+166	+13	−93	+45	+40	+4
0.10	+61	+52	−8	−54	+32	−59	−38	+31	−12	+162	+54	−51	+121	+21	−62	+29	+19	−12
0.14	+9	+8	+11	−47	+17	−60	−8	+20	+4	+101	+28	−37	+76	+4	−40	+18	+7	−22
0.18	−19	−18	+21	−33	+5	−60	+10	+11	+10	+31	+11	−25	+32	−25	−22	+9	−3	−23
0.22	−27	−25	+30	−20	−11	−54	+23	+4	+13	−40	−6	−12	−12	−49	−6	0	−11	−23
0.26	−28	−34	+38	−5	−20	−48	+30	−2	+16	−106	−22	−2	−50	−56	+15	−6	−16	−19
0.30	−30	−35	+34	+7	−21	−29	+28	−7	+19	−155	−33	+9	−81	−51	+39	−14	−21	−12
0.34	−37	−25	+29	+20	−27	−4	+21	−12	+22	−178	−44	+19	−102	−39	−60	−20	−25	−4
0.38	−47	−10	+21	+29	−32	+20	+20	−17	+24	−181	−51	+30	−116	−25	+68	−26	−28	+3
0.42	−57	+8	+17	+38	−38	+47	+21	−23	+25	−172	−55	+42	−123	−8	+75	−30	−29	+10
0.46	−63	+21	+9	+43	−43	+67	+26	−29	+25	−156	−58	+54	−125	+13	+81	−36	−27	+14
0.50	−63	+31	+8	+46	−47	+91	+36	−35	+23	−133	−56	+61	−120	+31	+74	−40	−25	+17
0.54	−57	+40	+4	+48	−49	+110	+43	−41	+20	−104	−53	+72	−115	+50	+66	−45	−22	+18
0.58	−52	+46	0	+49	−45	+122	+51	−46	+16	−71	−42	+73	−100	+65	+60	−46	−18	+19
0.62	−44	+50	−5	+48	−36	+125	+53	−48	+11	−37	−32	+73	−84	+77	+51	−46	−13	+17
0.66	−33	+50	−8	+47	−23	+125	+52	−48	+6	−3	−21	+68	−66	+81	+45	−41	−10	+16
0.70	−17	+47	−8	+45	−6	+126	+43	−43	+1	+30	−10	+55	−42	+80	+37	−32	−5	+12
0.74	−2	+38	−9	+43	+14	+111	+29	−33	−4	+58	0	+43	−19	+72	+29	−20	+1	+9
0.78	+13	+28	−8	+33	+33	+88	+7	−20	−8	+83	+11	+22	+9	+55	+13	−4	+6	+6
0.82	+20	+15	−7	+17	+48	+41	−11	−4	−11	+98	+21	−3	+40	+31	−17	+9	+12	+1
0.86	+26	−6	−7	−7	+57	−22	−33	+19	−15	+103	+32	−30	+71	−2	−45	+31	+15	−5
0.90	+35	−31	−7	−39	+48	−103	−55	+47	−18	+94	+43	−64	+105	−46	−71	+49	+21	−12
0.94	+58	−67	−6	−88	+22	−192	−76	+79	−21	+72	+53	−101	+137	−99	−98	+69	+26	−18
0.98	+112	−111	−6	−152	−11	−293	−96	+113	−24	+36	+65	−145	+178	−162	−126	+72	+30	−25

TABLE XXIX.

No.	Objective		ε	Z_1	Z	$D\sqrt{Z}$	T	T'	$\frac{RT}{10^6 \varepsilon}$
			μμ			cm			
1	Yerkes	101.6 cm	56	0.67	0.68	83.7	0.20	0.16	1.8
2	Potsdam	80 "	47	0.62	0.63	63.5	0.30	0.34	2.6
3	Pulkowa	76.2 "	25	0.92	0.92	73.0	0.08	0.18	1.2
4	Vienna-Währing	67.5 "	50	0.72	0.73	57.7	0.37	0.46	2.5
5	Berlin-Bab.	65 "	37	0.84	0.84	59.6	0.27	0.22	2.4
6	Potsdam	50 "	104	0.23	0.29	27.0	1.07	1.08	2.6
7	Strassburg	49 "	49	0.73	0.74	42.1	0.35	0.34	1.8
8	Berlin-Bab.	40 "	41	0.69	0.70	33.4	0.53	0.48	2.6
9	Ottawa	38.1 "	24	0.93	0.93	36.7	0.14	0.30	1.1
10	Potsdam	32.5 "	123	0.08	0.002	1.5	1.22	1.30	1.6
11	Potsdam	30 "	15	0.77	0.77	26.3	0.42	0.44	1.4
12	Vienna-Währing	30 "	59	0.64	0.64	24.0	0.79	0.84	2.0
13	Leipzig	30 "	105	0.22	0.21	13.8	1.00	0.95	1.4
14	Hamburg	25.6 "	59	0.64	0.65	20.6	1.26	—	2.7
15	Potsdam	20.6 "	56	0.67	0.66	16.7	1.03	0.92	1.9
16	Helsinki	17.5 "	38	0.83	0.83	15.9	0.72	—	1.7
17	Helsinki	16 "	25	0.92	0.92	15.3	0.40	—	1.3
18	(Mirror)	17.5 "	16	0.97	0.97	17.2	0.35	—	1.9

of the zonal aberrations. For comparison, we repeat that this constant is 1.59 in the case of pure spherical aberration and 2.53 for typical zonal aberration.

40. Looking at the wave fronts depicted near the end of this report, it can be seen that certain objectives could be brought significantly closer to the ideal objective if the lens aperture were stopped down in an appropriate manner.[4] For instance, if the edge of the Potsdam visual 50-cm objective is masked, leaving an aperture 44 cm in diameter ($\rho = 0.88$), the objective can be greatly improved. In that case, namely, $\varepsilon = 22$ nm, $Z_1 = 0.94$, and $D\sqrt{Z_1} = 42.6$ cm. The center of the pattern is therefore considerably brighter when the objective is partially masked than when the aperture is completely open.

The curves illustrating the wave fronts demonstrate that several of the objectives in question could be successfully corrected by refinishing. As long as the deviations of the /127

[4]For this purpose, it would be best to plot q on the horizontal axis instead of ρ in the drawings of the wave fronts.

light front are known, it is easy to tell which zones of the objective and how much to polish. Let n be the average refractive index of the glass of an objective which is to be corrected by polishing a face. If, at this point, a layer of glass 1 unit thick is removed, the deviation of the wave front is reduced here by n - 1 units. Therefore, in order to suppress the deviation h all the way to zero, a layer h/(n - 1) units of length thick must be removed from the glass at this point. Hence, if the deviations of the light front are multiplied by 1/(n - 1), the aberration of a face of the objective is obtained, while the other faces are considered to be aberration-free. For mirrors, one must write n = -1 and hence 1/(n - 1) = -1/2. For lenses, the corresponding number varies between the values 1.6 and 2.0, depending on the refractive index. This shows that a grinding error in the surface of a mirror causes a deviation in the light front about 3.2-4.0 times as great as a corresponding error in the surface of a lens.

The correction of zonal aberrations in an objective can be conducted in infinitely many ways. As an illustration, we take the Leipzig 30-cm refractor. In Fig. 14, the curve H reproduces the light front of this refractor. To a large degree, the zonal aberrations carry the stamp of pure spherical aberration, and the spherical aberration is overcorrected in this case, since the focal length of the peripheral beams is greater than that for the central beams, as can be seen immediately from curve H. In the drawing, each spherical surface corresponds to a parabola, and the limiting case is a straight line. Three different corrections are illustrated in the diagram, corresponding to the corrected wave fronts A, B, and C. In the first case, the center and edge of the objective are to be polished until the curve representing the wave front turns into the straight line A. In the second case, polishing the peripheral sections gives rise to the zonal-aberration curve of parabola B, and in the third, polishing the center converts it to parabola C. In practice, the latter case is the simplest to accomplish, in the view of opticians. If the refinishing is achieved by polishing crown glass, the difference of the ordinates for curves H and C, multiplied by 2, is the thickness of the glass layer to be removed from each zone. At the center of the objective, therefore, there would be about 1.5 μm to be removed.

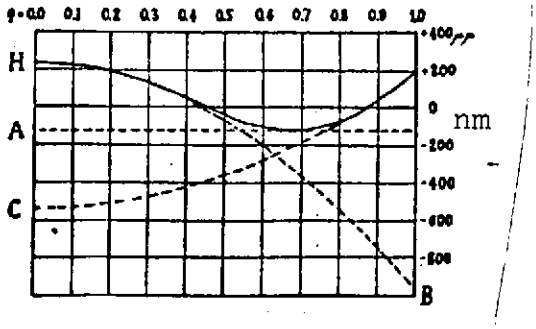

Fig. 14.

Refinishing just the middle sections of the objective could also correct several other of these objectives, e.g. the Potsdam

photographic 32.5-cm objective, which has large zonal aberrations. It is true that these aberrations could not be completely corrected just by polishing the central sections, and the zones closer to the edge would also have to be polished, but the remaining aberrations would not be very disturbing. Also, the large objective of the Yerkes observatory could be corrected by refinishing the central sections.

In this connection, I would like to mention that Schröder, /129 in manufacturing objectives, intentionally calculated the radii of the faces so that spherical aberration would be overcorrected. Once all the faces of the objective had been prepared as precisely as possible in accordance with the calculations, he refinished the central section of the last face of the objective, until the spherical aberration was corrected exactly. By using this procedure, he avoided the case of undercorrected spherical aberration, which is more difficult to eliminate by refinishing. Undercorrection might well have been produced by grinding and polishing errors than by the nonuniform density of the glass if the spherical aberration of the mathematically calculated objective had been precisely equal to zero.

Five years ago, I had already produced a parabolic mirror using the method described earlier, in which the light fronts are used to correct the aberrations of an objective. Since, at that time, I had not yet discovered how to ascertain the deviations of the wave front directly by the interference methods, I first determined the focal-length deviations using the previously known procedures, and then integrated them to obtain the deviations of the light front. By inspecting the latter, I immediately saw which part of the face and how much to polish. My methods for determining the light wave front, for which any person can very quickly fabricate the required equipment, supply every optician with the means to check the quality of an objective with great precision, and, by careful refinishing, to obtain objectives which are practically ideal. It will not be absolutely necessary to restrict refinishing just to the central portions of the objective. My experience indicates that all types of zonal aberration can be successfully refinished away, although refinishing the center is the easiest.

REFERENCES

1. On the adjustment and testing of telescopic objectives, T. Cooke and Sons, Buckinham Works, New York. German edition by Dr. R. Straubel, Berlin, 1894.

2. Publ. Astrophys. Obs. Potsdam, No. 46.

3. Publ. Astrophys. Obs. Potsdam, No. 48.

4. First publication: Zeitschr. f. Instrk. 20, 51 (1900); further details: Zeitschr. f. Instrk. 24, 1 (1904); application to a large refractor: [2].

5. Hartmann, "Studies of telescopic lenses," Zeitschr. f. Instrk. 24, 6 (1904).

6. Zeitschr. f. Instrk. 22, 108 (1902).

7. Zeitschr. f. Instrk. 22, 213 (1902).

8. Astrophysical Journal 47, 283 (1918).

9. Classen, J., Mathematische Optik [Mathematical Optics], Leipzig, 1901, pp. 182-185.

10. Publ. Astroph. Obs. Potsdam, No. 45, p. 43.

11. Zeitschr. f. Instrk. 24, 12 (1904).

12. Zeitschr. f. Instrk. 22, 325 (1902).

13. Zeitschr. f. Instrk. 24, 46 (1904).

14. Astrophysical Journal 27, 242 (1908).

15. Strehl, K., Theorie des Fernrohrs [Theory of the telescope], Leipzig, 1894, p. 30.

16. Strehl, K., "Zones and power of refractors," Zeitschr. f. Instrk. 24, 323 (1904).

17. Mascart, Traité d'optique [Treatise on optics], Vol. I, Paris, 1889, p. 269.

18. Muller, G., Die Photometrie des Gestirne [Stellar photometry], Leipzig, 1897, p. 166.

19. Publ. Astroph. Obs. Potsdam, No. 48, 1903.